UNIVERSITY OF OKLAHOMA

GRADUATE COLLEGE

EFFECT OF OSMOLYTES ON REGULATING THE ACTIVITIES OF THE SSK1 RESPONSE REGULATOR FROM *SACCHAROMYCES CEREVISIAE*

A DISSERTATION

SUBMITTED TO THE GRADUATE FACULTY

in partial fulfillment of the requirements for the

Degree of

DOCTOR OF PHILOSOPHY

BY

ALLA OLEGIVNA KASERER
Norman, Oklahoma
2009

EFFECT OF OSMOLYTES ON REGULATING THE ACTIVITIES OF THE SSK1 RESPONSE REGULATOR FROM *SACCHAROMYCES CEREVISIAE*

A DISSERTATION APPROVED FOR THE
DEPARTMENT OF CHEMISTRY AND BIOCHEMISTRY

BY

_____
Dr. Ann H. West

_____
Dr. Paul F. Cook

_____
Dr. George Richter-Addo

_____
Dr. Tyrrell Conway

_____
Dr. Jana Shen

Acknowledgements

This Ph.D. thesis would not be possible without years of research and support of many people I came to know at the University of Oklahoma, who deserve special mention. It is a pleasure to express my gratitude to them all in this acknowledgment.

I would like to convey my deep and sincere gratitude to my supervisor, Professor Ann West. Her wide knowledge, guidance from the very early stage of this research and her support has been a great value to me. Her passions in science, encouragement and understanding have enriched me as a researcher and provided a good basis for the present thesis. I would especially like to thank her for her patience and inspiration throughout my scientific career. I am indebted to her in every possible way.

Many special thanks I would like to express, in particular, to Professor Paul F. Cook for his valuable scientific discussions, guidance in kinetic analysis, for his detailed and constructive comments, criticism and explanations. Thank you, for granting me your precious time and answering all my questions.

I gratefully acknowledge the members of my advisory committee, Professors Bruce Roe, George Richter-Addo, Tyrrell Conway and Jana Shen for their fruitful discussions and guidance.

It is also a pleasure to pay tribute to our collaborators, Professor Richard Calderone from Georgetown University and Professor Christopher Halkides from University of North Carolina, Wilmington. I would like to thank Dr. Calderone for

giving me the opportunity to collaborate on the *C. albicans* project and Dr. Halkides and his research group for helping me with the creation of a phosphono-SSK1-R2 analog.

Collective and individual thanks are also owed to my colleagues in the West and Cook labs that came and left during the time I spent in the lab. It is my pleasure to mention: Dr. Fabiola Janiak-Spens, Dr. Hui Tan, Dr. Stace Porter, Dr. Daniel Copland, Dr. Xiaodong Zhao and Dr. Babak Andi. Your help, invaluable assistance and guidance will always be appreciated and remembered by me. Without the contribution of all the members of the laboratory it would be impossible to finish this research project. Itôs been wonderful working with you all!

Furthermore I would like to thank my family and my husband Wallace for their love, support during challenging times and persistent confidence in me. Special thanks and love to my mom and dad Viktoria and Oleg, who pushed me to pursue a Ph.D. program and who were not afraid to let me go so far away from home. I am also deeply grateful to my parents in law, Alana and Peter, for accepting me as a member of the family and supporting and loving me through all these years.

Finally, I would like to thank everyone who helped me in finishing this thesis and I would like to dedicate this work to my grandmother Erika N. Ivannikova.

Table of Contents

List of Tables

List of Figures

Abstract

The multi-step His-Asp phosphorelay system in *Saccharomyces cerevisiae* allows cells to adapt to osmotic, oxidative and other environmental stresses. The pathway consists of a hybrid histidine kinase SLN1, a histidine-containing phosphotransfer (HPt) protein YPD1 and two response regulator proteins, SSK1 and SKN7. Under non-osmotic stress conditions, the SLN1 sensor kinase is active and phosphoryl groups are shuttled through YPD1 to SSK1, therefore maintaining the response regulator protein in a constitutively phosphorylated state. The cellular response to hyperosmotic stress involves rapid efflux of water and changes in intracellular ion and osmolyte concentration. To address the effect of osmolytes on the regulation of this signaling pathway, the individual and combined effects of NaCl and glycerol on phosphotransfer rates within the SLN1-YPD1-SSK1 phosphorelay were examined. In addition, the effect of osmolyte concentration on the half-life of the phosphorylated SSK1 receiver domain in the presence/absence of YPD1 was evaluated. The results show that the combined effects of glycerol and NaCl on the phosphotransfer reaction rates are different from the individual effects of glycerol and NaCl. The combinatory effect is likely more representative of the *in vivo* changes that occur during hyperosmotic stress. The results revealed that increasing osmolyte concentrations negatively affects the YPD1ÅSSK1~P interaction thereby facilitating dephosphorylation

of SSK1 and activating the HOG1 MAP kinase cascade. At high osmolyte concentrations, the kinetics of the phosphorelay favors production of SSK1~P and inhibition of the HOG1 pathway.

A similar multi-step signaling pathway is also utilized by *Candida albicans*, which is known for adaptation to oxidative stress, morphogenesis, cell wall biosynthesis and virulence in this opportunistic pathogenic yeast. To biochemically characterize major components of this pathway, studies were focused on *in vitro* reconstitution of the multi-step phosphorelay from *C. albicans* and biochemical characterization of the CaYPD1 (HPt protein) and CaSSK1 (response regulator protein). The heterologous phosphoryl transfer system SLN1-HK-RR Ÿ CaYPD1Ÿ CaSSK1 (or SSK1) was established and examined. The CaYPD1 histidine phosphotransfer protein exhibited similar phosphotransfer specificity *in vitro* towards the response regulator domain of CaSSK1-RR and SSK1-RR. The half-life of the phosphorylated regulatory domain of CaSSK1-RR was also measured and was approximately 9 min with a corresponding rate constant of 0.078 min^{-1}. This result demonstrates a similar rate of CaSSK1-RR dephosphorylation compared to SSK1-RR suggesting possible functional similarities between these two response regulator proteins.

Mutational analysis of the CaSSK1 response regulator domain was also performed. Mutants were expressed, purified and their activity was analyzed using an *in vitro* phosphorylation assay. Little or no phosphorylation was observed for the

CaSSK1-RR D556N mutant. The radiolabel primarily resided with the CaYPD1 protein and did not get transferred to the D556N mutant. Likewise, the D513K mutant was also severely impaired in its ability to be phosphorylated by CaYPD1. The receiver domains of the D556N and the D513K mutants could not be appreciably phosphorylated *in vitro* indicating that constitutive activation of HOG1 occurs *in vivo* due to the inability of CaSSK1 to be phosphorylated.

Chapter 1

1. Introduction

ñPortions of this chapter are reproduced in part with automatic permission from [Kaserer, A.O. and West, A.H. (2007) Histidine kinases in two-component signaling pathways, *The Handbook of Cell Signaling,* (2nd edition by Bradshaw R.A., Dennis E.A., eds.), In press] Academic Press, San Diegoò.

In order to sense and respond to their environment, cells need to transform one kind of signal or stimuli into another. This type of transformation is called signal transduction. Most signal transduction processes inside the cell involve ordered biochemical reactions carried out by protein participants of the signaling pathways. These events have a different nature and duration, lasting from milliseconds and minutes up to hours and days depending on the output response. The amount of proteins and other molecules participating in the signaling system may also vary starting from the initial stimuli and to signal amplification and finally to alterations in gene expression.

Signaling systems are widely spread among all living organisms. Bacteria, archaea and lower eukaryotes utilize similar mechanisms to survive exposure to the environment. The signal transduction mechanism that they have in common is the so-called two-component system. This system adopts protein phosphorylation as a means of information transfer. The minimal signaling system consists of a sensor histidine kinase (HK) and its downstream partner, a response regulator (RR) protein (Parkinson,

Kofoid 1992; Stock, Surette *et al.,* 1995; Mizuno 1998; Stock, Robinson *et al.,* 2000; West, Stock 2001).

1.1. Significance

The significance of this work lies within three major areas of scientific and biomedical importance:

1) Cell signaling mechanisms;

2) Protein-protein interactions;

3) Development of novel antibacterial and antifungal drugs;

1) *Cell signaling mechanism*

Cell signaling is the main element of the cell communication system that manages basic cellular activities and coordinates cell actions. The ability of cells to perceive and correctly respond to environmental changes is the basis of development and survival. The study of the cell signaling of *S. cerevisiae* via its multi-step two-component signaling system will advance our knowledge in understanding of the mechanism underlying adaptation to hyperosmotic stress and provide insights as to the mechanism of phosphorylation-dependent activation/deactivation of the SSK1 response regulator and its protein partners.

2) *Protein-protein interactions*

For any signal transduction pathway, it is extremely important that its proteins interact with each other in a specific and highly regulated manner. Correct information

should be carried out through the cell to modulate vital cellular responses. Specific protein-protein interactions in *Saccharomyces cerevisiae* should secure signal transmission with high fidelity in response to hyperosmotic stress to compensate for water loss from the cell and produce osmolytes (glycerol *etc.*) to sustain constant internal equilibrium (Hohmann 2002).

The effect of osmolytes on protein-protein interactions between histidine kinases, histidine-containing phosphotransfer proteins and response regulators are critical not only in understanding multi-step phosphorelay system regulation, but also maintenance of the yeast cell homeostasis.

3) *Development of novel antibacterial and antifungal drugs*

Practical implications of this study involve development of new antibacterial and antifungal drugs on the basis of multi-step phosphorelay systems from *Saccharomyces cerevisiae* (a well-studied model organism) and *Candida albicans* (pathogenic fungi). The real need for new antibacterial and antifungal drugs especially against the latter arises from the emergence of multi-drug resistant strains. Two-component regulatory proteins, and specifically CaSSK1, are involved in activation of the downstream genes that contribute to virulence of *C. albicans* and are attractive targets for drug design and drug screening (Stephenson, Hoch 2002; Chauhan, Latge *et al.,* 2008). Thus, because of the involvement of these signaling proteins in fungal pathogenesis, biochemical characterization of the participants of the two-component

system in *C. albicans* will provide useful information for drug design including design of possible peptide inhibitors that can inhibit these proteins, specifically CaSSK1.

A significant proportion of human infections involve biofilms (Kojic, Darouiche 2004). Organisms in biofilms behave differently from freely suspended microbes and are less susceptible to different antibacterial and antifungal drugs. An increasing amount of device-related infections, particularly those involving the bloodstream and urinary tract, is being caused by *Candida albicans*. *C. albicans* is emerging as important nosocomial pathogen with detectable biofilms formation on and in implanted devices. These studies will provide useful knowledge for novel approaches to the biofilm antifungal drug design.

1.2. Signaling through two-component systems

Two-component signaling systems couple extracellular stimuli to cellular responses. The information processing and transfer occurs via phosphorylation. The minimal signaling system consists of a sensor histidine kinase (HK) and its downstream partner, a response regulator (RR) protein. It is also referred to as a ñHis-Asp phosphorelay signal transduction systemò.

The HK catalyzes ATP-dependent autophosphorylation of its conserved histidine residue (within the HK dimerization domain) and then transfers phosphoryl groups to a conserved aspartate residue within the receiver domain of the RR protein

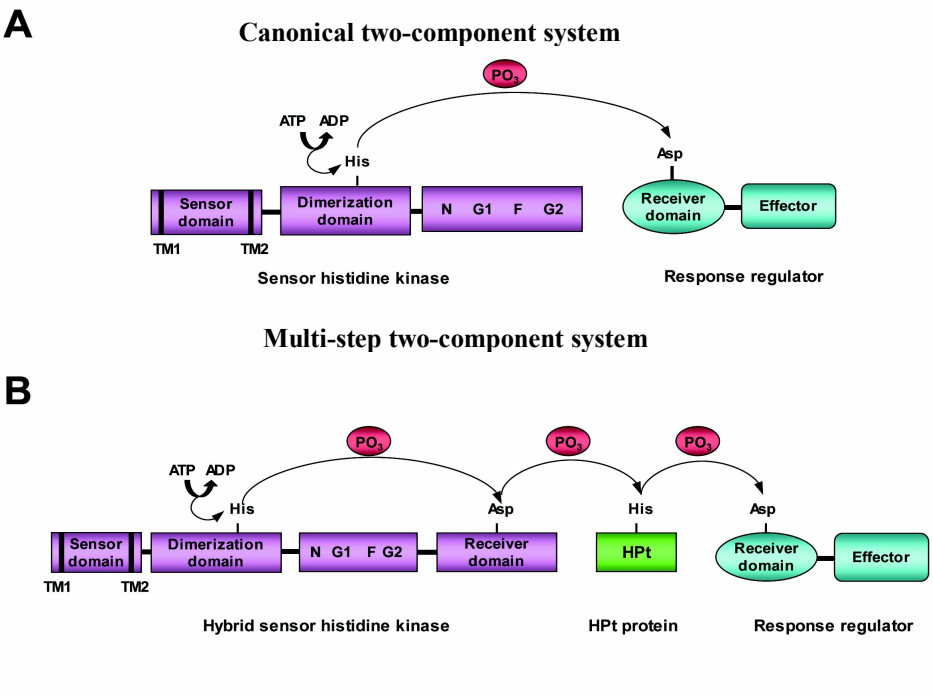

Figure 1-1. His-to-Asp Phosphotransfer Schemes. (A) A canonical two-component system consists of a membrane-bound HK and cytoplasmic RR protein. The HK is anchored to the membrane by transmembrane segments TM1 and TM2. Autophosphorylation of the HK requires ATP as a phosphoryl donor. The phosphoryl group is then transferred to an aspartic acid residue within the receiver domain of the RR. (B) A multi-step phosphorelay system typically contains a hybrid HK, which possesses a C-terminal receiver domain, a histidine-containing phosphotransfer (HPt) protein and an RR protein (Kaserer, West 2009).

(Figure 1-1A). Phosphorylation of the RR typically results in activation of the effector domain function, which commonly possesses DNA-binding activity resulting in transcriptional regulation of genes involved in output responses.

Expanded and more complex multi-step His-to-Asp phosphorelay systems also exist (Figure 1-1B). These consist of a hybrid HK with a C-terminal aspartate-containing phosphoreceiver domain, an essential histidine phosphotransfer (HPt) protein, and a downstream RR protein. The HPt protein functions as a histidine-phosphorylated intermediate and transfers phosphoryl groups between the hybrid HK and its cognate RR.

1.3. Histidine kinases

Signal transduction pathways involving a His-to-Asp phosphorelay regulate important cellular processes such as nutrient acquisition, adaptation to environmental stress, cell motility, development, virulence, and intercellular communication. HKs in particular, have become attractive targets for the development of novel antibacterial or antifungal drugs (Matsushita, Janda 2002; Stephenson, Hoch 2002; Chauhan, Kruppa *et al.,* 2007; Boisnard, Ruprich-Robert *et al.,* 2008; Chauhan, Calderone 2008).

1.3.1 Abundance and evolutionary diversity of HKs

Up to now, close to 905 bacterial genomes and 182 fungal genomes have been sequenced and made available to the public (http://www.ncbi.nlm.nih.gov/genomes/ lproks.cgi?view=1 and http://www.ncbi.nlm.nih.gov/genomes/ leuks.cgi). In a survey of the SENTRA database there are >11,228 predicted HK genes of prokaryotic signal transduction proteins (http://compbio.mcs.anl.gov/sentra/) (D'Souza, Glass *et al.,*

2006), of which as many as 25% are predicted to be hybrid HKs (Zhang, Shi 2005). Approximately 5700 of these HKs are fully annotated in a curated set of 202 prokaryotic organisms (Galperin 2005). Despite the large number of HKs that are found, they are unevenly distributed across microbial species. For example, the genome of *Streptomyces coelicolor* contains 95 HKs, *Vibrio cholerae* has 44 HKs, while *Fusobacterium nucleatum* has none (Galperin 2005). Very often HKs and their cognate RRs are encoded whether adjacent to each other or in the same operon. However, there are many "orphan" HK and RR genes that cannot be placed into a predictable TCS pathway. An *in vitro* phosphotransfer-profiling assay is an answer to this problem. The method was specifically developed to identify cognate HK, HPt or RR proteins on a proteome-wide basis that most likely would function together in a His-to-Asp phosphorelay system (Laub, Biondi *et al.,* 2007).

Phylogenetic analysis of HK proteins indicated a possible common origin with heat-shock protein Hsp90, type II topoisomerases and DNA-mismatch repair protein MutL (Dutta, Qin *et al.,* 1999; Koretke, Lupas *et al.,* 2000). HKs have diverged via gene family expansion, gene duplication, gene fusion/fission, domain gain/loss and domain shuffling (Alm, Huang *et al.,* 2006; Cock, Whitworth 2007). Some species have adapted by forming new combinations of signaling domains, while others have relied on horizontal gene transfer to produce a larger number of HKs at their disposal (Brinkman, MacFarlane *et al.,* 2001; Alm, Huang *et al.,* 2006). It appears that hybrid HKs evolved in bacteria in the manner of lateral recruitment of an aspartate-containing

receiver domain into an HK molecule, which then duplicated as one unit (Koretke, Lupas *et al.,* 2000). Interestingly, most if not all, of the HKs found in eukaryotic organisms are of the hybrid variety suggesting that hybrid HKs most likely originated in bacteria and were acquired by eukaryotes through horizontal gene transfer (Pao, Saier 1997; Koretke, Lupas *et al.,* 2000).

1.3.2 Sensory domains of HKs

Most histidine kinases exist as membrane-embedded dimeric proteins with N-terminal periplasmic sensory domain (as depicted in Figure 1-1) (Mascher, Helmann *et al.,* 2006). On the other hand, there are some transmembrane HKs, which do not possess an extracellular sensory domain and presumably are receptive to membrane-associated signals. In addition, there are HKs that are cytoplasmic proteins, which tether sensory domains to detect intracellular changes. Sensory domains were grouped according to their domain topology (Mascher, Helmann *et al.,* 2006). This type of classification explains their role in cell communication with environmental stimuli, stimuli perception and processing. It includes:

1) Periplasmic (or extracellular)-sensing HKs;
2) HKs with transmembrane helices (2-20 transmembrane regions involved in signal perception) lacking sensing domains and using membrane associated stimuli or membrane surface for direct signal perception;

3) Cytoplasmic-sensing HKs, implying membrane-anchored or soluble proteins with sensing domains inside the membrane.

Overall, sensory domains of HKs are extremely diverse not only in terms of sequence variability but also in terms of signals they perceive. The signal perception occurs by direct interaction between the sensory domain and a stimulant molecule. There are a number of other stimuli that can activate histidine kinases: chemical, mechanical or other. Still, for many HKs the exact stimulus remains unknown.

Recently, a number of three-dimensional structures of periplasmic and cytoplasmic sensory domains of HKs have been reported (Pappalardo, Janausch *et al.,* 2003; Reinelt, Hofmann *et al.,* 2003; Neiditch, Federle *et al.,* 2006; Cheung, Hendrickson 2009). Although each of these bind to different ligands, interestingly, several are structurally related to the PAS (Period-ARNT-Single-minded) domain superfamily of prokaryotic and eukaryotic ligand-binding light, oxygen, and redox sensing modules (Taylor, Zhulin 1999).

PAS domains have been found in almost 2000 sensor kinases (Letunic, Copley *et al.,* 2006). They are present in enzymes, transcription factors, ion channels *etc* and belong to all three kingdoms of life (Taylor, Zhulin 1999). The domains share approximately 110 amino acids which constitute the α/β fold. They are able to interact with other protein domains via surface-exposed central β-sheet. These domain/domain interactions can modulate kinase activity by perturbing the arrangement of the core HK domains (catalytic and dimerization domains) within the protein (Lee 2008).

1.3.3 HK core domains

Based upon their domain organization all HKs are divided into two major classes: class I and class II (Bilwes, Alex *et al.,* 1999).

Class I HK family is represented by EnvZ protein which contains an N-terminal periplasmic sensor domain, a transmembrane domain and a core kinase domain consisting of the catalytic domain and dimerization domain. In class I HKs the phosphorylatable histidine residue, part of the H-box sequence motif, is located in the dimerization domain His-box and is directly linked to the catalytic domain comprising the unique conserved set of sequence motifs designated as N, G1, F and G2 boxes (Figure 1-2). These conserved sequences are essential for Mg^{2+} and ATP-binding. Furthermore, residues in the F and G2 boxes constitute part of a ñlidò that closes upon nucleotide binding (Bilwes, al. 2001; Marina, Mott *et al.,* 2001).

The class II HK family, represented by the CheA protein, possesses a different domain organization. The H-box is secluded from the ATP-binding domain and resides in the phosphotransfer (HPt) domain located at the N-terminus of the kinase. It is followed by a dimerization domain and ATP-binding domain similar to class I HKs.

Structural information for the class II HK ATP-binding core domain was first determined for CheA from *Thermatoga maritima* (Parkinson, Kofoid 1992). One of the major advances in recent years was the crystal structure determination of the entire cytoplasmic portion of the histidine kinase HK853 from *Thermatoga maritima* (Figure 1-3) (Marina, Waldburger *et al.,* 2005). In the dimeric structure, the ATP-binding

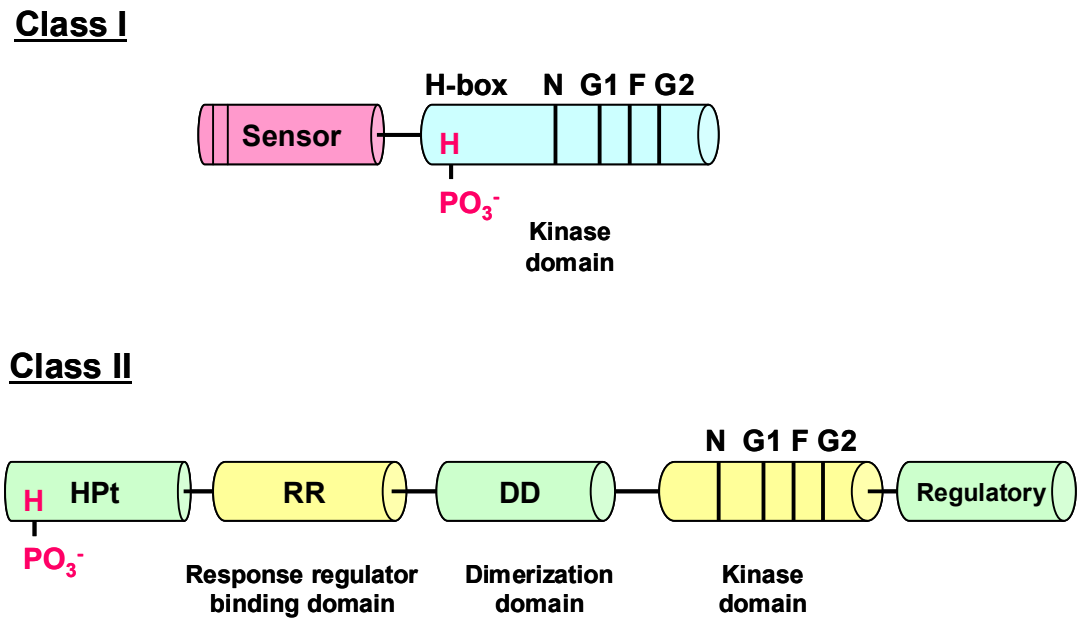

Figure 1-2. Class I and Class II histidine kinases. Schematic diagram of two classes of HKs. Figure adapted from (Bilwes, Alex *et al.,* 1999; Dutta, Qin *et al.,* 1999).

catalytic domains flank the central histidine-containing helical hairpin dimerization domains. During catalysis, the ATP-binding domain of one monomer *trans*-phosphorylates the H- box of the opposite subunit. This would necessitate significant conformational changes during catalysis in which the flexible hinge regions between these two domains are predicted to play an important role and emphasizes the importance of interdomain contacts (Marina, Waldburger *et al.,* 2005).

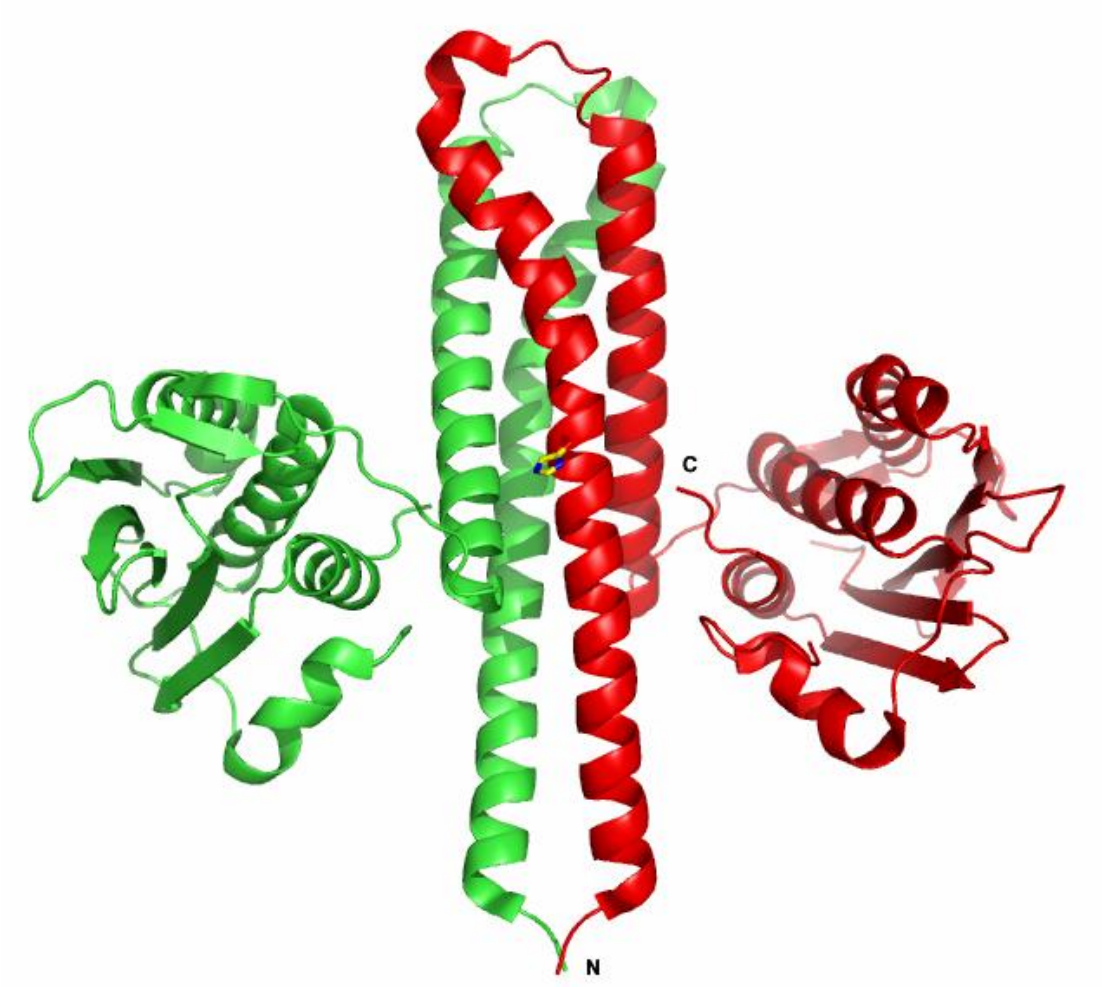

Figure 1-3. Crystal structure of the histidine kinase HK853 from *Thermatoga maritima*. Ribbon representation of the entire cytoplasmic portion of HK853, which includes an N-terminal His-containing dimerization domain and C-terminal catalytic core domain. ATP binds to the α/β "wing" domains that flank the central four-helix bundle. The side chain for the conserved histidine (His260) residue is shown in stick representation.

1.3.4 Signaling through the membrane

The mechanism of signal propagation of HKs remains elusive. Upon ligand binding, bacterial chemoreceptors undergo subtle changes which involve subsequent participation of specific helices. These helices were discovered in 1994 by Inouye and coworkers as ñlinker regionsò (Jin, Inouye 1994) and specified as ñHAMPò domain by Aravind and Ponting in 1999 (Aravind, Ponting 1999). Despite its low sequence homology, it is present in bacteria, fungi, plants and protists, compiling about one-fifth of all HK proteins and sharing a helix-turn-helix conformation according to secondary structure predictions.

The HAMP domain consists of two amphipathic helices (AS1 and AS2) connected by a long loop adopting a four-helix bundle conformation in the dimerized HK, placing two AS2s adjacent to each other and two AS1s further apart (Singh, Berger *et al.,* 1998; Appleman, Stewart 2003; Zhu, Inouye 2004). Mutational analysis of HAMP domain AS2 resulted in reversed-response phenotype and defective or constitutive HK activation for AS1 and AS2, revealing the importance of the HAMP domain as a negative regulator for output HK domain activity (Butler, Falke 1998; Appleman, Stewart 2003). The NMR structure of a HAMP domain from the Af1503 protein of *Archaeoglobus fulgidus* was recently solved by Hulko *et al.* (Hulko, Berndt *et al.,* 2006). The Af1503 protein forms a homodimer with a unique parallel four-helical coiled-coil structure and unusual interhelical packing that suggests two distinct packing geometries are possible.

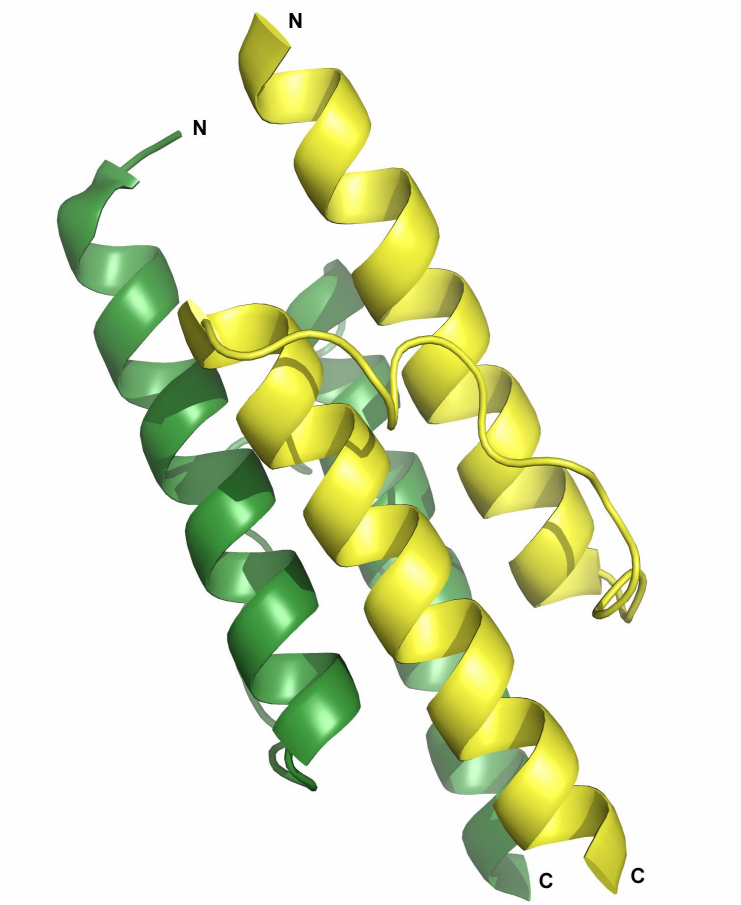

Figure 1-4. The HAMP domain from the Af1503 protein of *Archaeoglobus fulgidus*. A schematic ribbon side view of the HAMP domain dimer (Stock, Stock *et al.,* 1990; Kosinsky, Volynsky *et al.,* 2004). Monomers are in yellow (α1) and in green (α2). The helices of the HAMP domain have typical coiled-coil crossing angles of 3°ï 13° within a monomer and 10°ï 15° relative to the central axis of the bundle.

Additional data support a helical rotational model in which adjacent helices can interconvert between two possible packing modes rotating 26° between ñonò and ñoffò

conformations to facilitate signal transmission to and from the HAMP domain (Figure 1-4).

However an alternative model of HAMP function was earlier put forward by Williams and Stewart (Williams, Stewart 1999) implying direct interaction of AS1 with AS2 or its interaction with cell membrane. Undoubtedly, HAMP domains have a flexible structural organization and might play multiple roles in facilitating transmembrane signal propagation for diverse types of receptors.

1.3.5 Histidine phosphorylation and regulation of HKs

Phosphorylation of the conserved histidine residue in HKs leads to the creation of a high-energy phosphoramidate (N-P) bond. Solution studies of phosphohistidine residues show that it is stable only at high pH values and undergoes rapid hydrolysis (Klumpp, Krieglstein 2002). Hydrolysis of the phosphohistidine molecule is accompanied by the release of around 40 kJ/mol for the free amino acid and around 55 kJ/mol for the residue within a protein (Inouye, Duttu *et al.,* 2003). Thus, chemically, a phosphorylated histidine is very unstable in comparison with Ser, Thr, and Tyr phosphoamino acids, which form a relatively stable phosphoester bond (Hoch, Silhavy 1995).

The events leading to histidine autophosphorylation of an HK is relatively complex and involves the coupling of a series of steps. The HK sensory domain must first accept input signals that in turn somehow modulate the rate of kinase

autophosphorylation. Ligand-binding to the sensory domain presumably induces a conformational change that is transmitted through the membrane to the cytoplasmic kinase domain, often through a HAMP domain linker region. Domain-domain interactions clearly are an important key to understanding signal transmission and regulation of HKs.

In a simple two-component signaling scheme, phosphoryl groups are transferred from an HK to an RR. However, some HKs also affect the rate of dephosphorylation of their cognate RRs. Two alternative models have been put forth to explain how external environmental signals regulate these two opposing functions of HKs, *i.e.* both kinase and phosphatase activities of the cytoplasmic domain (Gao, Mack *et al.,* 2007). The first model, the so-called switch model, proposes a simple ñonò or ñoffò mode of the cytoplasmic domain. The other, the rheostat model, suggests that the ratio of the opposing activities is controlled by the external signal. Hence, the balance between kinase and RR phosphatase activity is affected by external stimuli. For example, when the rate of histidine autophosphorylation is high, the balance shifts predominantly towards the phosphotransfer reaction and RR phosphorylation. When the rate of histidine autophosphorylation is low, the equilibrium shift favors RR phosphatase activity (Gao, Mack *et al.,* 2007).

1.4. Response regulator proteins

HKs transmit environmental signals to cytoplasmic response regulator (RR) proteins, which in turn control signal output responses. Most bacterial RRs have a two-domain architecture with a conserved N-terminal regulatory domain (also called a receiver domain) that controls the function of a variable C-terminal effector domain. In many cases, the RR serves as a transcriptional regulator by virtue of a C-terminal DNA-binding domain. According to phylogenetic analysis, these types of RRs can be divided into major subfamilies: OmpR/PhoB, NarL/FixJ, NtrC/DctD and LytTR, ActR, YesN of which the OmpR/PhoB subfamily accounts for almost 30% of all RRs (West, Stock 2001; Galperin 2006).

1.4.1 RR diversity and classification

Recent studies identified around 9000 RRs in bacterial and archaeal genome databases (Mayover, Halkides *et al.,* 1999; D'Souza, Glass *et al.,* 2006). However, many of these RRs are not characterized and their regulatory functions are yet to be defined. Although most of the RRs are encoded in the genome in close proximity with their HKs, many of them are located discretely, making it difficult to find their true partners. Furthermore, some of the HKs interact with more then one RR or multiple HKs interact with one RR creating branched networks and implicating potential cross-talk among the pathways. Phosphotransfer profiling and phenotype microarray analysis were recently established to facilitate identification of cognate HK-RR

partners uncovering new pathways for characterization (Zhou, Lei *et al.,* 2003; Laub, Biondi *et al.,* 2007).

With the advent of the large-scale genomic sequencing, many new RRs were discovered and studied. Close to 17% of all RRs constitute single domain proteins, such as the chemotaxis protein CheY and Spo0F that signal to effector proteins via protein-protein interactions. The rest of the RRs are classified according to their effector domain sequence similarity: DNA-binding domains, enzymatic, protein-protein interactions and RNA-binding domains (Figure 1-5) (Gao, Mack *et al.,* 2007; Laub, Biondi *et al.,* 2007). Another approach for organizing RRs in the OmpR subfamily from *B. subtilis* and *E. coli* is to classify them on the basis of their surface interfaces (Kojetin, Thompson *et al.,* 2003). Despite only 20-30% amino acid sequence identity, the regulatory domain of RRs all share a dynamic conserved $(\beta\alpha)_5$ fold (West, Stock 2001; Gao, Stock 2009). The active site of RRs is composed of several carboxylate-containing amino acids that coordinate an essential Mg^{2+} ion and a highly conserved lysine residue. Residues that constitute the interface surface between HK and the receiver domain of the RRs were taken into account and classified into three major types (Kojetin, Sullivan *et al.,* 2007):

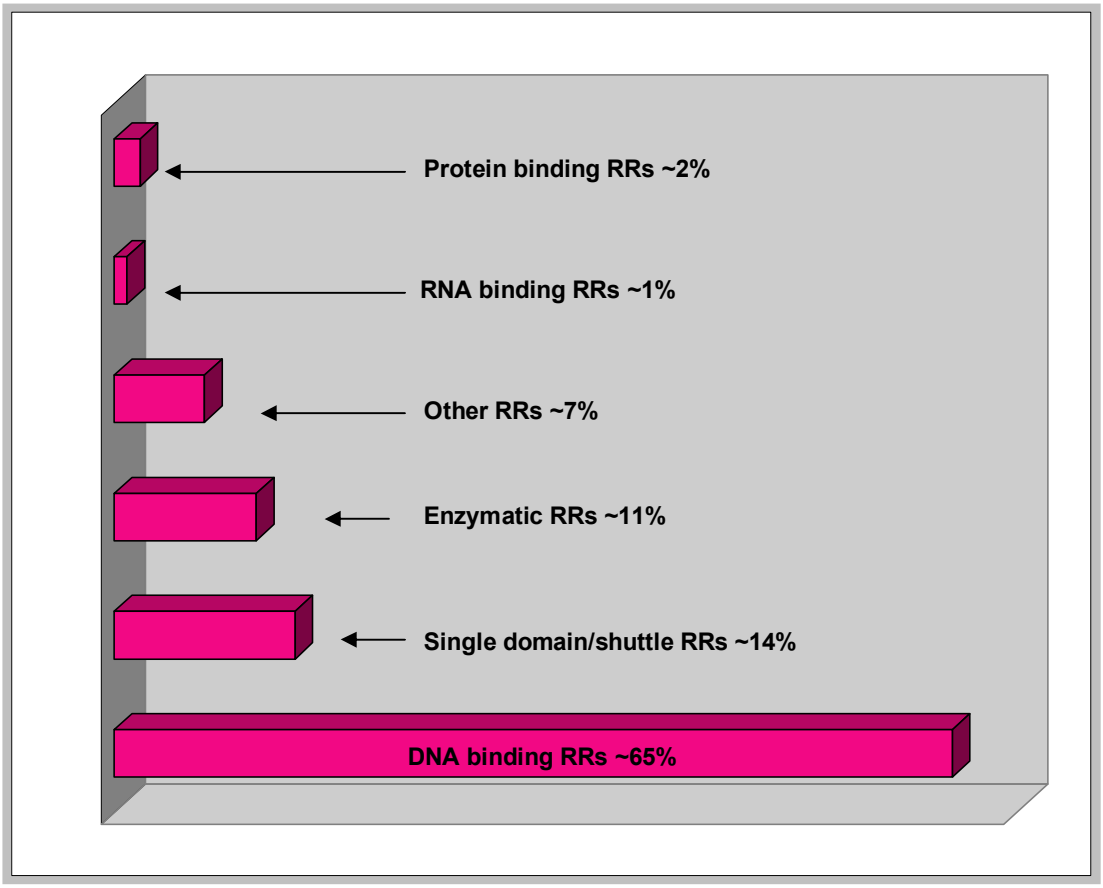

Figure 1-5. Classification of bacterial RRs. Classification is done according to the RRs effector domains and 9000 RRs is taken as a 100% value (Gao, Mack *et al.,* 2007).

a) conserved catalytic residues directly involved in phosphotransfer;

b) tethering residues, creating broad orientational contacts for catalysis;

c) recognition residues, providing correct HK-RR interaction.

Using a comparative modeling approach, Kojetin and colleges categorized the OmpR subfamily onto six subclasses (A-F) based on the existing conserved hydrophobic

interfaces of the α-helix 1 and α-helix 1/α-helix 5, taking into account individual side-chain composition, residue clustering and relative amino acid localization (Fabret, Feher *et al.,* 1999; Kojetin, Sullivan *et al.,* 2007).

1.4.2 Receiver and effector domains activities

A typical RR consists of two domains, a C-terminal effector domain, and an N-terminal domain referred to as a regulatory or receiver domain. The receiver (α/β) domain comprises three major activities such as phosphotransfer, regulation of effector domain function and autodephosphorylation. RRs regulate a variety of output responses. Their regulatory domain structures are conformationally dynamic, allowing modulation of the effector domain activities or direct interaction with other protein partners during phosphotransfer. These domains catalyze phosphoryl group transfer from the histidine residue of the HK onto a conserved aspartate residue within the RR protein.

The regulatory domains of RRs are enzymatically active and capable of catalyzing not only phosphotransfer from phospho-His of the HKs to its own Asp residue, but also autophosphorylation using small molecule phosphodonors (Lukat, McCleary *et al.,* 1992; McCleary, Stock 1994). However, the transfer of phosphoryl groups from a cognate HK is far more efficient. Small molecule phosphodonors are represented by acetyl phosphate, phosphoramidate and carbamoyl phosphate. Acetyl phosphate is the high-energy acid/base-labile intermediate of the reversible acetate

kinase-phosphotransacetylase pathway in *E. coli* (Klein, Shulla *et al.,* 2007). It has been shown that CheY, OmpR and PhoB response regulators can be phosphorylated by acetyl phosphate *in vitro* and the sensor kinase EnvZ is capable of activating PhoB response regulator using acetyl phosphate *in vivo* (Lukat, McCleary *et al.,* 1992; McClearly, Stock 1994; Hiratsu, Nakata *et al.,* 1995; Kim, Wilmes-Riesenberg *et al.,* 1996). In addition, intracellular concentrations of acetyl phosphate in *E. coli* are sufficient for direct phosphorylation of response regulators which led to a suggestion that this small molecule phosphodonor can trigger global signal propagation by directly affecting the activation state of at least one global RR (Klein, Shulla *et al.,* 2007). However, a major role of this metabolite in catalyzing RR receiver domain autophosphorylation is yet to be determined.

Additional characteristics of RR receiver domains include modulation of the effector domain activity and autodephosphorylation. The autodephosphorylation of the conserved Asp can vary from one RR to another ranging from seconds to hours depending on the specific system it belongs to. The mechanism of RR dephosphorylation has been considered as a phosphatase reaction with water or hydroxide molecule substituting the histidine imidazole side chain (Lukat, Lee *et al.,* 1991).

A lot of research has been also carried out to elucidate the mechanism by which RR receiver domains modulate the activity of their effector domains (Stock, Robinson *et al.,* 2000; Stock, Da Re 2000). The direct regulation of the effector

domains upon phosphorylation of the receiver domains has been shown in detail for the methylesterase CheB and transcription factor NarL. The CheB receiver domain phosphorylation relieves inhibition of its methylesterase domain allowing access to the catalytic triad, while phosphorylation of NarL disrupts the interdomain interface exposing DNA-binding residues of the effector domain (Anand, Goudreau *et al.,* 1998; Djordjevic, Goudreau *et al.,* 1998; Eldridge, Kang *et al.,* 2002). For these two RRs, intermolecular changes within the receiver domains lead to two discrete forms of effector domain activation upon phosphorylation.

Effector domains, on the other hand, mediate the outcome responses of the signaling systems. Most effector domains of the prokaryotic two-component systems are transcriptional activators or repressors, capable of DNA binding or direct interaction with transcriptional machinery and its components. In contrast, eukaryotic two-component systems effector domains mainly possess enzymatic activity or regulate signaling activities through protein-protein interactions (Chang, Stewart 1998; Loomis, Kuspa *et al.,* 1998; West, Stock 2001).

1.4.3 Activation and phosphorylation of RRs

The phosphorylated lifetime of the conserved Asp can vary from one RR to another, presenting an obstacle to their characterization in active conformation. To elucidate the mechanism of RRs activation by phosphorylation and capture RRs in their active state a variety of biochemical approaches has been used in the past decade:

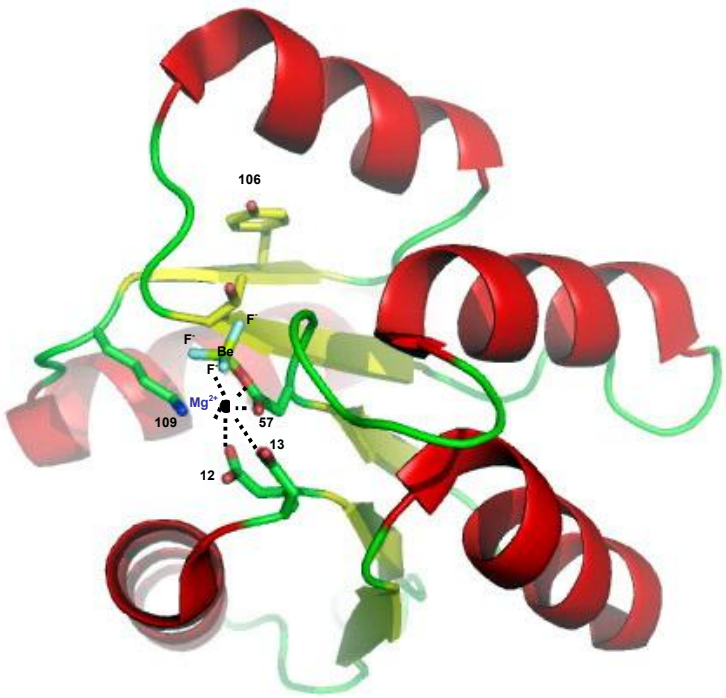

Figure 1-6. The crystal structure of the CheY- $BeF_3^-$$Mg^{2+}$-FliM peptide complex from *E.coli*. A ribbon diagram of the activated RR CheY bound to Mg^{2+} and BeF_3^-. Mg^{2+} has an octahedral coordination, BeF_3^- comprises tetrahedral coordination. Mg^{2+} interacts with Asp12, Asp13, the backbone of Asn59, one of the fluorine atoms and a water molecule as the sixth ligand. Two other fluorine atoms are hydrogen bonded to Thr87 and Asn89.

protein NMR, synthesis of phosphono-analogs, removal of metal ions to reduce the rate of RR dephosphorylation, utilization of the stable acyl phosphates from *Thermatoga maritima* and utilization of phosphate analogs (BeF_3^-) (Halkides, Zhu *et*

al., 1998; Birck, Mourey *et al.,* 1999; Kern, Volkman *et al.,* 1999; Lewis, Brannigan *et al.,* 1999; Yan, Cho *et al.,* 1999).

Receiver domains of RRs undergo conformational changes upon phosphorylation. The crystal structure of the CheY- BeF_3^--Mg^{2+}-FliM peptide complex offered new insights into the active form of the single domain RR CheY (Figure 1-6) (Lee, Cho *et al.,* 2001). The active site of the CheY RR, located in a structurally conserved $(\alpha/\beta)_5$ domain, comprises of a cluster of acidic residues: Asp12, Asp13 (α1-β1 loop ï metal binding site) and Asp57 (β3 - site of phosphorylation). It is also surrounded by other conserved residues (Thr87 in β4, Lys109 and Tyr106 in β5) participating in the conformational changes which accompany phosphorylation. Upon phosphorylation, positioning of the Thr87 residue undergoes significant perturbations along with the flipped ñoutwardò to an ñinwardò orientation of the Tyr106 residue. Residue Lys109 directly interacts with phosphate (BeF_3^-). A majority of displacements within RRs are limited to the α4-β4-α5 face of the protein and range from 1 to 6 Å for different regulatory domains (Robinson, Buckler *et al.,* 2000; Stock, Robinson *et al.,* 2000).

The phosphorylated and unphosphorylated forms of the receiver domains can represent the active conformations of the RRs. Several studies have shown an existence of the equilibrium between phosphorylated and unphosphorylated forms of the proteins (Kern, Volkman *et al.,* 1999; Simonovic, Volz 2001; Volkman, Lipson *et al.,* 2001). This information allowed developing of the ñtwo-stateò activation model

for RRs which described the concurrent existence of active and non-active conformations of the RRs in equilibrium. According to this model, phosphorylation or protein-protein interactions would shift the equilibrium towards the active conformation of the RRs.

1.4.4 Structures of RRs

There have been major advances in the structural characterization of RR proteins in recent years. More than a dozen RR receiver domain structures have been solved: CheY, Spo0F, NtrC, NarL, CheB, FixJ, PhoB and many others (Volz, Matsumura 1991; Volkman, Nohaile *et al.,* 1995; Baikalov, Schröder *et al.,* 1996; Madhusudan, Zapf *et al.,* 1996; Djordjevic, Goudreau *et al.,* 1998; Birck, Mourey *et al.,* 1999; Sola, Gomis-Rüth *et al.,* 1999).

Some of the activated RRs are determined in large part due to the use of the phosphoryl analog, beryllium fluoride or other phosphoryl mimics. Comparison of the activated and inactive conformations of RRs showed subtle conformational rearrangements within the protein molecule leading to its stabilization (Lee, Cho *et al.,* 2001). In addition, structures of complexes between RRs and their signaling partners have begun to emerge (Varughese, Tsigelny *et al.,* 2006; Yamada, Akiyama *et al.,* 2006; Zhao, Copeland *et al.,* 2008).

1.5. HPt domains

1.5.1 HPt domain discovery

Canonical two-component signaling system consists of a sensor histidine kinase and its downstream partner, a response regulator protein. However, more complex systems, multi-step phosphorelays, also exist consisting of a hybrid HK, an essential histidine phosphotransfer (HPt) protein, and a downstream RR protein. The HPt protein functions as a histidine-phosphorylated intermediate (or alternative transmitter) and transfers phosphoryl groups between the hybrid HK and its cognate RR, playing a crucial role in the His Ÿ Asp Ÿ His Ÿ Asp phosphorelay (Appleby, Parkinson *et al.,* 1996).

The HPt containing protein, ArcB, from *E. coli* was discovered in 1994 by Ishige and colleges (Ishige, Nagasawa *et al.,* 1994). ArcB is a hybrid histidine kinase consisting of a histidine kinase domain, and receiver domain followed by an HPt domain. The ArcB C-terminal region, containing His-717, was shown to be phosphorylatable *in vitro* and serve as a supplementary transmitter domain for the RR ArcA phosphorylation (Tsuzuki, Ishige *et al.,* 1995).

Many HPt proteins has been discovered since then, most of which participate in His Ÿ Asp phosphorelay systems (Appleby, Parkinson *et al.,* 1996; Inouye 1996; Mizuno 1998). The analysis of the *E.coli* genome uncovered four more hybrid kinases, containing HPt domains: BarA, EvgS, TorS and YojN (Mizuno 1997). Further studies identified HPt domains and HPt proteins in other organisms such as *B. pertussis*

(BvgS), *B. subtilis* (Spo0B), *S. cerevisiae* (YPD1) and *A. thaliana* (AHP1, AHP2 AHP3) *etc* (Arico, Miller *et al.,* 1989; Burbulys, Trach *et al.,* 1991; Maeda, Wurgler-Murphy *et al.,* 1994; Uhl, Miller 1996; Suzuki, Imamura *et al.,* 1998). The amount of HPt containing proteins and their distribution among different species demonstrate an important role these mediators play within multi-step phosphorelay systems.

1.5.2 HPt structures – ArcB and YPD1

Most of the prokaryotic HPt domains are part of the hybrid histidine kinases, whereas eukaryotic HPts evolved to function as separate proteins. The HPt domains/proteins are hard to recognize in the genome sequence databases since the amino acid composition of these domains/proteins is variable and relatively short. However, the central phosphorylated His residue remains invariant surrounded by a set of conserved amino acids aiding in HPt recognition (Xu, West 1999).

The X-ray structure of ArcB-HPt domain was determined to a resolution of 2.06 Å using multiple isomorphous replacement method (Kato, Mizuno *et al.,* 1997). It consists of about 120 amino acids organized into six anti-parallel α helices. The domain has elongated shape with dimensions 30 x 30 x 45 Å. Four of the six helices are packed into a coiled-coil arrangement with a sterically close-packed hydrophobic core in the center, the so-called ñfour-helix bundleò. The bundle is arranged in an up-down-up-down topology with left-handed twist (Figure 1-7).

The site of phosphorylation His-715 is located on the surface of the αD helix. Conserved residues Glu-714, Lys-718, Lys720 and Gln-736, Gln-739 are located in close proximity on the αD helix and C-terminus of the αE helix. It was shown (Kato, Mizuno *et al.,* 1997) that the αD and αE helices regions constitute the most conserved area of ArcB HPt domain. This region has a 20% identity with the HPt protein YPD1 from *S. cerevisiae.*

The structure of YPD1 protein, a HPt protein of the SLN1-YPD1-SSK1 multi-step phosphorelay system from *S. cerevisiae,* is very similar to that of the C-terminal ArcB HPt domain. Like ArcB, YPD1 forms a four-helix bundle with a sterically close-packed hydrophobic core in the center. The crystal of YPD1 protein was obtained by hanging-drop diffusion method and the structure was solved to a resolution of 2.7 Å using multiple isomorphous replacement and anomalous scattering methods by the West group (Xu, Nguyen *et al.,* 1999; Xu, West 1999). Another group also independently solved YPD1 structure to a resolution of 1.8 Å (Song, Lee *et al.,* 1999).

The YPD1 protein has an elongated shape with dimensions 30 x 30 x 60 Å. The site of phosphorylation, His 64, is located on the surface of helix αC. Compared to ArcB, YPD1 contains an extended loop stretching from the αD helix and reaching the αG helix of the

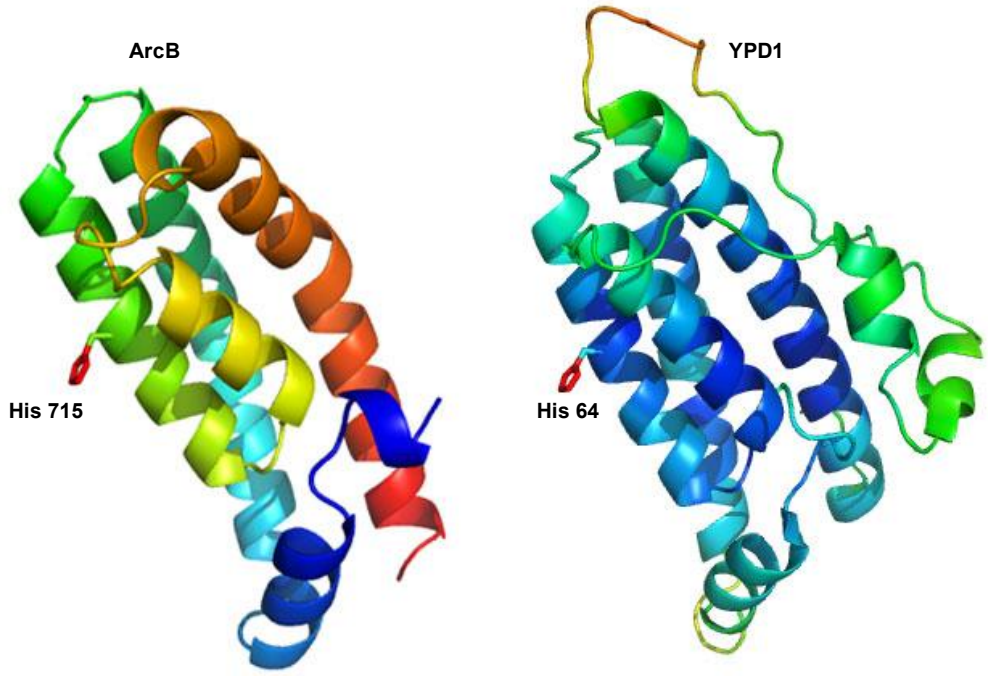

Figure 1-7. The crystal structure of ArcB HPt domain from *E.coli* and YPD1 from *S. cerevisiae.* A ribbon diagram of both the ArcB HPt domain (left) and YPD1 HPt protein (right). The site of phosphorylation for ArcB is His 715 and the site of phosphorylation for YPD1 is His 64 (Kato, Shimizu *et al.,* 1999; Xu, West 1999).

bundle. The response regulator binding site is formed between His64 and the αA helix comprised mostly of hydrophobic residues creating a common docking site for SSK1 and SKN7 response regulators (Porter, West 2005). Finally, the response regulator binding specificity was proposed to occur through interactions at the hydrophobic docking site concentrated within the non-conserved residues of the β4ï α4 and β5ï α5 loops (Porter, West 2005). The crystal structure of the SLN1-RR·YPD1 complex and

BeF_3^- activated SLN1-RR·YPD1 complex, solved by the members of the West group in 2003 and 2008 (Xu, Porter *et al.,* 2003; Zhao, Copeland *et al.,* 2008), provided detailed insight into molecular recognition between a RR and HPt protein. Several hydrophobic residues located along α1 of the response regulator SLN1-RR and several loops surrounding active site such as β1ï α1, β3ï α3 and β4ï α4 mainly constitute the binding interface of the SLN1-RR forming interactions with αA, αB and αC of YPD1 (Zhao, Copeland *et al.,* 2008).

1.6. Multi-step two-component system in *Saccharomyces cerevisiae*.

The multi-step phosphorelay system from *Saccharomyces cerevisiae* was one of the first identified and is one of the best characterized eukaryotic system. It is responsible for cellular adaptation to osmotic, oxidative and other environmental stresses (Blomberg, Adler 1989; Mager, Varela 1993; Ota, Varshavsky 1993; Albertyn, Hohmann *et al.,* 1994; Brown, Bussey *et al.,* 1994; Maeda, Wurgler-Murphy *et al.,* 1994; Posas, Wurgler-Murphy *et al.,* 1996; Hohmann 2002). The branched pathway consists of a hybrid histidine kinase SLN1, a histidine-containing phosphotransfer (HPt) protein YPD1, and two independent response regulator proteins, SSK1 and SKN7 (Figure 1-8).

The *SLN1* gene encodes a transmembrane sensor kinase with histidine kinase and aspartate transferase activities. It was discovered as a synthetically lethal allele with *ubr1*Δ, encoding the recognition component of the N-end-rule ubiquitin system

(Ota, Varshavsky 1992). SLN1 possess an extracellular domain and two transmembrane domains like some bacterial sensor kinases (Ostrander, Gorman 1999). The architecture of the SLN1 protein differs from the typical bacterial sensor kinase by the unconventional fusion of a sensor kinase and a response regulator module. The hybrid histidine kinase exists as a dimer in the yeast membrane and autophosphorylates in *trans* via cytosolic ATP (Maeda, Wurgler-Murphy *et al.,* 1994; Posas, Wurgler-Murphy *et al.,* 1996). The sites of phosphorylation are His576 for histidine kinase domain and Asp1144 for response regulator domain (Maeda, Wurgler-Murphy *et al.,* 1994). The phosphorylation of response regulator domain leads to the subsequent transfer of the phosphoryl groups to the downstream HPt protein YPD1. The crystal structure of the SLN1-RRÅYPD1 complex in active and inactive conformations was solved by the members of the laboratory (Chooback, West 2003; Xu, Porter *et al.,* 2003; Zhao, Copeland *et al.,* 2008).

It has also been shown that the SLN1 kinase monitors changes in turgor pressure caused by hyperosmotic stress, and that its activity is independently affected by the presence/absence of specific outer cell wall proteins (Reiser, Raitt *et al.,* 2003; Shankarnarayan, Malone *et al.,* 2008).

The HPt protein YPD1 is involved in mediating transfer of the phosphoryl group from the transmembrane HK SLN1 to response regulator proteins SSK1 and SKN7 (Posas, Wurgler-Murphy *et al.,* 1996; Li, Ault *et al.,* 1998).

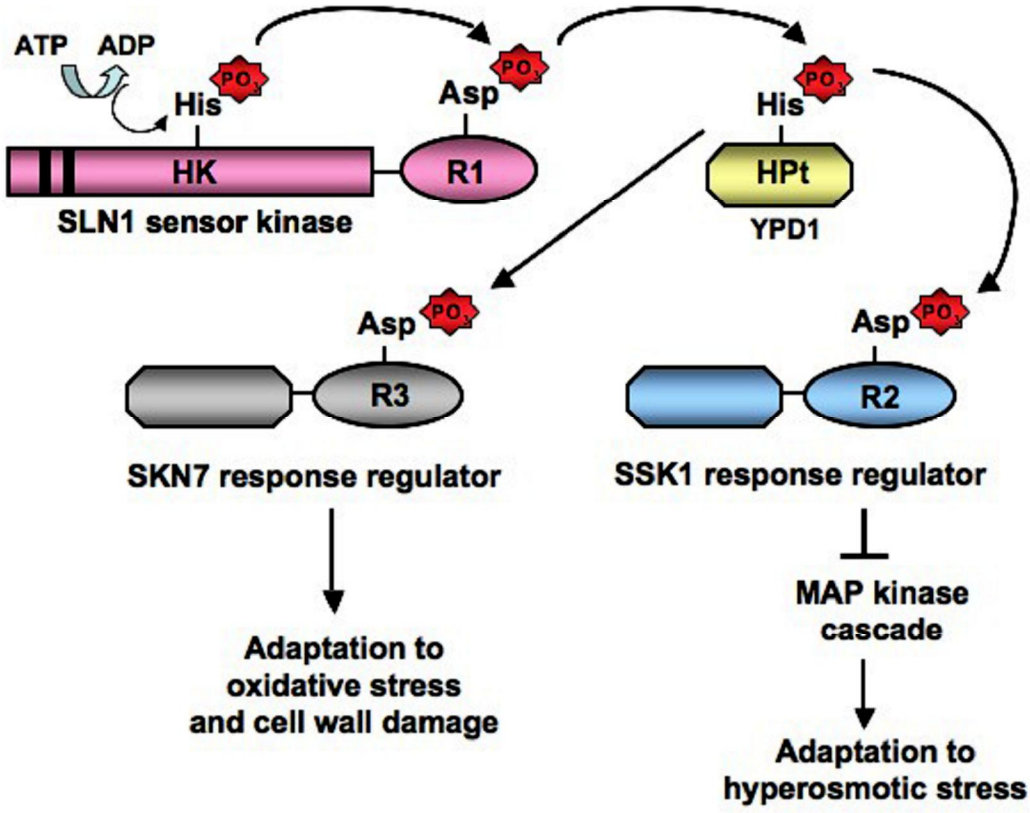

Figure 1-8. Multi-step phosphorelay signaling pathway in *S. cerevisiae*. Components of the system are: SLN1- hybrid sensor kinase, YPD1-histidine phosphotransfer protein, SSK1/SKN7-response regulator proteins. Under normal conditions phosphotransfer occurs from SLN1 to SSK1, under non-osmotic conditions, unphosphorylated SSK1 activates the MAP kinase cascade.

SKN7 is one of the RRs of the multi-step phosphorelay. It has an atypical domain organization in that the DNA binding domain is located at the N-terminus and the response regulator domain is located at the C-terminus. The SKN7 response regulator is involved in different cellular processes: oxidative stress (Morgan, Banks *et*

al., 1997; Li, Ault *et al.,* 1998; Raitt, Johnson *et al.,* 2000) and cell wall damage (Brown, North *et al.,* 1993; Morgan, Bouquin *et al.,* 1995). During adaptation to oxidative stress SKN7 regulates transcription of TRX2, SSA1 and heat-shock like genes in a phosphorylation-independent manner (Li, Ault *et al.,* 1998; Raitt, Johnson *et al.,* 2000). The mechanism of this regulation is not known. On the other hand regulation of the response to the cell wall damage requires SKN7 phosphorylation leading to OCH1 gene activation (Li, Dean *et al.,* 2002).

The domain organization of SSK1 is similar to SKN7 and consists of the response regulator domain at the C-terminus and a putative effector domain at the N-terminal end, but is devoid of DNA-binding activity. Phosphorylation of SSK1 negatively regulates a downstream MAP kinase cascade. Only under hyperosmotic conditions the unphosphorylated SSK1 protein can activate downstream target genes by direct binding to the first members of the MAP kinase cascade SSK2/SSK22, redundant MAP kinase kinase kinases (Maeda, Wurgler-Murphy *et al.,* 1994; Posas, Saito 1998; Posas, Takekawa *et al.,* 1998; Horie T., Tatebayashi K. *et al.,* 2008). These two kinases activate the MAP kinase kinase PBS2 (Maeda, Takekawa *et al.,* 1995; Posas, Saito 1997). PBS2 in turn activates HOG1, the final MAP kinase in this pathway. Phosphorylated HOG1 migrates into the nucleus where it interacts with different transcription factors and regulates the expression level of the *GPD1* gene (glycerol-3 phosphate dehydrogenase) and other genes, which leads to the production of glycerol (Albertyn, Hohmann *et al.,* 1994; Ferrigno, Posas *et al.,* 1998; Madhani, Fink 1998;

Posas, Saito 1998). The two-component signal transduction in the yeast *S. cerevisiae* uses two mechanisms for signal transduction: the histidine-aspartate phosphorelay mechanism commonly observed in bacteria and the serine/threonine/tyrosine phosphorylated MAP kinase cascade typically found in eukaryotes.

1.7. Pathogenic yeast - *Candida albicans*

Candida albicans is a pathogenic yeast of both clinical and research interest. A crucial feature of this microorganism is its versatility. The organism has the ability to invade kidney, liver, and brain (Calderone 2002; Soll 2002; Romani, Bistoni *et al.,* 2003). In some patient groups, whose defense system is severely compromised (AIDS patients, prematurely born infants, leukemics and burn patients), *Candida* turns into a deadly pathogen causing systemic infections with mortality rate as high as 50% (Wenzel 1995). The incidence of such infections is rapidly increasing. *Candida* species are fourth in frequency among all microorganisms isolated from blood samples in US hospitals and fourth in causing nosocomial infections (Calderone 2002). Furthermore, oropharyngeal candidiasis occurs in approximately 70% of patients with AIDS, ~70% of all women will experience at least one episode of vaginitis caused by *Candida albicans* and ~ 20% will experience recurrent disease (Calderone 2002; Soll 2002).

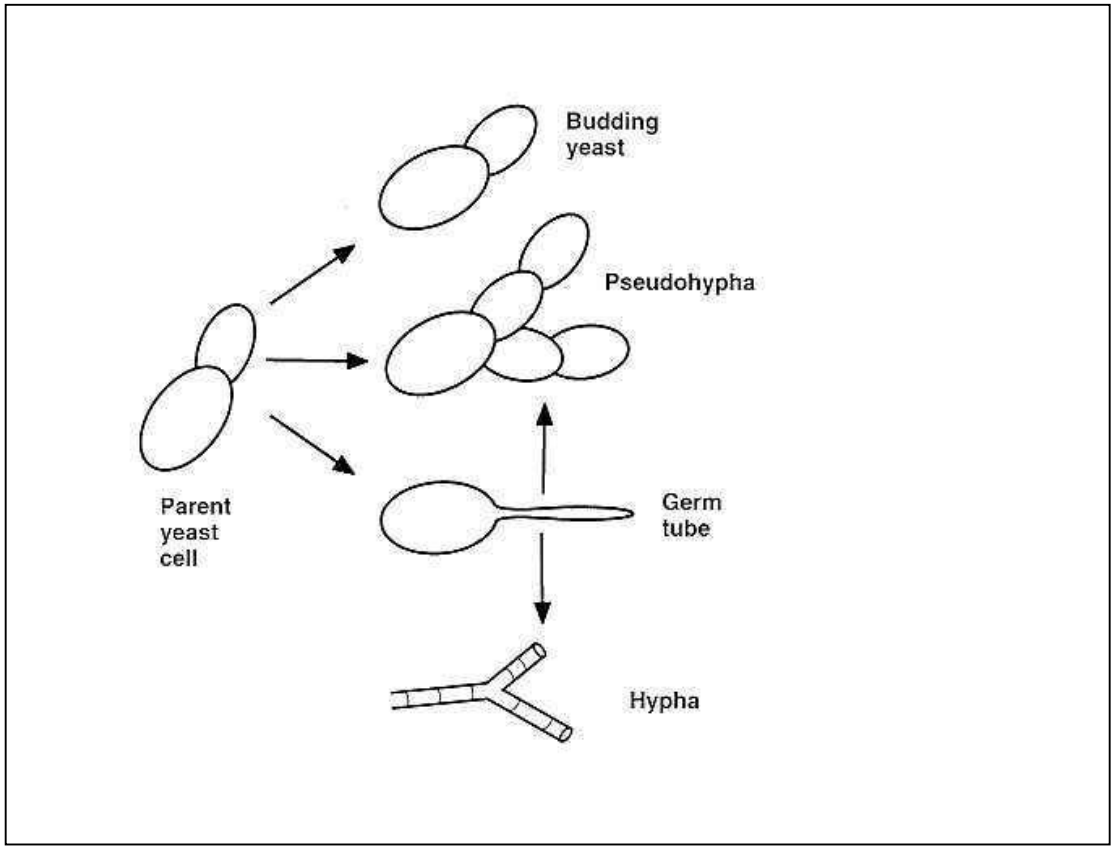

Figure 1-9. Germination of *C. albicans*. Parental yeast cells can germinate into five different morphological forms depending on the growth conditions: budding yeast, pseudohypha, germ tubes, and hypha (Walsh, Dixon 1996).

C. albicans grows vegetatively in a variety of morphogenic forms: it can exist as simple budding yeast or undergo morphogenesis and produce filaments in the form of pseudohypha and/or hypha (Figure 1-9). Additional electron microscopy studies have revealed ultrastructural organization in the *C. albicans* cell wall, which changes

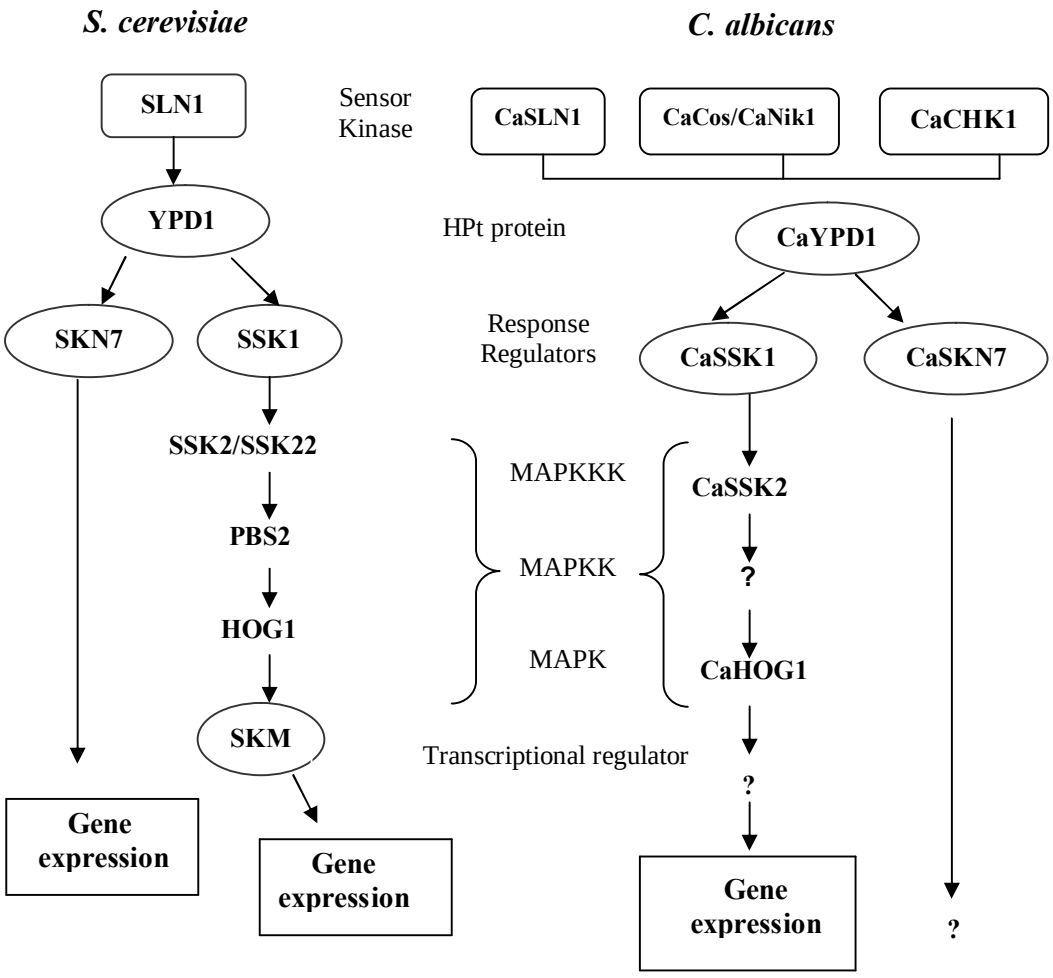

Figure 1-10. Multi-Step Phosphorelay Signaling Pathways in *S. cerevisiae* and *C. albicans*. Comparison of the multi-step systems in both organisms. Both systems control a downstream MAP kinase cascade and are responsible for environmental stress adaptation.

during germ-tube formation, the onset of stationary phase, and reinitiation of growth (Djaczenko, Cassone 1972; Scherwitz, Martin *et al.,* 1978). The yeast cell wall

contains the following composition: lipid 2%, protein 3-6%, chitin 1-2%, mannoprotein 35-40%, and glucan 48-60% (Klis, de Groot *et al.,* 2001).

Due to the morphological switch (unicellular yeast into filamentous yeast); *C. albicans* is able to survive under variety of stress conditions. A number of factors have been associated with the virulence properties of *C. albicans*: adherence to host cells, ability to turn on several degradative enzymes and the phenomenon of ñphenotypic switchingò (Brown, Gow 1999; Soll 2002; Romani, Bistoni *et al.,* 2003). Little is known about the mechanism of adaptation of *C. albicans*. The multi-step His-Asp phosphorelay signal transduction pathways is known as one of the major pathways by which adaptation to oxidative stress occurs (Calera, Calderone 1999).

Homologues of two-component signal transduction proteins were found in *C.albicans* (Figure 1-10). Three histidine kinases CaSLN1, Cos/CaNik1 and CHK1 were found in *C.albicans* (Calera, Calderone 1999; Deschenes, Lin *et al.,* 1999; Yamada-Okabe, Mio *et al.,* 1999). CaSLN1 is a transmembrane kinase that complements SLN1 in *S. cerevisiae*. This suggests that it has a similar role in *C. albicans* (Nagahashi, Mio *et al.,* 1998). Cos/CaNik1 is a gene homologue of NIK1 protein from *Neurospora crassa*. Similarities in structure were found in the N-terminus region with *S.cerevisiae*. It is known that deletions of the *CaNIK1* gene suggest that the protein is involved in hyphal development in *C. albicans* and is responsible for the frequency of the phenotype switch (Alex, Korch *et al.,* 1998; Nagahashi, Mio *et al.,* 1998; Srikantha, Tsai *et al.,* 1998).

CaCHK1 is a hybrid kinase with a Ser/Thr MAP kinase domain and an ATP/GTP binding loop. Deletion of the *CaCHK1* gene resulted in avirulence and flocculation of the strains that may indicate that CaCHK1 is a part of a signal transduction pathway associated with regulating hyphal-specific cell surface proteins (Calera, Choi *et al.,* 1998; Calera, Calderone 1999; Calera, Zhao *et al.,* 1999; Torosantucci, Chiani *et al.,* 2002). As in *S.cerevisiae*, the histidine-containing phosphotransfer protein CaYPD1 is found in *C. albicans*. The CaYPD1 gene can complement the *ypd1* gene deletion in *S. cerevisiae* (Calera, Herman *et al.,* 2000).

Two response regulators have been identified to date in *C. albicans* ï CaSKN7 (orf6.8220, http://genolist.pasteur.fr/CandidaDB) and CaSSK1. It is known that the *CaSSK1* gene is unable to complement a *SSK1* gene deletion in *S. cerevisiae* (Calera, Calderone 1999), thus it is expected to have functions not only in regulating the response to the hyperosmotic stress, but also other functions (functions that are associated with virulence and cell wall biosynthesis) (Chauhan, Inglis *et al.,* 2003). Additionally, Δ*ssk1* in *C. albicans* causes cell flocculation and avirulence (Calera, Zhao *et al.,* 2000). The *CaSKN7* response regulator gene has been identified by the *C. albicans* genome-sequencing project, but the protein has not yet been studied. However, the deletion mutant of *CaSKN7* was constructed. The mutant strain was sensitive to H_2O_2 *in vitro*, but its virulence was only mildly attenuated (Singh, Chauhan *et al.,* 2004).

Virulence of *C. albicans*

The ability of *C. albicans* to survive, as a commensal organism, under different stress conditions inside the host is well known. The spectrum of diseases, attributed to *C. albicans* is much greater than that of any other commensal microorganism. It is able to invade the host under a wide variety of predisposing conditions that range from specific immune defects to esophageal candidiasis (Kodsi, Wickremesinghe *et al.,* 1976; Bernhardt, Herman *et al.,* 2001). For any disease establishment, *C. albicans* requires virulence factors, which can be strictly associated with the pathogenic state of the organism or can also influence survival of *C. albicans* as a commensal organism. They include (Calderone, Fonzi 2001):

a) host recognition biomolecules; b) morphogenesis; c) expression of invasive enzymes; c) phenotypic switching.

Host recognition biomolecules Numerous studies showed that *C. albicans* non-adhesive strains are avirulent (Gale 1998; Staab, Bradway *et al.,* 1999; Sundstrom 1999). The adhesive proteins, which bind the organism to mammalian cells include: Als1, Als5 (agglutinin-like proteins), Hwp1 (mannoprotein), Int1 (integrin-like protein), Mnt1 (membrane protein) and mannan-binding proteins.

Morphogenesis *C. albicans* is polymorphic in their growth pattern. They can grow isotropically (budding yeast) or apically (hyphae, pseudohyphae). This yeast-to-hyphal conversion is important because it is associated with biofilm formation by the organism in mucosal infections and invasion in systemic disease. Two signal

transduction pathways are associated with morphogenesis (Brown, Gow 1999; Lengeler, Davidson *et al.,* 2000).

Expression of invasive enzymes There are two groups of enzymes that contribute to the *C. albicans* virulence ï secreted aspartyl proteinases (SAP) and phospholipases (PL). Among four PLs, only PLB1 protein is required for virulence (Ghannoum 2000). Six out of seven existing SAPs in *C. albicans* are required for virulence and express in different manner, which depends on tissue specificity (Schaller M., Schafer W. *et al.,* 1998; Schaller M., Bein *et al.,* 2003).

Phenotypic switching The phenotypic switch in *C. albicans* occurs frequently and is reversible. The mechanism for the switch has been suggested to include chromosomal rearrangements (aneuploidy) (Rustchenko-Bulgac, Sherman *et al.,* 1990). The most studied phenotypic switch is the white-opaque system in strain WO-1 (Slutsky, Buffo *et al.,* 1985). Opaque cell colonize the skin more than white-phase cells, but are less virulent (Kvaal, Lachke *et al.,* 1999).

All above-mentioned factors expressed by *C. albicans* are important in its adaptation and virulence to specific anatomical sites and include multiple protein signaling cascades that help to effect and turn on downstream genes.

1.8. Research focus

The multi-step His-Asp phosphorelay system in *Saccharomyces cerevisiae* which allows cells to adapt to osmotic, oxidative and other environmental stresses has

been comprehensively studied. However there are still questions yet to be answered: what is the mechanism of signal recognition by SLN1 histidine kinase? How is the signal transmitted and processed under hyperosmotic stress? What triggers SSK1 protein dephosphorylation during hyperosmotic stress? How does ion-solute concentrations affect the SLN1-YPD1-SSK1 phosphorelay pathway?

The research in our laboratory has been focused on investigating on how changes in intracellular ion and osmolyte concentration upon hyperosmotic shock may affect pathway regulation and protein-protein interactions involving YPD1 and SSK1. Elucidating the molecular events that trigger the cellular responses to hyperosmotic stress is important for fully understanding the overall regulation of this signaling pathway. Therefore, we examined the effect of solute concentration not only on phosphotransfer rates within SLN1-YPD1-SSK1 phosphorelay but also on YPD1/SSK1 interactions and dephosphorylation of SSK1. This study will provide new insights into the mechanisms that underlie the osmoregulatory pathway in *S. cerevisiae* and the specific effects of osmolytes in regulating the pathway.

Additionally, we have also focused our attention on the *in vitro* reconstitution of the multi-step phosphorelay from pathogenic yeast *C. albicans* and biochemical characterization of the CaYPD1 and CaSSK1 proteins. This study will establish a basis for the future biochemical characterization of this multi-step His-to-Asp phosphorelay and its components and possibly for anti-fungal drug design.

References

Albertyn, J., Hohmann, S., Thevelein, J. M. and Prior, B. A. (1994). "*GPD1*, which encodes glycerol-3-phosphate dehydrogenase, is essential for growth under osmotic stress in *Saccharomyces cerevisiae*, and its expression is regulated by the high-osmolarity glycerol response pathway." Mol. Cell. Biol. **14**(6): 4135-4144.

Alex, L. A., Korch, C., Selitrennikoff, C. P. and Simon, M. I. (1998). "*COS1*, a two-component histidine kinase that is involved in hyphal development in the opportunistic pathogen *Candida albicans*." Proc. Natl. Acad. Sci. (USA) **95**(June): 7069-7073.

Alm, E., Huang, K. and Arkin, A. (2006). "The evolution of two-component systems in bacteria reveals different strategies for niche adaptation." PLoS Comp. Biol. **2**(11): e143.

Appleby, J. L., Parkinson, J. S. and Bourret, R. B. (1996). "Signal transduction via the multi-step phosphorelay: not necessarily a road less traveled." Cell **86**: 845-848.

Aravind, L. and Ponting, C. P. (1999). "The cytoplasmic helical linker domain of receptor histidine kinase and methyl-accepting proteins is common to many prokaryotic signalling proteins." FEMS Microbiol. Lett. **176**: 111-116.

Bernhardt, J., Herman, D., Sheridan, M. and Calderone, R. (2001). "Adherence and invasion studies of *Candida albicans* strains, using in vitro models of esophageal candidiasis." J. Infect. Dis. **184**: 1170-1175.

Bilwes, A. M. and al., e. (2001). "Nucleotide binding by the histidine kinase CheA." Nat. Struct. Biol. **8**: 353-360.

Bilwes, A. M., Alex, L. A., Crane, B. R. and Simon, M. I. (1999). "Structure of CheA, a signal-transducing histidine kinase." Cell **96**(Jan. 8): 131-141.

Brown, A. J. and Gow, N. A. (1999). "Regulatory networks controlling Candida albicans morphogenesis." Trends Microbiol. **7**(8): 333-338.

Brown, J. L., North, S. and Bussey, H. (1993). "*SKN7*, a yeast multicopy suppressor of a mutation affecting cell wall β-glucan assembly, encodes a product with domains homologous to prokaryotic two-component regulators and to heat shock transcription factors." J. Bacteriol. **175**(21): 6908-6915.

Calderone, R., Ed. (2002). *Candida* and Candidiasis. Washington, D.C., ASM Press.

Calderone, R. and Fonzi, W. A. (2001). "Virulence factors of *Candida albicans*." Trends Microbiol. **9**(7): 327-335.

Calera, J. A. and Calderone, R. (1999). "Flocculation of hyphae is associated with a deletion in the putative *CaHK1* two-component histidine kinase gene from *Candida albicans*." Microbiol. **145**: 1431-1442.

Calera, J. A. and Calderone, R. (1999). "Histidine kinase, two-component signal transduction proteins of *Candida albicans* and the pathogenesis of candidosis." Mycoses **42**(Suppl. 2): 49-53.

Calera, J. A. and Calderone, R. A. (1999). "Identification of a putative response regulator two-component phosphorelay gene (*CaSSK1*) from *Candida albicans*." Yeast **15**: 1243-1254.

Calera, J. A., Choi, G. H. and Calderone, R. A. (1998). "Identification of a putative histidine kinase two-component phosphorelay gene (*CaHK1*) in *Candida albicans*." Yeast **14**: 665-674.

Calera, J. A., Herman, D. and Calderone, R. (2000). "Identification of *YPD1*, a gene of *Candida albicans* which encodes a two-component phosphohistidine intermediate protein." Yeast **16**: 1053-1059.

Calera, J. A., Zhao, X.-J. and Calderone, R. (2000). "Defective hyphal development and avirulence caused by a deletion of the SSK1 response regulator gene in *Candida albicans*." Infect. Immun. **68**(2): 518-525.

Calera, J. A., Zhao, X. J., De Bernardis, F., Sheridan, M. and Calderone, R. (1999). "Viruence of Candida albicancs CaHK1 mutants in a murine model of hematogenously disseminated candidiasis." Infect Immun. **67**(8): 4280-4284.

Chauhan, N., Inglis, D., Roman, E., Pla, J., Li, D., Calera, J. A. and Calderone, R. (2003). "*Candida albicans* response regulator gene *SSK1* regulates a subset of genes whose functions are associated with cell wall biosynthesis and adaptation to oxidative stress." Euk. Cell **2**(5): 1018-1024.

Chauhan, N., Latge, J. P. and Calderone, R. (2008). "Two-component signal transduction proteins as potential drug targets in medically important fungi." Infect Immun **76**(11): 4795-4803.

Cock, P. J. and Whitworth, D. E. (2007). "Evolution of prokaryotic two-component system signaling pathways: gene fusions and fissions." Mol. Biol. Evol. **24**(11): 2355-2357.

D'Souza, M., Glass, E. M., Syed, M. H., Zhang, Y., Rodriguez, A., Maltsev, N. and Galperin, M. Y. (2006). "Sentra: a database of signal transduction proteins for comparative genome analysis." Nuc. Acids Res **35**: D217-D273.

Deschenes, R. J., Lin, H., Ault, A. D. and Fassler, J. S. (1999). "Antifungal properties and target evaluation of three putative bacterial histidine kinase inhibitors." Antimicrob. Agents Chemother. **43**(7): 1700-1703.

Djaczenko, W. and Cassone, A. (1972). "Visualization of new ultrastructural components in the cell wall of Candida albicans with fixatives containing TAPO." J. Cell Biol. **52**(1): 186-190.

Dutta, R., Qin, L. and Inouye, M. (1999). "Histidine kinases: diversity of domain organization." Mol. Microbiol. **34**(4): 633-640.

Fabret, C., Feher, V. A. and Hoch, J. A. (1999). "Two-component signal transduction in *Bacillus subtilis*: How one organism sees its world." J. Bacteriol. **181**(7): 1975-1983.

Ferrigno, P., Posas, F., Koepp, D., Saito, H. and Silver, P. A. (1998). "Regulated nucleo/cytoplasmic exchange of HOG1 MAPK requires the importin β homologs NMD5 and XPO1." EMBO J. **17**(19): 5606-5614.

Gale, C. (1998). "Linkage of adhesion, filamentous growth, and virulence in Candida albicans to a single gene, INT1." Science. **279**(5355): 1355-1358.

Galperin, M. Y. (2005). "A census of membrane-bound and intracellular signal transduction proteins in bacteria: bacterial IQ, extroverts and introverts." BMC Microbiol. **5**(htttp://www.biomedcentral.com/1471-2180/5/35): 1-19.

Galperin, M. Y. (2006). "Structural classification of bacterial response regulators: diversity of output domains and domain combinations." J. Bacteriol. **188**(12): 4169-4182.

Gao, R., Mack, T. R. and Stock, A. M. (2007). "Bacterial response regulators: versatile regulatory strategies from common domains." TRENDS in Biochemical Sciences **32**(5): 226-234.

Gao, R., Mack, T. R. and Stock, A. M. (2007). "Bacterial response regulators: versatile regulatory strategies from common domains." Trends Biochem. Sci. **32**(6): 225-234.

Gao, R. and Stock, A. M. (2009). "Biological insights from structures of two-component proteins." Annu Rev Microbiol **63**: 133-154.

Ghannoum, M. A. (2000). "Potential role of phospholipases in virulence and fungal pathogenesis." Clin. Microbiol. Rev. **13**(1): 122-143.

Hoch, J. A. and Silhavy, T. J., Eds. (1995). Two-component signal transduction. Washington, D.C., American Society for Microbiology Press.

Hohmann, S. (2002). "Osmotic stress signaling and osmoadaptation in yeasts." Microbiol. Mol. Biol. Rev. **66**(2): 300-372.

Hulko, M., Berndt, F., Gruber, M., Linder, J. U., Truffault, V., Schultz, A., Martin, J., Schultz, J. E., Lupas, A. N. and Coles, M. (2006). "The HAMP domain structure implies helix rotation in transmembrane signaling." Cell **126**(Sept. 8): 929-940.

Inouye, M., Duttu, R. and Zhu, Y. (2003). "Regulation of porins in Eschirichia coli by the osmosensing histidine kinase/phosphatase EnvZ." In "Histidine kinases in signal transduction" (M. Inouye and R. Duttu, Eds.): 25-46. Academic Press, San Diego.

Ishige, K., Nagasawa, S., Tokishita, S. and Mizuno, T. (1994). "A novel device of bacterial signal transducers." EMBO J. **13**: 5195-5202.

Jin, T. and Inouye, M. (1994). "Transmembrane signaling: Mutational analysis of the cytoplasmic linker region of Taz1-1, a Tar-EnvZ chimeric receptor in *Escherichia coli*." J. Mol. Biol. **244**: 477-481.

Kaserer, A. O. and West, A. H. (2009). "Histidine kinases in two-component signaling pathways." *The Handbook of Cell Signaling,* (2nd edition by Bradshaw R.A., Dennis E.A., eds.) Academic Press, San Diego.

Kato, M., Mizuno, T., Shimizu, T. and Hakoshima, T. (1997). "Insights into multistep phosphorelay from the crystal structure of the C-terminal HPt domain of ArcB." Cell **88**: 717-723.

Kato, M., Shimizu, T., Mizuno, T. and Hakoshima, T. (1999). "Structure of the histidine-containing phosphotransfer (HPt) domain of the anaerobic sensor protein ArcB complexed with the chemotaxis response regulator CheY." Acta Cryst. **D55**: 1257-1263.

Klein, A. H., Shulla, A., Reimann, S. A., Keating, D. H. and Wolfe, A. J. (2007). "The intracellular concentration of Acetyl phosphate in *Escherichia coli* is sufficient for direct phosphorylation of two-compnent response regulators." J. Bacteriol. **189**(15): 5574-5581.

Klis, F. M., de Groot, P. and Hellingwerf, K. (2001). "Molecular organization of the cell wall of Candida albicans." Med Mycol. **39**: Suppl 1: 1-8.

Klumpp, S. and Krieglstein, J. (2002). "Phosphorylation and dephosphorylation of histidine residues in proteins." Eur. J. Biochem. **269**: 1067-1071.

Kodsi, B. E., Wickremesinghe, P. C., Kozinn, P. J., Iswara, K. and Goldberg, P. K. (1976). "*Candida esophagitis*: a prospective study of 27 cases." Gastroenterology **71**: 715-719.

Kojetin, D. J., Sullivan, D., Thompson, R. J. and Cavanagh, J. (2007). "Classification of response regulators based on their surface properties." Methods Enzymol. **422**: 141-169.

Kojetin, D. J., Thompson, R. J. and Cavanagh, J. (2003). "Sub-classification of response regulators using the surface characteristics of their receiver domains." FEBS Lett. **554**: 231-236.

Kojic, E. M. and Darouiche, R. O. (2004). "*Candida* infections of medical devices." Clin. Microbiol. Rev. **17**(2): 255-267.

Koretke, K. K., Lupas, A. N., Warren, P. V., Rosenberg, M. and Brown, J. R. (2000). "Evolution of two-component signal transduction." Mol. Biol. Evol. **17**(12): 1956-1970.

Kosinsky, Y. A., Volynsky, P. E., Lagant, P., Vergoten, G., Suzuki, E., Arseniev, A. S. and Efremov, R. G. (2004). "Development of the force field parameters for phosphoimidazole and phosphohistidine." J. Comput. Chem. **25**: 1313-1321.

Kvaal, C., Lachke, S. A., Srikantha, T., Daniels, K., McCoy, J. and Soll, D. R. (1999). "Misexpression of the opaque-phase-specific gene PEP1 (SAP1) in the white phase of Candida albicans confers increased virulence in a mouse model of cutaneous infection." Infect Immun. **67**(12): 6652-6662.

Laub, M. T., Biondi, E. G. and Skerker, J. M. (2007). "Phosphotransfer profiling: systematic mapping of two-component signal transduction pathways and phosphorelays." Meth. Enzymol. **423**: 531-548.

Laub, M. T., Biondi, E. G. and Skerker, J. M. (2007). "Phosphotransfer profiling: systematic mapping of two-component signal transduction pathways and phosphorelays." Methods Enzymol. **423**: 531-548.

Lee, J. *e. a.* (2008). "Changes at the KinA PAS-A Dimerization interface influence histidine kinase function." Biochem **47**: 4051-4064.

Lee, S.-Y., Cho, H. S., Pelton, J. G., Yan, D., Henderson, R. K., King, D. S., Huang, L.-S., Kustu, S., Berry, E. A. and Wemmer, D. E. (2001). "Crystal structure of an activated response regulator bound to its target." Nat. Struct. Biol. **8**(1): 52-56.

Lengeler, K. B., Davidson, R. C., D'Souza, C., Harashima, T., Shen, W.-C., Wang, P., Pan, X., Waugh, M. and Heitman, J. (2000). "Signal transduction cascades regulating fungal development and virulence." Microbiol. Mol. Biol. Rev. **64**(4): 746-785.

Letunic, I., Copley, R. R., Pils, B., Pinkert, S., Schultz, J. and Bork, P. (2006). "SMART 5: domains in the context of genomes and networks." Nucleic Acids Res. **34(Database issue)**(D257-60).

Li, S., Ault, A., Malone, C. L., Raitt, D., Dean, S., Johnston, L. H., Deschenes, R. J. and Fassler, J. S. (1998). "The yeast histidine protein kinase, Sln1p, mediates phosphotransfer to two response regulators, Ssk1p and Skn7p." EMBO J. **17**(23): 6952-6962.

Li, S., Dean, S., Li, Z., Horecka, J., Deschenes, R. J. and Fassler, J. S. (2002). "The eukaryotic two-component histidine kinase Sln1p regulates OCH1 via the transcription factor, Skn7p." Mol. Biol. Cell **13**(Feb.): 412-424.

Lukat, G. S., Lee, B. H., Mottonen, J. M., Stock, A. M. and Stock, J. B. (1991). "Roles of the highly conserved aspartate and lysine residues in the response regulator of bacterial chemotaxis." J. Biol. Chem. **266**: 8348-8354.

Lukat, G. S., McCleary, W. R., Stock, A. M. and Stock, J. B. (1992). "Phosphorylation of bacterial response regulator proteins by low molecular weight phospho-donors." Proc. Natl. Acad. Sci. USA **89**: 718-722.

Madhani, H. D. and Fink, G. R. (1998). "The riddle of MAP kinase signaling specificity." Trends Genet. **14**(4): 151-155.

Maeda, T., Takekawa, M. and Saito, H. (1995). "Activation of yeast PBS2 MAPKK by MAPKKKs or by binding of an SH3-containing osmosensor." Science **269**: 554-558.

Maeda, T., Wurgler-Murphy, S. M. and Saito, H. (1994). "A two-component system that regulates an osmosensing MAP kinase cascade in yeast." Nature **369**: 242-245.

Marina, A., Mott, C., Auyzenberg, A., Hendrickson, W. A. and Waldburger, C. D. (2001). "Structural and mutational analysis of the PhoQ histidine kinase catalytic domain." J. Biol. Chem. **276**(44): 41182-41190.

Marina, A., Waldburger, C. D. and Hendrickson, W. A. (2005). "Structure of the entire cytoplasmic portion of a sensor histidine-kinase protein." EMBO J. **24**: 4247-4259.

Mascher, T., Helmann, J. D. and Unden, G. (2006). "Stimulus perception in bacterial signal-transducing histidine kinases." Microbiol. Mol. Biol. Rev. **70**(4): 910-938.

Mayover, T. L., Halkides, C. J. and Stewart, R. C. (1999). "Kinetic characterization of CheY phosphorylation reactions: Comparison of P-CheA and small-molecule phosphodonors." Biochemistry **38**: 2259-2271.

McCleary, W. R. and Stock, J. B. (1994). "Acetyl phosphate and the activation of two-component response regulators." J. Biol. Chem. **269**(50): 31567-31572.

Mizuno, T. (1997). "Compilation of all genes encoding two-component phosphotransfer signal transducers in the genome of *Escherichia coli*." DNA Res. **4**: 161-168.

Mizuno, T. (1998). "His-Asp phosphotransfer signal transduction." J. Biochem. **123**: 555-563.

Morgan, B. A., Bouquin, N., Merrill, G. F. and Johnston, L. H. (1995). "A yeast transcription factor bypassing the requirement for SBF and DSC1/MBF in budding yeast has homology to bacterial signal transduction proteins." EMBO J. **14**: 5679-5689.

Nagahashi, S., Mio, T., Ono, N., Yamada-Okabe, T., Arisawa, M., Bussey, H. and Yamada-Okabe, H. (1998). "Isolation of *CaSLN1* and *CaNIK1*, the genes for osmosensing histidine kinase homologues, from the pathogenic fungus *Candida albicans*." Microbiology **144**: 425-432.

Ostrander, D. B. and Gorman, J. A. (1999). "The extracellular domain of the Saccharomyces cerevisiae Sln1p membrane osmolarity sensor is necessary for kinase activity." J. Bacteriol. **181**(8): 2527-2534.

Ota, I. M. and Varshavsky, A. (1992). "A gene encoding a putative tyrosine phosphatase suppresses lethality of an N-end rule-dependent mutant." Proc. Natl. Acad. Sci. (USA) **89**: 2355-2359.

Pao, G. M. and Saier, M. H., Jr. (1997). "Nonplastid eukaryotic response regulators have a monophyletic origin and evolved from their bacterial precursors in parallel with their cognate sensor kinases." J. Mol. Evol. **44**: 605-613.

Parkinson, J. S. and Kofoid, E. C. (1992). "Communication modules in bacterial signaling proteins." Annu. Rev. Genet. **26**: 71-112.

Porter, S. W. and West, A. H. (2005). "A common docking site for response regulators on the yeast phosphorelay protein YPD1." Biochim. Biophys. Acta **1748**: 138-145.

Posas, F. and Saito, H. (1997). "Osmotic activation of the HOG MAPK pathway via Ste11p MAPKKK: Scaffold role of Pbs2p MAPKK." Science **276**: 1702-1705.

Posas, F. and Saito, H. (1998). "Activation of the yeast SSK2 MAP kinase kinase kinase by the SSK1 two-component response regulator." EMBO J. **17**(5): 1385-1394.

Posas, F., Wurgler-Murphy, S. M., Maeda, T., Witten, E. A., Thai, T. C. and Saito, H. (1996). "Yeast HOG1 MAP kinase cascade is regulated by a multistep phosphorelay mechanism in the SLN1-YPD1-SSK1 "two-component" osmosensor." Cell **86**: 865-875.

Raitt, D. C., Johnson, A. L., Erkine, A. M., Makino, K., Morgan, B., Gross, D. S. and Johnston, L. H. (2000). "The Skn7 response regulator of Saccharomyces cerevisiae interacts with Hsf1 in vivo and is required for the induction of heat shock genes by oxidative stress." Mol. Biol. Cell **11**(July): 2335-2347.

Reiser, V., Raitt, D. C. and Saito, H. (2003). "Yeast osmosensor Sln1 and plant cytokinin receptor Cre1 respond to changes in turgor pressure." J. Cell Biol. **161**(6): 1035-1040.

Robinson, V. L., Buckler, D. R. and Stock, A. M. (2000). "A tale of two components: a novel kinase and a regulatory switch." Nat. Struct. Biol. **7**(6): 626-633.

Romani, L., Bistoni, F. and Puccetti, P. (2003). "Adaptation of *Candida albicans* to the host environment: the role of morphogenesis in virulence and survival in mammalian hosts." Curr. Opin. Microbiol. **6**: 338-343.

Rustchenko-Bulgac, E. P., Sherman, F. and Hicks, J. B. (1990). "Chromosomal rearrangements associated with morphological mutants provide a means for genetic variation of Candida albicans. ." J. Bacteriol. **172**(3): 1276-1283.

Schaller M., Bein, M., Korting, H. C., Baur, S., Hamm, G., Monod, M., Beinhauer, S. and B., H. (2003). "The secreted aspartyl proteinases Sap1 and Sap2 cause tissue damage in an in vitro model of vaginal candidiasis based on reconstituted human vaginal epithelium." Infect Immun. **71**(6): 3227-3234.

Schaller M., Schafer W., Korting H.C. and B., H. (1998). "Differential expression of secreted aspartyl proteinases in a model of human oral candidosis and in patient samples from the oral cavity. ." Mol Microbiol. **29**(2): 605-615.

Scherwitz, C., Martin, R. and Ueberberg, H. (1978). "Ultrastructural investigations of the formation of Candida albicans germ tubes and septa." Sabouraudia **16**(2): 115-124.

Shankarnarayan, S., Malone, C. L., Deschenes, R. J. and Fassler, J. S. (2008). "Modulation of yeast Sln1 kinase activity by the CCW12 cell wall protein. ." J Biol Chem **283**(4): 1962-73.

Singh, P., Chauhan, N., Ghosh, A., Dixon, F. and Calderone, R. (2004). "SKN7 of *Candida albicans*: mutant construction and phenotypic analysis." Infect. Immun. **72**(4): 2390-2394.

Slutsky, B., Buffo, J. and Soll, D. R. (1985). "High-frequency switching of colony morphology in Candida albicans. ." Science. **230**(4726): 666-669.

Soll, D. R. (2002). "Candida commensalism and virulence: the evolution of phenotypic plasticity." Acta Trop. **81**(2): 101-110.

Song, H. K., Lee, J. Y., Lee, M. G., Min, J. M. K., Yang, J. K. and Suh, S. W. (1999). "Insights into eukaryotic multistep phosphorelay signal transduction revealed by the crystal structure of Ypd1p from *Saccharomyces cerevisiae*." J. Mol. Biol. **293**(Nov. 5): 753-761.

Srikantha, T., Tsai, L., Daniels, K., Enger, L., Highley, K. and Soll, D. R. (1998). "The two-component hybrid kinase regulator *CaNIK1* of *Candida albicans*." Microbiology **144**: 2715-2729.

Staab, J. F., Bradway, S. D., Fidel, P. L. and Sundstrom, P. (1999). "Adhesive and mammalian transglutaminase substrate properties of Candida albicans Hwp1." Science **283**(Mar. 5): 1535-1538.

Stephenson, K. and Hoch, J. A. (2002). "Two-component and phosphorelay signal-transduction systems as therapeutic targets." Curr. Opin. Pharm. **2**: 1-6.

Stock, A. M., Robinson, V. L. and Goudreau, P. N. (2000). "Two-component signal transduction." Annu. Rev. Biochem. **69**: 183-215.

Stock, J. and Da Re, S. (2000). "Signal transduction: Response regulators on and off." Curr. Biol. **10**: R420-R424.

Stock, J. B., Stock, A. M. and Mottonen, J. M. (1990). "Signal transduction in bacteria." Nature **344**: 395-400.

Stock, J. B., Surette, M. G., Levit, M. and Park, P. (1995). Two-component signal transduction systems: Structure-function relationships and mechanisms of catalysis. Two-component signal transduction. J. A. Hoch and T. J. Silhavy. Washington, D.C., American Society for Microbiology**:** 25-51.

Sundstrom, P. (1999). "Adhesins in Candida albicans." Curr. Opin. Microbiol. **2**(4): 353-357.

Taylor, B. L. and Zhulin, I. B. (1999). "PAS domains: Internal sensors of oxygen, redox potential, and light." Microbiol. Mol. Biol. Rev. **63**(2): 479-506.

Torosantucci, A., Chiani, P., De Bernardis, F., Cassone, A., Calera, J. A. and Calderone, R. (2002). "Deletion of the two-component histidine kinase gene (*CHK1*) of *Candida albicans* contributes to enhanced growth inhibition and killing by human neutrophils in vitro." Infect. Immun. **70**(2): 985-987.

Tsuzuki, M., Ishige, K. and Mizuno, T. (1995). "Phosphotransfer circuitry of the putative multi-signal transducer, ArcB, of *Escherichia coli*: *in vitro* studies with mutants." Mol. Microbiol. **18**: 953-962.

Walsh, T. J. and Dixon, D. M. (1996). "Deep mycosis." Medical microbiology (4th edition by Baron S.) The University of Texas Medical Branch at Galveston.

Wenzel, R. P. (1995). "Nosocomial candidemia: risk factors and attributable mortality." Clin. Infect. Dis. **20**: 1531-1534.

West, A. H. and Stock, A. M. (2001). "Histidine kinases and response regulator proteins in two-component signaling systems." Trends Biochem. Sci. **26**(6): 369-376.

Williams, S. B. and Stewart, V. (1999). "Functional similarities among two-component sensors and methyl-accepting chemotaxis proteins suggest a role for linker region amphipathic helices in transmembrane signal transduction." Mol. Microbiol. **33**(6): 1093-1102.

Xu, Q., Nguyen, V. and West, A. H. (1999). "Purification, crystallization, and preliminary X-ray diffraction analysis of the yeast phosphorelay protein YPD1." Acta Cryst. **D55**: 291-293.

Xu, Q., Porter, S. W. and West, A. H. (2003). "The yeast YPD1/SLN1 complex: Insights into molecular recognition in two-component systems." Structure **11**(Dec. 2003): 1569-1581.

Xu, Q. and West, A. H. (1999). "Conservation of structure and function among histidine-containing phosphotransfer (HPt) domains as revealed by the crystal structure of YPD1." J. Mol. Biol. **292**: 1039-1050.

Yamada-Okabe, T., Mio, T., Ono, N., Kashima, Y., Matsui, M., Arisawa, M. and Yamada-Okabe, H. (1999). "Roles of three histidine kinase genes in hyphal development and virulence of the pathogenic fungus *Candida albicans*." J. Bacteriol. **181**(23): 7243-7247.

Zhang, W. and Shi, L. (2005). "Distribution and evolution of multi-step phosphorelay in prokaryotes:lateral domain recruitment involved in the formation of hybrid-type histidine kinases." Microbiol. **151**: 2159-2173.

Zhao, X., Copeland, D. M., Soares, A. S. and West, A. H. (2008). "Crystal structure of a complex between the phosphorelay protein YPD1 and the response regulator domain of SLN1 bound to a phosphoryl analog." *J. Mol. Biol.* **375**: 1141-1151.

Zhou, L., Lei, X.-H., Bochner, B. R. and Wanner, B. L. (2003). "Phenotype Microarray analysis of Escherichia coli K-12 mutants with deletions of all two-component systems." J. Bacteriol. **185**: 4956-4972.

Chapter 2

Effect of osmolytes on the half-life of phosphorylated SSK1-RR in the presence and absence of YPD1

ñPortions of this chapter are reproduced with automatic permission from [Kaserer A.O., Babak A., Cook P.F., West A.H. (2009) Effects of Osmolytes on the SLN1-YPD1-SSK1 Phosphorelay system from *Saccharomyces cerevisiae*., *Biochemistry.* v. 48(33), p. 8044-50]ò.

Two-component signal transduction systems in prokaryotes and eukaryotes regulate cellular responses to a variety of environmental stresses (Stock, Robinson *et al.,* 2000). In *Saccharomyces cerevisiae*, a multi-step phosphorelay system is responsible for adaptation to osmotic, oxidative and other environmental stresses (Blomberg, Adler 1989; Albertyn, Hohmann *et al.,* 1994; Saito 2001; Hohmann 2002). The branched pathway consists of a sensor histidine kinase SLN1, a histidine-containing phosphotransfer (HPt) protein YPD1, and two independent response regulator proteins, SSK1 and SKN7. The *SLN1* gene encodes a hybrid histidine kinase with two membrane spanning regions and an extracellular sensing domain (Ota, Varshavsky 1993). The HPt protein, YPD1, serves as a non-enzymatic but essential mediator between SLN1 and two downstream RR proteins SSK1 and SKN7 (Posas, Wurgler-Murphy *et al.,* 1996; Li, Ault *et al.,* 1998).

Phosphoryl group transfer from YPD1 to SSK1-RR allows constitutive phosphorylation of this response regulator to occur under normal osmotic conditions (Posas, Saito 1998; Janiak-Spens, Cook *et al.,* 2005; Horie T., Tatebayashi K. *et al.,* 2008). However, the life-time of response regulators in the presence of magnesium ions is relatively short, ranging from seconds (CheY) to about 10 hrs (VanR) (Hess,

Oosawa *et al.,* 1988; Wright, Holman *et al.,* 1993). Half-life studies were previously carried out in our laboratory for all three isolated response regulator domains: phospho-SSK1-RR, phospho-SLN1-RR and phospho-SKN7-RR (Janiak-Spens, Sparling *et al.,* 1999). The analysis revealed that phospho-SLN1-RR exhibited a half-life of $t_{1/2} = 13 \pm 2$ min, phospho-SSK1-RR with $t_{1/2} = 13 \pm 3$ min and phospho-SKN7-RR with $t_{1/2} = 144 \pm 6$ min (Janiak-Spens, Sparling *et al.,* 1999; Janiak-Spens, Sparling *et al.,* 2000).

Furthermore, the unprecedented regulatory role for an HPt domain YPD1 in a phosphorelay signaling system was uncovered using a gel mobility shift assay and half-life studies of the phosphorylated SSK1-RR in the presence of YPD1 (Janiak-Spens, Sparling *et al.,* 2000). It was demonstrated *in vitro*, that YPD1 is able to form a complex with phosphorylated SSK1 response regulator domain shielding its phosphoryl group from rapid hydrolysis. This stabilization effect of nearly 200-fold appeared to be protein specific and was observed only for SSK1-RR, increasing the half-life of the phosphorylated SSK1-RR from $t_{1/2} = 13 \pm 3$ min to $t_{1/2} = 38 \pm 4$ hrs. It also suggested a possible mechanism according by which SSK1 can be maintained in its phosphorylated inactive state under normal physiological conditions (Janiak-Spens, Sparling *et al.,* 2000). However, a major question still remained: how is the SSK1 response regulator protein rapidly dephosphorylated under hyperosmotic shock conditions?

Phosphorylation and dephosphorylation of SSK1 functions as an on/off switch in controlling the activity of the downstream HOG1 mitogen-activated protein (MAP) kinase cascade, responsible for production of glycerol (Posas, Saito 1998; Horie T., Tatebayashi K. *et al.,* 2008). Accumulation of intracellular glycerol, a chemically inert osmolyte, allows yeast cells to adapt to hyperosmotic stress conditions.

A number of different osmolytes are found inside yeast and other fungi including monovalent salts, amino acids, polyols and carbohydrates (Blomberg, Adler 1992; Millar 1999; Hohmann 2002). *S. cerevisiae*, *S. pombe*, *C. albicans*, and *D. hansenii* almost exclusively employ glycerol as an osmolyte in osmoregulation (Aiba, Yamada *et al.,* 1995; Thomé 1999; Hohmann 2002; Fan, Whiteway *et al.,* 2005; Burg 2008). Osmoadaptation is achieved through a series of cellular responses that are temporally regulated. For instance, closure of the osmotically sensitive glycerol channel (Fps1) upon hyperosmotic shock provides an additional route to increase the glycerol concentration inside the cell almost immediately to compensate for water efflux (Shankarnarayan, Malone *et al.,* 2008). HOG1 phosphorylation occurs in the cell during the first 1-3 min after exposure to osmotic shock (Brewster, de Valoir *et al.,* 1993). Both GPD1 and glycerol concentrations are at half-maximal level within 20 min (Klipp, Nordlander *et al.,* 2005). An increase in intracellular glycerol concentration increases the turgor pressure which is mediated by the elasticity of the plasma membrane and cell wall upon water exchange (Klipp, Nordlander *et al.,* 2005).

Elucidating the molecular events that trigger the cellular responses to hyperosmotic stress including the rapid efflux of water, changes in intracellular ion and osmolyte concentration, phosphorylation/dephosphorylation of SSK1-R2 is important for fully understanding the overall regulation of this signaling pathway. We hypothesized that the change in ion/solute concentration under hyperosmotic conditions disrupts the YPD1–SSK1-RR~P complex, thus facilitating dephosphorylation of SSK1 and subsequent MAP kinase cascade activation. We therefore examined the effect of osmolyte concentrations on the half-life of the phosphorylated SSK1-RR in the presence and absence of YPD1 and present data in support of our hypothesis.

2.2 Materials and methods

2.2.1 Materials

All chemicals and biochemicals were of ultrapure grade. Glutathione-Sepharose 4B resin was purchased from Amersham. HiTrapQ columns were purchased from GE Healthcare. [γ-^{32}P] ATP (3000 Ci/mmol) was purchased from Perkin-Elmer. Chymostatin, aprotinin, pepstain, phosphoramidon, E-64, leupeptin, antipain, sodium metabisulfite were purchased from Sigma and benzamidine was purchased from Fluka. Ficoll 400, D-(+)-trehalose, proline and betaine were purchased from Sigma-Alrdich. NaCl and glycerol were from Mallinckrodt Chemicals and Pharmco-Aaper, respectively.

2.2.2 Protein expression and purification

All strains used for protein purification are presented in Table 2-1.

GST-SLN1-HK protein expression and purification (Li, Ault et al., 1998)

Escherichia coli DH5Ŭcells (strain OU246) containing the pGEX-GST-SLN1-HK (plasmid OU70 including SLN1-HK 530 ï 970 amino acids) vector were inoculated into 10 mL of LB medium with 100 ε g $mL^{\bar{I}\,1}$ of ampicillin and shaken overnight at 37 ºC. The cell culture was further inoculated into 1 L of prewarmed LB medium in the presence of 100 ε g $mL^{\bar{I}\,1}$ of ampicillin at 37°C. When the optical density (at 600 nm) of the culture reached 0.9, the cells were cooled to room

Protein expressed	Plasmid number	Plasmid name	Strain number	*E. coli* strain, antibiotic resistance
GST-SLN1-HK	OU70	pGEX-GST-HK	OU246	DH5Ŭ Amp^R
YPD1	OU15	pUC12-YPD1	OU6	DH5Ŭ Amp^R
SSK1-RR	OU26	pETCYB-SSK1-RR	OU357	BL21 (DE3)/ Amp^R, Cm^R

Table 2-1. Plasmid constructs used for protein expression and purification. An OU number was assigned for each individual plasmid construct and transformed in *E. coli* strain.

temperature and expression of SLN1-HK was induced by the addition of IPTG to a final concentration of 0.2 mM. The cultures were shaken overnight at 16°C and then harvested, resuspended at 4 mL $g^{\bar{I}\,1}$ (wet weight) of the cell buffer SP-1 (50 mM Tris-

HCl, pH 8, 150 mM NaCl, 1 mM EDTA, 1% Triton X-100, 0.1% ϐME, 1 mM PMSF and 1 x protease inhibitor cocktail)[1]. Cells were lysed by sonication, and the lysates were clarified by centrifugation in a JA-20 rotor at 27,200 *x g* for 1 h at 4°C. The supernatant was loaded onto a 2 mL glutathioneï sepharose 4B bead column equilibrated in SP1 buffer at 4°C. The column was washed sequentially with 20 mL of SP1 buffer and incubated overnight at 4°C. Thereafter the column was washed with 10 mL of SP2 buffer (50 mM Tris-HCl, pH 8, 2 mM DTT and 1 mM EDTA) and 20 mL of SP3 buffer (50 mM Tris-HCl, pH 8, 100 mM KCl, 2 mM DTT, 1 mM EDTA and 10% glycerol). Next, 2 mL of SP3 buffer was left above the column bed and gently mixed with the beads. The suspension was immediately aliquoted (50 εL) in the eppendorf tubes and stored at ï20°C. The protein was judged to be 90% homogeneous based on analysis by SDS-PAGE.

YPD1 protein expression and purification (Xu, Nguyen *et al.,* 1999).

Escherichia coli DH5Ŭcells (strain OU6) containing the pUC12-YPD1 vector (plasmid OU 15 including YPD1 full length protein) were inoculated into 1 mL of LB medium with 100 εg mL^{ï1} of ampicillin and shaken overnight at 37 ºC. The cell culture was further inoculated into 1 L of prewarmed LB medium in the presence of 100 εg mL^{ï1} of ampicillin and grown for 19 hrs at 37°C. The culture was harvested,

[1] Protein inhibitor mix (100x) with final concentrations of the components: Chymostatin (10 εg/mL), Aprotinin (200 εg/mL), pepstatin (100 εg/mL), Phosphoramidon (110 εg/mL), E-64 (720 εg/mL), Leupeptin (50 εg/mL), Antipain (250 εg/mL), Benzamidine (10 mM) and Sodium metabisulfite (10 mM).

washed and suspended at 5 mL g^{-1} (wet weight) of cells in lysis buffer (0.1 M sodium phosphate, pH 7.0, 1 mM EDTA and 1.4 mM ϐME). Cells were lysed by sonication, and the lysate was clarified by centrifugation at 27, 200 *x g* for 1 h at 4°C (JA-20 rotor). The supernatant was separated from pellet and its volume was measured. Next, an ammonium sulfate precipitation was performed: clarified cell lysate was transferred to a small beaker and placed on the stirplate at 4°C, gently stirring with the slow addition of saturated ammonium sulfate to a final concentration of 55 %. The suspension was centrifuged in a JA-20 rotor at 12, 100 *x g* for 45 min at 4°C. The pellet was resuspended in 6-7 mL of dialysis buffer (20 mM BisTris, pH 6.5 and 1.4 mM ϐME) and dialyzed against 2 L of dialysis buffer. Subsequently, the protein was recovered from the dialysis bag and clarified by centrifugation in a JA-20 rotor at 12,100 *x g* for 1 h at 4°C. The supernatant was filtered through a 0.2 εm syringe filter and loaded onto a pre-equilibrated 5 ml HiTrapQ column with buffer A (20 mM BisTris, pH 6.5). The column was washed sequentially with 100 mL of buffer A and the protein was eluted with the linear salt gradient 0 - 1 M NaCl in buffer A. Fractions were analyzed by SDS-PAGE and YPD1-containing fractions were pooled and concentrated to approximately 8 mL using a Centricon 10 (Amicon) filter. The protein was then loaded onto a Sephadex G-50 gel-filtration column (300 ml bed volume) equilibrated in 50 mM sodium phosphate, pH 7, 1 mM EDTA and 1.4 mM ϐME. Fractions containing pure YPD1 protein were identified by SDS-PAGE and pooled, subsequently concentrated to 10 mg/mL. The protein concentration was determined by

absorbance at 280 nm using a calculated extinction coefficient of 15,280 $M^{-1}cm^{-1}$. Purified YPD1 protein was stored in gel filtration buffer in the presence of 1mM DTT and 15 % glycerol at ī 20°C.

SSK1-RR protein expression and purification (Janiak-Spens, Sparling *et al.,* 1999)

Escherichia coli BL21 (DE3) RIL cells (strain OU357) containing the pETCYB-SSK1-RR (plasmid OU26 including SSK1-RR 495 ï 712 amino acids) vector were inoculated into 10 mL of LB medium with 100 ε g mL^{-1} of ampicillin and shaken overnight at 37 ºC. The cell culture was further inoculated into 1 L of prewarmed LB medium in the presence of 100 ε g mL^{-1} of ampicillin and shaken at 37°C. When the optical density (at 600 nm) of the culture reached 0.8, the cells were cooled to room temperature and expression of SSK1-RR was induced by the addition of IPTG to a final concentration of 1 mM. The cultures were shaken overnight at 16°C and then harvested, washed with cell wash buffer (0.1 M Na-phosphate, pH 7 and 1 mM EDTA), then resuspended at 5 mL g^{-1} (wet weight) of cells in lysis buffer (20 mM Tris-HCl, pH 8, 500 mM NaCl, 1 mM EDTA, 0.1% Triton X-100). Cells were lysed by sonication, and the lysate was clarified by centrifugation at 27,200 *x g* for 1 h at 4°C. The supernatant was loaded onto a 3 mL chitin bead column equilibrated in lysis buffer at 4°C. The column was washed sequentially with 100 mL of lysis buffer and 25 mL of cleavage buffer (20 mM Tris-HCl, pH 8, 50 mM NaCl, 1 mM EDTA, 5 mM ATP, 10 mM $MgCl_2$). Thereafter the column was washed

immediately with 25 mL of cleavage buffer containing 30 mM ϐME and incubated overnight at 4°C. The protein was eluted with cleavage buffer and further purified by separation on a gel filtration column (Sephadex G75, 300 ml bed volume) equilibrated in 20 mM Tris-HCl, pH 8, 50 mM NaCl, 1 mM EDTA, 1.4 mM ϐME and 10% glycerol. Fractions containing SSK1-RR were pooled and concentrated using a Centricon 10 (Amicon) filter unit. The protein was judged to be 90% homogeneous based on analysis by SDS-PAGE. The protein concentration was determined by absorbance at 280 nm using a calculated extinction coefficient of 25,440 $M^{-1}cm^{-1}$. Typical yields were 1 mg L^{-1} of cells. Purified SSK1-RR protein was stored in gel filtration buffer in the presence of 10% glycerol at − 20°C.

2.2.3 Measurement of phosphorylated protein half-life

Phosphorylation of the response regulator domain SSK1-RR was achieved by incubation with GST-SLN1-HK and [γ-^{32}P] ATP. GST-tagged SLN1-HK (7 µM) bound to glutathione-Sepharose 4B resin was incubated with 7 µM [γ-^{32}P] ATP in 100 µL of 50 mM Tris-HCl (pH 8.0), 100 mM KCl, 10 mM $MgCl_2$, 2 mM DTT and 20% glycerol for 30 min at room temperature. Phosphorylated GST-SLN1-HK was recovered in the pellet after three consecutive centrifugation steps (1 min at 100 × *g*). Purified SSK1-RR (12 µM) in 50 mM Tris-HCl (pH 8.0), 100 mM KCl, 10 mM $MgCl_2$, 2 mM DTT was added and the mixture was incubated for 30 min at room temperature in a total reaction volume of 40 µL. Phospho-SSK1-RR was recovered in

the supernatant after gently pelleting the resin-bound GST-SLN1-HK. The isolated phosphorylated SSK1-RR (30 εL) was added to a reaction mixture containing 3 μM YPD1 and indicated osmolyte concentrations (NaCl, trehalose, glycerol, proline, betaine) in a total reaction volume of 120 μL. For the reaction in the absence of YPD1, the isolated SSK1-RR (12 μM) in 50 mM Tris-HCl (pH 8.0), 100 mM KCl, 10 mM $MgCl_2$, 2 mM DTT was added to the indicated osmolyte concentrations in a total reaction volume of 75 μl. Aliquots (15 εL) were removed at indicated time points for both reactions, mixed with 5 εL of 4X stop buffer (0.25 M Tris-HCl pH 8.0, 8% SDS, 60 mM EDTA, 40% glycerol, 0.008% bromophenol blue) to terminate the reaction, and kept at 20 °C until gel analysis. Samples were analyzed by SDS-PAGE followed by phosphorimager analysis (STORM 860, Molecular Dynamics) to quantitate radiolabeled band intensity. Dephosphorylation of phospho-SSK1-R2 followed first-order rate kinetics and the half-life of phospho-SSK1-R2 was determined according to the formula $t_{1/2} = ln2/k$, where k is the rate constant for the dephosphorylation reaction.

2.3 Results

2.3.1 Effect of osmolytes on the stability of the YPD1•SSK1-RR complex

A value of 13 ± 3 min was previously measured for the half-life of phosphorylated SSK1-R2 in the absence of YPD1 (Janiak-Spens, Sparling *et al.,* 2000). However, in the presence of YPD1, the phosphorylated SSK1-R2 half-life increased to 38 ± 4 hrs (Janiak-Spens, Sparling *et al.,* 2000). Thus, it was proposed

that the HPt protein YPD1 forms a complex with SSK1 and sterically shields the phosphorylated aspartate residue from hydrolysis. However, the mechanism of rapid dephosphorylation of SSK1-RR~P under conditions of hyperosmotic stress remains unclear.

In order to assess the stability of the phosphorylated form of SSK1-RR under conditions of hyperosmotic stress, the half-life of SSK1-RR~P was first measured as a function of osmolyte concentration in the presence of YPD1. Osmolytes used were glycerol (Figure 2-1), betaine (Figure 2-2), proline (Figure 2-3), sodium chloride (Figure 2-4), and trehalose (Figure 2-5). Ficoll 400 was also tested as a control for viscosity (Figure 2-6). Throughout the course of the experiment, no trace of phosphorylated YPD1 was detectable, suggesting that there is no observable reverse phosphotransfer reaction between the two proteins. Our results demonstrate an approximately 2-fold decrease in the life-time of phosphorylated SSK1-RR in the presence of YPD1 and osmolytes (with the exception of proline) (Figure 2-7).

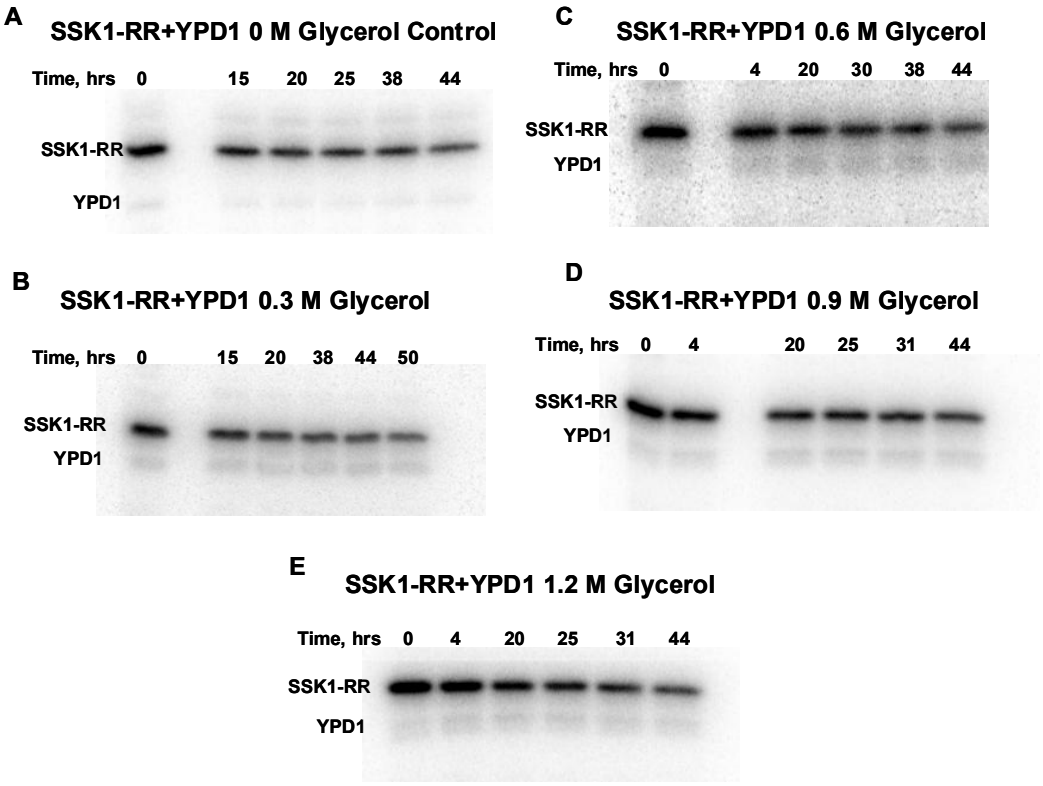

Figure 2-1. ***In vitro*** **dephosphorylation of SSK1-RR in the presence of YPD1 and glycerol.** The dephosphorylation reaction mixtures contained equimolar amounts of SSK1-RR and YPD1 in all reactions mixtures. Various concentrations of glycerol were examined: A) 0 M glycerol; B) 0.3 M glycerol; C) 0.6 M glycerol; D) 0.9 M glycerol; E) 1.2 M glycerol. After incubation for the specified amount of time, sample aliquots were taken and quenched by addition of 5 εl of 4 × stop buffer (8% SDS and 80 mM EDTA). Reaction products were separated by 15% SDS-PAGE and the gel was then subjected to phosphorimager analysis.

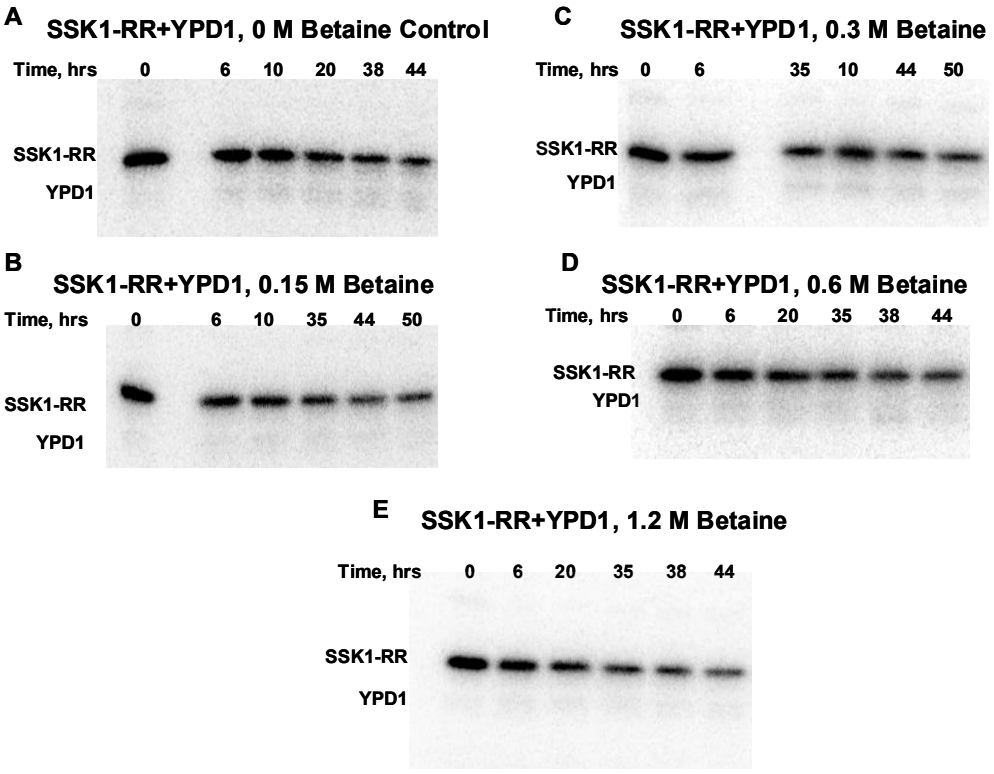

Figure 2-2. *In vitro* dephosphorylation of SSK1-RR in the presence of YPD1 and betaine. The dephosphorylation reaction mixtures contained equimolar amounts of SSK1-RR and YPD1 in all reactions mixtures. Various concentrations of betaine were examined: A) 0 M Betaine; B) 0.15 M Betaine; C) 0.3 M Betaine; D) 0.6 M Betaine; E) 1.2 M Betaine. After incubation for the specified amount of time, sample aliquots were taken and quenched by addition of 5 εl of 4 × stop buffer (8% SDS and 80 mM EDTA). Reaction products were separated by 15% SDS-PAGE and the gel was then subjected to phosphorimager analysis.

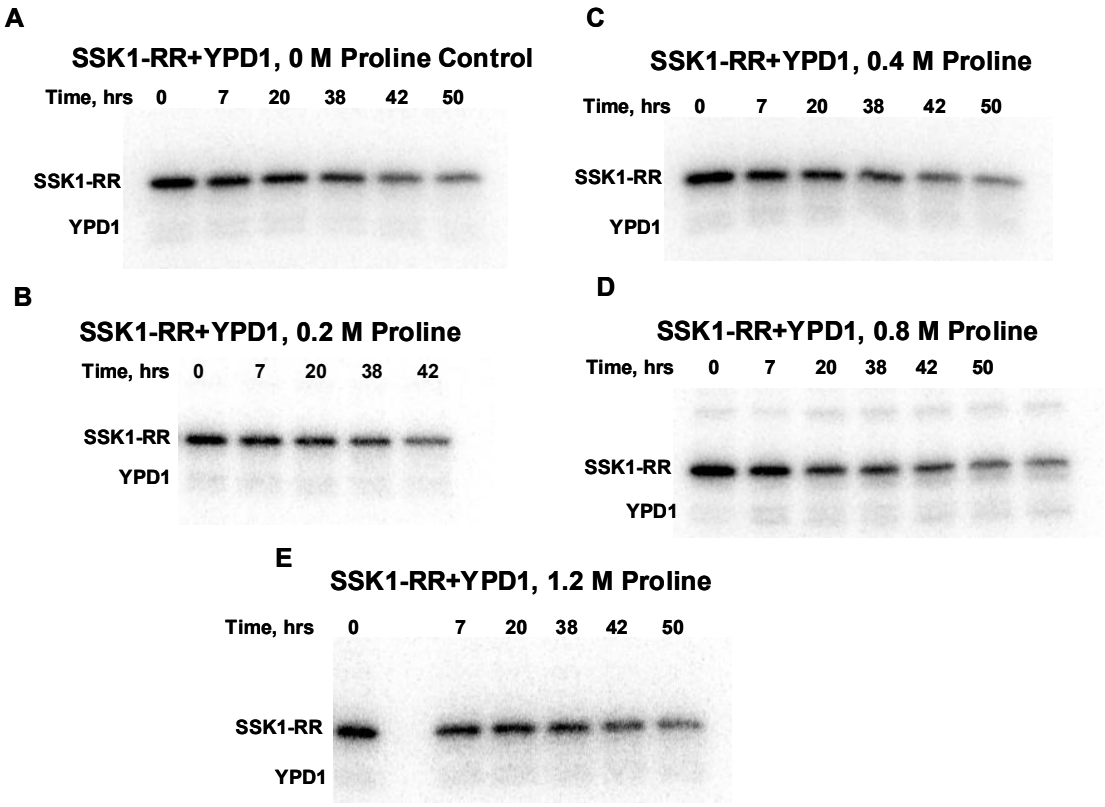

Figure 2-3. *In vitro* dephosphorylation of SSK1-RR in the presence of YPD1 and proline. The dephosphorylation reaction mixtures contained equimolar amounts of SSK1-RR and YPD1 in all reactions mixtures. Various concentrations of proline were examined: A) 0 M Proline; B) 0.2 M Proline; C) 0.4 M Proline; D) 0.8M Proline; E) 1.2 M Proline. After incubation for the specified amount of time, sample aliquots were taken and quenched by addition of 5 εl of 4 × stop buffer (8% SDS and 80 mM EDTA). Reaction products were separated by 15% SDS-PAGE and the gel was then subjected to phosphorimager analysis.

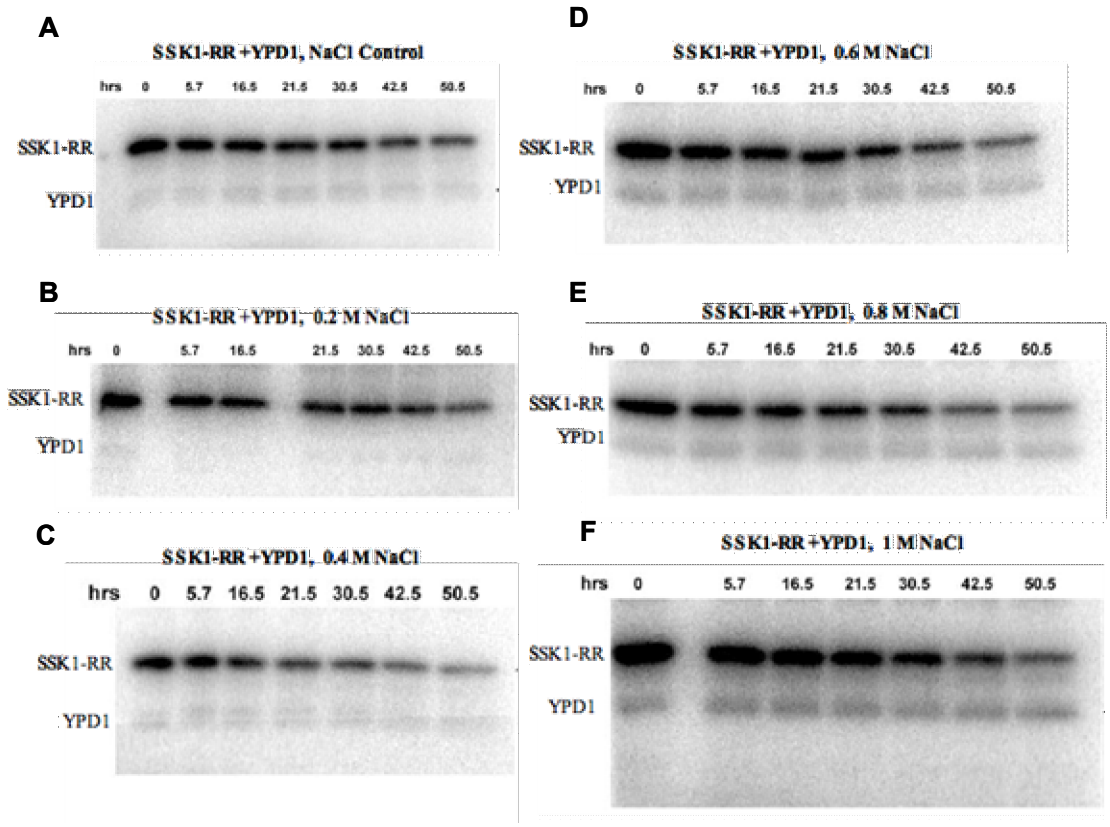

Figure 2-4. ***In vitro*** **dephosphorylation of SSK1-RR in the presence of YPD1 and sodium chloride.** The dephosphorylation reaction mixtures contained equimolar amounts of SSK1-RR and YPD1 in all reactions mixtures. Various concentrations of sodium chloride were examined: A) 0 M NaCl; B) 0.2 M NaCl; C) 0.4 M NaCl; D) 0.6 M NaCl; E) 0.8 M NaCl; F) 1 M NaCl. After incubation for the specified amount of time, sample aliquots were taken and quenched by addition of 5 εl of 4 × stop buffer (8% SDS and 80 mM EDTA). Reaction products were separated by 15% SDS-PAGE and the gel was then subjected to phosphorimager analysis.

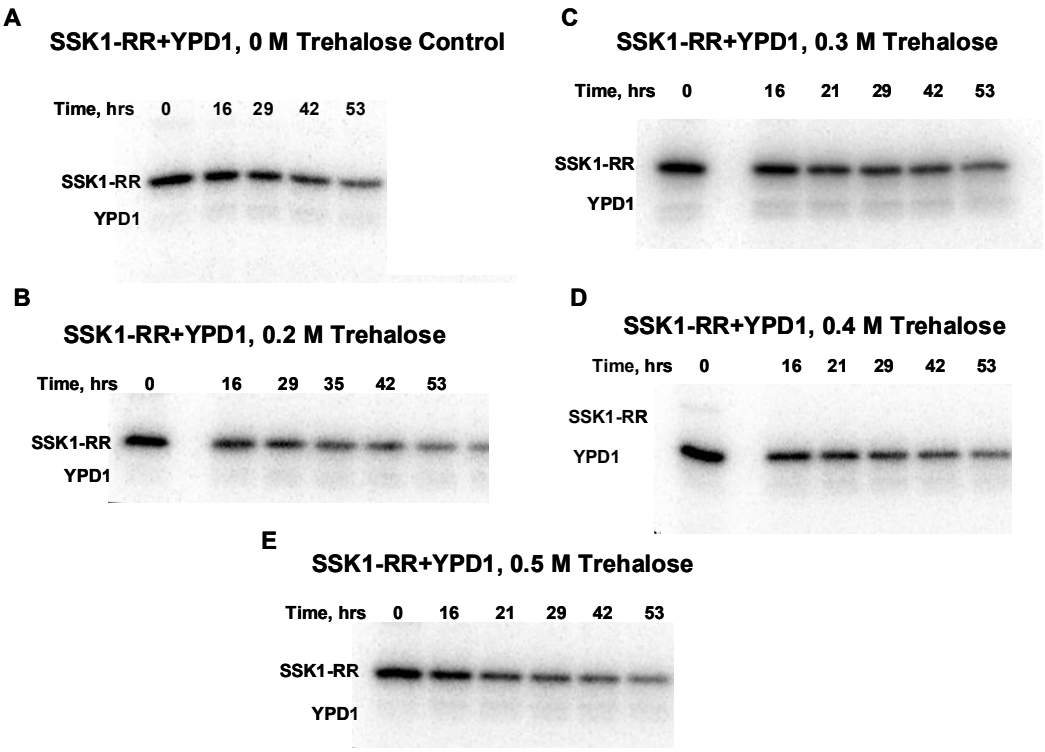

Figure 2-5. ***In vitro*** **dephosphorylation of SSK1-RR in the presence of YPD1 and trehalose.** The dephosphorylation reaction mixtures contained equimolar amounts of SSK1-RR and YPD1 in all reactions mixtures. Various concentrations of trehalose were examined: A) 0 M Trehalose; B) 0.2 M trehalose; C) 0.3 M Trehalose; D) 0.4 M Trehalose; E) 0.5 M Trehalose. After incubation for the specified amount of time, sample aliquots were taken and quenched by addition of 5 εl of 4 × stop buffer (8% SDS and 80 mM EDTA). Reaction products were separated by 15% SDS-PAGE and the gel was then subjected to phosphorimager analysis.

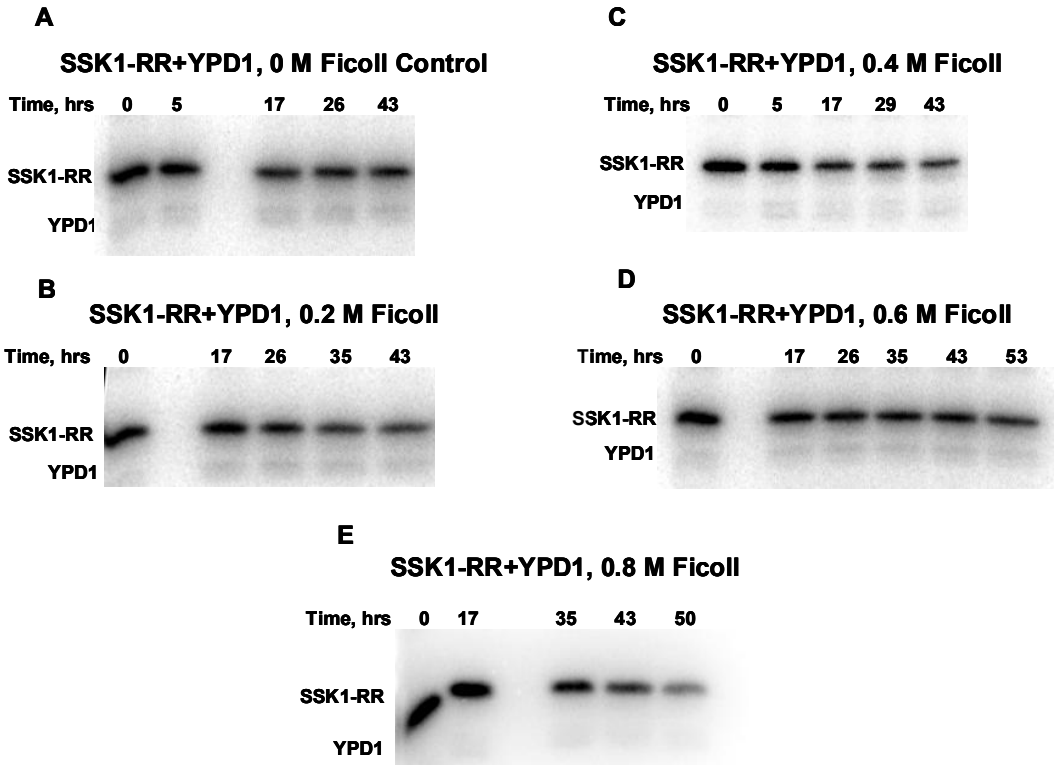

Figure 2-6. *In vitro* dephosphorylation of SSK1-RR in the presence of YPD1 and Ficoll 400. The dephosphorylation reaction mixtures contained equimolar amounts of SSK1-RR and YPD1 in all reactions mixtures. Various concentrations of Ficoll were examined: A) 0 M Ficoll 400; B) 0.2 M Ficoll 400; C) 0.4 M Ficoll 400; D) 0.6 M Ficoll 400; E) 0.8 M Ficoll 400. After incubation for the specified amount of time, sample aliquots were taken and quenched by addition of 5 εl of 4 × stop buffer (8% SDS and 80 mM EDTA). Reaction products were separated by 15% SDS-PAGE and the gel was then subjected to phosphorimager analysis.

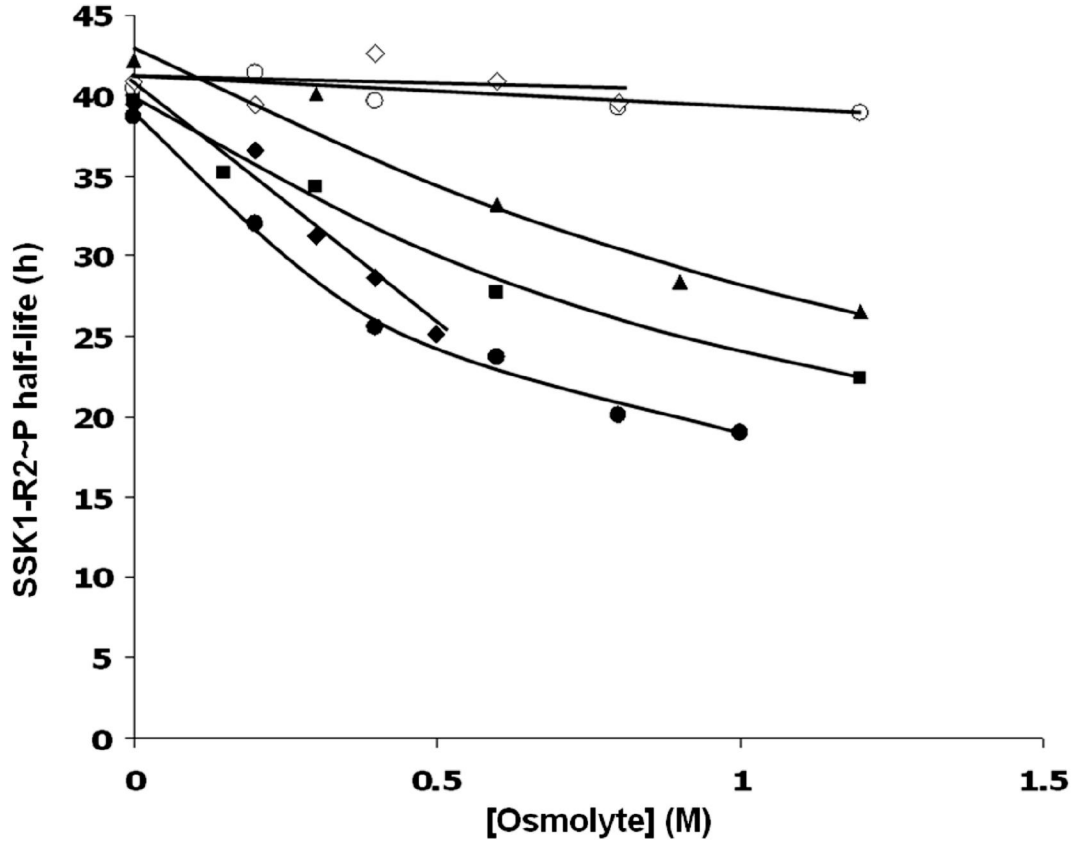

Figure 2-7. Effects of osmolytes on the half-life of SSK1-RR~P. Curves are drawn by hand for (ʒ) proline, (ö) Ficoll 400, (ʑ) glycerol, (ƴ) betaine, (Dƶtrehalose, and (ŏ) NaCl.

2.3.2 Effect of osmolytes on the SSK1-RR phosphorylated half-life

To determine if the observed effect of osmolytes on the SSK1-RR phosphorylated lifetime is due to an affect on protein-protein interaction between YPD1 and SSK1-RR or a direct influence on SSK1-RR~P intrinsic stability, the same experiments were repeated in the absence of YPD1.

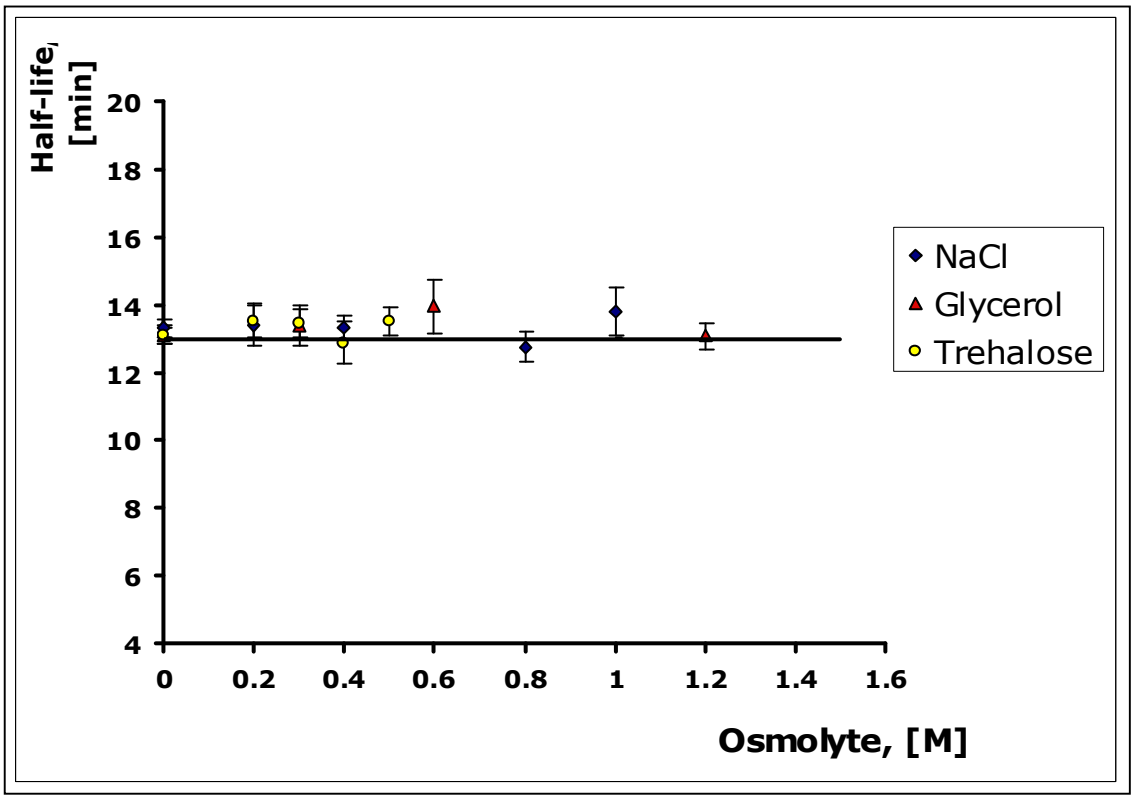

Figure 2-8. Effects of osmolytes on the half-life of SSK1-RR~P in the absence of YPD1. (D,ŽNaCl, (z) glycerol, (ŏ) (ʒ) trehalose.

Osmolytes used were glycerol, sodium chloride and trehalose (Figure 2-8). In contrast to the experiments carried out in the presence of YPD1, experiments conducted in the absence of YPD1 showed no effect of osmolytes on the intrinsic stability of SSK1-RR~P.

2.4 Discussion

The nature of the interaction between SSK1-RR and YPD1 is important due to the regulatory function of SSK1-RR and its phosphorylation state that controls to activation or inactivation of the HOG1 MAP kinase cascade. Previous *in vitro* studies have suggested a protective role for YPD1 in shielding the phosphoryl group of SSK1-RR from hydrolysis (Janiak-Spens, Sparling *et al.,* 1999; Janiak-Spens, Sparling *et al.,* 2000). A protein-protein interaction such as this would help prevent activation of HOG1 under non-osmotic stress conditions. Increasing osmolyte concentrations caused a reduction in the half-life of SSK1-RR~P in the presence of YPD1 by approximately 2-fold (Figure 2-7). Ficoll 400 was used as a control for viscosity and had shown no effect on the SSK1-RR~P stability in the presence of YPD1 (Figure 2-7). Additionally, in the absence of YPD1, osmolytes had also no effect on the intrinsic stability of SSK1-RR~P (Figure 2-8). Our data suggest that osmolytes negatively affect the stability of the SSK1-RR~P·YPD1 complex in a concentration-dependent manner (Figure 2-7) and, as a consequence, the rate of phosphate hydrolysis increases. The underlying mechanism for complex destabilization can be explained as the ability

of osmolytes to create extensive hydrogen bonding and or ionic interactions with surface residues of the proteins involved in the complex as well as conformational changes. Proline was an exception in this case, suggesting that its structural rigidity and higher hydrophobicity compared to other osmolytes, renders it incapable of influencing complex stability. We suggest that this modest 1.5- to 2-fold decrease observed for the SSK1-RR~P half-life in the presence of osmolytes is only one of potentially multiple contributing factors that lead to dephosphorylation of SSK1 and subsequent activation of the HOG1 MAPK cascade. The existence of an SSK1-specific aspartyl phosphatase, for example, cannot be ruled out.

References

Aiba, H., Yamada, H., Ohmiya, R. and Mizuno, T. (1995). "The osmo-inducible *gpd1*$^{+}$ gene is a target of the signaling pathway involving Wis1 MAP-kinase kinase in fission yeast." FEBS Lett. **376**: 199-201.

Blomberg, A. and Adler, L. (1992). "Physiology of osmotolerance in fungi." Adv. Micro. Physiol. **33**: 145-212.

Brewster, J. L., de Valoir, T., Dwyer, N. D., Winter, E. and Gustin, M. C. (1993). "An osmosensing signal transduction pathway in yeast." Science **259**: 1760-1763.

Burg, M. B., and Ferraris, J. D. (2008). "Intracellular organic osmolytes: function and regulation." *J. Biol. Chem.* **283**: 7309-7313.

Fan, J., Whiteway, M. and Shen, S. H. (2005). "Disruption of a gene encoding glycerol 3-phosphatase from *Candida albicans* impairs intracellular glycerol accumulation-mediated salt-tolerance." FEMS Microbiol. Letts. **245**: 107-116.

Hess, J. F., Oosawa, K., Kaplan, N. and Simon, M. I. (1988). "Phosphorylation of three proteins in the signaling pathway of bacterial chemotaxis." Cell **53**: 79-87.

Hohmann, S. (2002). "Osmotic stress signaling and osmoadaptation in yeasts." Microbiol. Mol. Biol. Rev. **66**(2): 300-372.

Horie T., Tatebayashi K., Yamada R. and H., S. (2008). "Phosphorylated Ssk1 prevents unphosphorylated Ssk1 from activating the Ssk2 mitogen-activated protein kinase kinase kinase in the yeast high-osmolarity glycerol osmoregulatory pathway." Mol Cell Biol **28**(17): 5172-83.

Janiak-Spens, F., Cook, P. F. and West, A. H. (2005). "Kinetic analysis of YPD1-dependent phosphotransfer reactions in the yeast osmoregulatory phosphorelay system." Biochemistry **44**(1): 377-386.

Janiak-Spens, F., Sparling, D. P. and West, A. H. (2000). "Novel role for an HPt domain in stabilizing the phosphorylated state of a response regulator domain." J. Bacteriol. **182**(23): 6673-6678.

Janiak-Spens, F., Sparling, J. M., Gurfinkel, M. and West, A. H. (1999). "Differential stabilities of phosphorylated response regulator domains reflect functional roles of the yeast osmoregulatory SLN1 and SSK1 proteins." J. Bacteriol. **181**(2): 411-417.

Klipp, E., Nordlander, B., Krüger, R., Gennemark, P. and Hohmann, S. (2005). "Integrative model of the response of yeast to osmotic shock." Nature Biotech. **23**(8): 975-982.

Li, S., Ault, A., Malone, C. L., Raitt, D., Dean, S., Johnston, L. H., Deschenes, R. J. and Fassler, J. S. (1998). "The yeast histidine protein kinase, Sln1p, mediates phosphotransfer to two response regulators, Ssk1p and Skn7p." EMBO J. **17**(23): 6952-6962.

Millar, J. B. A. (1999). "Stress-activated MAP kinase (mitogen-activated protein kinase) pathways of budding and fission yeast." Biochem. Soc. Symp. **64**: 49-62.

Ota, I. M. and Varshavsky, A. (1993). "A yeast protein similar to bacterial two-component regulators." Science **262**: 566-569.

Posas, F. and Saito, H. (1998). "Activation of the yeast SSK2 MAP kinase kinase kinase by the SSK1 two-component response regulator." EMBO J. **17**(5): 1385-1394.

Posas, F., Wurgler-Murphy, S. M., Maeda, T., Witten, E. A., Thai, T. C. and Saito, H. (1996). "Yeast HOG1 MAP kinase cascade is regulated by a multistep phosphorelay mechanism in the SLN1-YPD1-SSK1 "two-component" osmosensor." Cell **86**: 865-875.

Shankarnarayan, S., Malone, C. L., Deschenes, R. J. and Fassler, J. S. (2008). "Modulation of yeast SLN1 kinase activity by the CCW12 cell wall protein." J. Biol. Chem. **283**(4): 1962-1973.

Stock, A. M., Robinson, V. L. and Goudreau, P. N. (2000). "Two-component signal transduction." Annu. Rev. Biochem. **69**: 183-215.

Thomé, P. E., and Trench, R. K. (1999). "Osmoregulation and the Genetic Induction of Glycerol-3-phosphate Dehydrogenase by NaCl in the Euryhaline Yeast *Debaryomyces hansenii* " *Mar. Biotechnol.* ***1***: 230-238.

Wright, G. D., Holman, T. R. and Walsh, C. T. (1993). "Purification and characterization of VanR and the cytosolic domain of VanS: A two-component regulatory system required for vancomycin resistance in *Enterococcus faecium* BM4147." Biochemistry **32**: 5057-5063.

Xu, Q., Nguyen, V. and West, A. H. (1999). "Purification, crystallization, and preliminary X-ray diffraction analysis of the yeast phosphorelay protein YPD1." Acta Cryst. **D55**: 291-293.

Chapter 3

Effect of osmolytes on the phosphotransfer rates between SLN1-RR/YPD1 and YPD1/SSK1-RR protein pairs

ñPortions of this chapter are reproduced with automatic permission from [Kaserer A.O., Babak A., Cook P.F., West A.H. (2009) Effects of Osmolytes on the SLN1-YPD1-SSK1 Phosphorelay system from *Saccharomyces cerevisiae*., *Biochemistry.* v. 48(33), p. 8044-50]ò.

In Chapter 2, I described the effect of osmolytes on the half-life of the phosphorylated SSK1-RR in the presence and absence of YPD1. We showed that increasing osmolyte concentrations caused a reduction in the half-life of SSK1-RR~P in the presence of YPD1 by approximately 2-fold and had no effect on the SSK1-RR~P stability in the absence of YPD1, suggesting that osmolytes negatively affect YPD1·SSK1~P complex stability. In this chapter, I describe the effect of osmolyte concentrations on the phosphotransfer kinetics of the SLN1-YPD1-SSK1 multi-step phosphorelay pathway from *S. cerevisiae* can not be ruled out.

Previous studies conducted from the West laboratory used rapid-quench kinetics to characterize the individual phosphotransfer reactions between YPD1 and the response regulator domains associated with SLN1, SSK1 and SKN7 (Janiak-Spens, Cook *et al.,* 2005). For the SLN1-RR~P to YPD1 reaction, a maximum forward rate constant of 29 s^{-1} was determined with a K_d of 1.4 ε M for the SLN1-RR~P·YPD1 complex. A very rapid phosphotransfer rate of 160 s^{-1} was measured for the subsequent reaction between YPD1~P to SSK1-RR and the reaction was strongly favored over phosphotransfer to SKN7-RR. Phosphotransfer reactions between YPD1 and SLN1-RR or SKN7-RR were reversible; while reverse transfer from SSK1-RR~P

to YPD1 was not observed under the conditions tested. These parameters are in good agreement with the concept that SSK1 is constitutively phosphorylated under normal osmotic conditions (Posas, Saito 1998; Janiak-Spens, Cook *et al.,* 2005; Horie T., Tatebayashi K. *et al.,* 2008).

We therefore examined the effect of on osmolyte concentrations on the kinetics of the individual phosphotransfer reactions. This study provides new insights into the mechanisms that underlie the osmoregulatory pathway in *S. cerevisiae* and the specific effects of osmolytes in regulating the pathway.

3.2 Materials and methods

3.2.1 Materials

All chemicals and biochemicals were of ultrapure grade. Glutathione-Sepharose 4B resin was purchased from Amersham. [γ-^{32}P] ATP (3000 Ci/mmol) was purchased from Perkin-Elmer. Chymostatin, aprotinin, pepstain, phosphoramidon, E-64, leupeptin, antipain, sodium metabisulfite were purchased from Sigma and benzamidine was purchased from Fluka. Ficoll 400, D-(+)-trehalose, proline and betaine were purchased from Sigma. NaCl and glycerol were from Mallinckrodt Chemicals and Pharmco-Aaper, respectively.

3.2.2 Protein expression and purification

Bacterial strains used for protein purification are presented in Table 3-1.

Protein expressed	Plasmid number	Plasmid name	Strain number	*E. coli* strain, antibiotic resistance
GST-SLN1-HK-RR	OU119	pGEX-GST-HK-RR	OU253	BL21 (DE3) Star/ Amp^R
SLN1-RR	OU29	pETCYB-SLN1-RR	OU29	BL21 (DE3) Star/ Amp^R
YPD1	OU15	pUC12-YPD1	OU6	DH5Ŭ Amp^R
SSK1-RR	OU26	pETCYB-SSK1-RR	OU357	BL21 (DE3)/ Amp^R, Cm^R

Table 3-1. Plasmid constructs used for protein expression and purification. An OU number was assigned for each individual plasmid construct and transformed in *E. coli* strain.

GST-SLN1-HK-RR protein expression and purification (Janiak-Spens, Cook *et al.,* 2005)

Escherichia coli BL21 (DE3) Star cells (strain OU 253) containing the pGEX-GST-SLN1-HK-RR (plasmid OU 119 including SLN1-HK-RR 530 ï 1220 amino acids) vector were inoculated into 10 mL of LB medium with 100 ε g $mL^{ī 1}$ of ampicillin and shaken overnight at 37 ºC. The cell culture was further inoculated into 1 L of prewarmed LB medium in the presence of 100 ε g $mL^{ī 1}$ of ampicillin and shaken at 37°C. When the optical density (at 600 nm) of the culture reached 0.6, the cells were cooled to room temperature and expression of SLN1-HK-RR was induced by the addition of IPTG to a final concentration of 1 mM. The cultures were shaken for 20-22 hrs at 16°C and then harvested, washed with 50 ml of the wash buffer (50 mM Tris-HCl, pH 8, 1 mM EDTA and 2 mM DTT), then resuspended at 5 mL $g^{ī 1}$

(wet weight) with the cell buffer SP1 (50 mM Tris-HCl, pH 8, 150 mM NaCl, 1 mM EDTA, 1% Triton X-100, 0.1% ϐME, 1 mM PMSF and 1 x protease inhibitor cocktail, see Chapter 2). Cells were lysed by sonication, and the lysates were clarified by centrifugation in a JA-20 rotor at 27, 200 *x g* for 1 h at 4°C. The supernatant was loaded onto a 2 mL glutathione bead column equilibrated in SP1 buffer at 4°C. The column was washed sequentially with 20 mL of SP1 buffer and incubated overnight at 4°C. Thereafter the column was washed with 10 mL of SP2 buffer (50 mM Tris-HCl, pH 8, 2 mM DTT and 1 mM EDTA) and 20 mL of SP3 buffer (50 mM Tris-HCl, pH 8, 100mM KCl, 2 mM DTT, 1 mM EDTA and 10% glycerol). Next, 2 mL of the SP3 buffer was left above the column bed and gently mixed with the beads. The suspension was immediately aliquoted (50 εL) in eppendorf tubes and stored at ï 20°C. The protein was judged to be ~90% homogeneous based on analysis by SDS-PAGE.

SLN1-RR protein expression and purification (Janiak-Spens, Sparling *et al.,* 1999)

Escherichia coli BL21 (DE3) Star cells (strain OU 29) containing the pETCYB-SLN1-RR (plasmid OU 29) vector were inoculated into 10 mL of LB medium with 100 εg $mL^{ï 1}$ of ampicillin and shaken overnight at 37 ºC. The cell culture was further inoculated into 1 L of prewarmed LB medium in the presence of 100 εg $mL^{ï 1}$ of ampicillin and shaken at 37°C. When the optical density (at 600 nm) of the culture reached 0.8, the cells were cooled to room temperature and expression

of SLN1-RR was induced by the addition of IPTG to a final concentration of 0.4 mM. The cultures were shaken at room temperature for about 8 hrs and then harvested, washed with cell wash buffer (0.1 M Na-phosphate, pH 7 and 1 mM EDTA) resuspended at 5 mL g^{-1} (wet weight) of cells in lysis buffer (20 mM Tris-HCl, pH 7.5, 500 mM NaCl, 1 mM EDTA, 0.1% Triton X-100). Cells were lysed by sonication, and the lysates were clarified by centrifugation at 27, 200 *x g* for 1 h at 4°C. The supernatant was loaded onto a 3 mL chitin bead column equilibrated in lysis buffer at 4°C. The column was washed sequentially with 100 mL of lysis buffer and 25 mL of cleavage buffer (20 mM Tris-HCl, pH 7.5, 50 mM NaCl, 1 mM EDTA, 5 mM ATP, 10 mM $MgCl_2$). Thereafter the column was washed immediately with 25 mL of cleavage buffer containing 30 mM ϐME and incubated overnight at 4°C. The protein was eluted with the cleavage buffer and further purified by separation on a gel filtration column (Sephadex G50, 300 ml bed volume) equilibrated in 20 mM Tris-HCl, pH 7.5, 50 mM NaCl, 1 mM EDTA, and 1.4 mM ϐME. Fractions containing SLN1-RR were pooled and concentrated by using a Centricon 10 (Amicon) filter unit. The protein was judged to be ~90% homogeneous based on analysis by SDS-PAGE. The protein concentration was determined by absorbance at 280 nm using a calculated extinction coefficient of 4020 $M^{-1}cm^{-1}$. Typical yields were 1 mg L^{-1} of cells. Purified SLN1-RR protein was stored in gel filtration buffer in the presence of 10% glycerol at −20°C.

The GST-SLN1-HK-RR, YPD1 and SSK1-RR proteins were purified as described in Chapter 2.

3.2.3 *In vitro* phosphorylation

SLN1-RR Phosphorylation.

The SLN1-RR domain was phosphorylated via incubation with the SLN1-HK domain as follows. GST-tagged SLN1-HK (7 εM) bound to glutathione-Sepharose 4B resin was incubated with 7 εM [ɔ-^{32}P] ATP for 30 min. Unincorporated [ɔ-^{32}P] ATP was washed from phospho-SLN1-HK with 50 mM Tris-HCl, pH 8.0, 100 mM KCl, 15 mM $MgCl_2$, 2 mM DTT, and 20% glycerol by 3 consecutive centrifugations (1 min at 1000 x *g*). The SLN1-RR protein (18.6 εM) was then added in the same buffer and incubated for 10 min at room temperature in a total volume of 300 εL. Phospho-SLN1-RR was recovered in the supernatant after gently pelleting the GST-SLN1-HK bound to the resin. EDTA was added to the supernatant to a final concentration of 30 mM to prevent autodephosphorylation (Janiak-Spens, Cook *et al.,* 2005).

YPD1 Phosphorylation.

The YPD1 protein was phosphorylated similarly to that of SLN1-RR with the following modifications. Incubation of GST-tagged SLN1-HK-R1 (7 εM) and [ɔ-32P] ATP (7 εM) was for 60 min (Janiak-Spens, Cook *et al.,* 2005). YPD1 protein (18.6 εM) then was added in the reaction mixture for phosphorylation.

3.2.4 Measurement of phosphotransfer rates using quench-flow kinetics

Experiments were carried out to obtain rate data for the individual phosphotransfer steps using a rapid-quench kinetics instrument SFM-Q/4 Quench-Flow instrument (BioLogic). Phosphotransfer reactions were monitored in the millisecond timescale for acquisition of pre-steady state experimental data. The phosphodonor protein was diluted to 0.45 εM in 50 mM Tris-HCl, pH 8.0, 1 mM EDTA, 1 mM DTT and glycerol (0.3-1.2 M), or NaCl (0.2-1.0 M). The diluted phosphorylated protein (60 εL) was then mixed with 60 εL of phospho-accepting protein partner (0.45 εM-20 εM) in 50 mM Tris-HCl, pH 8.0, 20 mM $MgCl_2$, 1 mM DTT and 0.3-1.2 M glycerol, or 0.2-1 M NaCl, or glycerol/NaCl combinations (0.3/0.2 M, 0.55/0.4 M and 0.75/0.6 M). The reactions were quenched with 60 εL of stop buffer (8% SDS, 80 mM EDTA) after a specified time. To analyze the results, 30 εL of the quenched reaction was mixed with 10 εL of 4% SDS-PAGE loading buffer (200 mM Tris pH 6.8, 400 mM DTT or ϐ-mercaptoethanol, 8% SDS, 0.4 % bromophenol blue, and 40% glycerol) , and then 30 εL samples were loaded onto 15% SDS-PAGE gels. After gel electrophoresis, wet gels were wrapped in plastic wrap and analyzed using a phosphorimager (Molecular Dynamics, Storm 840). The phosphotransfer reaction kinetic parameters were quantified based on the disappearance of the ^{32}P-label from the phospho-donor protein or the appearance of ^{32}P-label in the phospho-accepting protein. The data were analyzed using the least squares fitting of Excel (Microsoft Office v. 10.1.12) and Enzfitter (version 2.04,

Biosoft, Cambridge, U.K.). Individual datasets were analyzed using eq 1 for experiments with NaCl, glycerol, Ficoll 400 and NaCl-glycerol combinations,

$$k_{obs} = k_{rev} + k_{fwd}\left(\frac{[S]}{K_d + [S]}\right) \quad (1)$$

where [S] is the concentration of the phospho-accepting protein, k_{obs} is the observed first order rate constant for the phosphotransfer reaction at a particular [S], k_{fwd} is the maximal forward net rate constant for phosphoryl transfer from the phosphorylated protein to the phospho-acceptor protein, k_{rev} is the corresponding maximum reverse net rate constant for the reaction between phospho-donor and phospho-acceptor proteins, and K_d is the dissociation constant of the phospho-donor-acceptor complex. The concentration of Ficoll 400 used in the control experiment was 0.75 M.

3.3. Results

3.3.1 Effect of individual osmolytes on the phosphotransfer rates from SLN1-RR to YPD1

Rapid mixing of SLN1-RR~P and YPD1 followed by rapid quench allowed measurement of first order rate constants by concurrently monitoring the disappearance of SLN1-RR~P and the appearance of YPD1~P (Scheme 3-1):

$$\text{SLN1-R1~P + YPD1} \underset{k_{-1}}{\overset{k_1}{\rightleftharpoons}} \text{[SLN1-R1~P·YPD1]} \underset{k_{-2}}{\overset{k_2}{\rightleftharpoons}} \text{[SLN1-R1·YPD1~P]} \underset{k_{-3}}{\overset{k_3}{\rightleftharpoons}} \text{SLN1-R1 + YPD1~P}$$

Reaction	SLN1-RR~P + YPD1			
NaCl	**0 M**	**0.2 M**	**0.6 M**	**1 M[b]**
k_{fwd} (s^{-1})	27.0 ±2.6	32.9 ±1.8	24.6 ±0.8	14.7 ± 0.8
k_{rev} (s^{-1})	9.2 ± 3.3	0.21 ± 2.1[c]	10.0 ±0.9	20.7 ± 0.4
K_d (εM)	2.8 ± 0.8	2.3 ± 0.6	2.6 ± 0.4	6.2 ± 1.6
k_{fwd}/K_d ($\varepsilon M^{-1} s^{-1}$)	9.6 ± 2.9	14.3 ± 3.8	9.5 ± 1.5	2.4 ± 0.6

Table 3-2. Kinetic constants[a] for phosphotransfer reactions in the absence and presence of NaCl. [a] The data used to calculate the values in this table were obtained in triplicate and the errors represent standard errors of the mean. [b] 1 M NaCl is considered not physiologically relevant. [c] Undefined.

All data were obtained in triplicate and were analyzed using eq 1 (in the methods section) to calculate the values shown in Tables 1-3. In the absence of osmolytes, the maximum forward rate constant, k_{fwd}, was 27.0 ± 2.6 s^{-1}, while the K_d for the SLN1-RR~P·YPD1 complex was 2.8 ± 0.8 μM, in good agreement with previously obtained data in the absence of osmolytes (Janiak-Spens, Cook *et al.,* 2005).

Subsequent phosphotransfer reactions between SLN1-RR~P and YPD1 were performed in the presence of different NaCl concentrations (as shown in Table 3-2, Figure 3-1). The value of k_{fwd} decreases from 27.0 ± 2.6 s^{-1} with no NaCl present to a

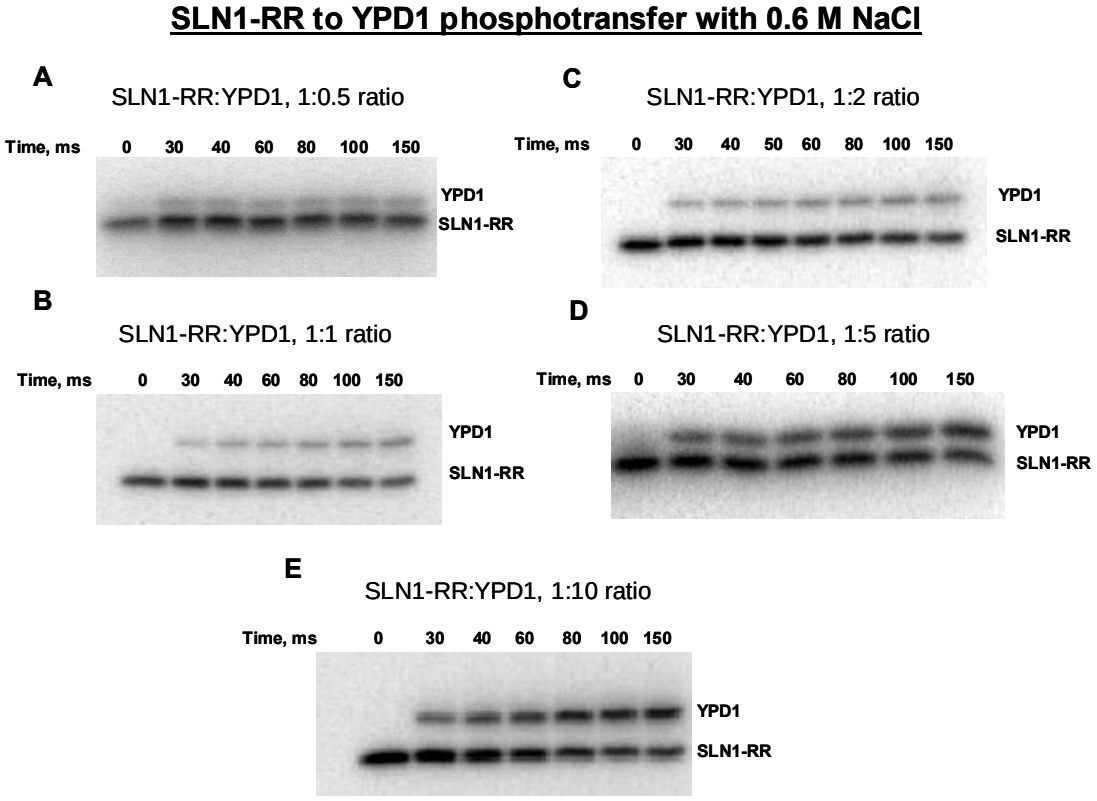

Figure 3-1. Phosphotransfer reaction from SLN1-RR to YPD1 in the presence of 0.6 M NaCl. Rapid mixing of specific molar ratios of SLN1-RR~P and YPD1 in the presence of 0.6 M NaCl followed by rapid quench with monitoring the disappearance of SLN1-RR~P and the appearance of YPD1~P . A) 1:0.5 ratio; B) 1:1 ratio; C) 1:2ratio; D) 1:5 ratio and E) 1:10 ratio.

value of 14.7 ± 0.8 s$^{ï 1}$ at 1 M NaCl, while k_{rev} increases from 9.2 ± 3.3 s^{-1} to 20.7 ± 0.4 s^{-1} at 1 M NaCl. No change in the dissociation constant was observed up to 0.6 M NaCl. A slight increase was observed at 1 M salt. For the second order rate constant

Reaction	SLN1-R1~P + YPD1			
Glycerol	**0 M**	**0.3 M**	**0.75 M**	**1.2 M**
k_{fwd} (s^{-1})	27.0 ±2.6	36.5 ±1.4	48.3 ± 2.1	62.3 ± 1.0
k_{rev} (s^{-1})	9.2 ± 3.3	7.5 ± 1.1	11.3 ± 0.6	14.5 ± 0.1
K_d (εM)	2.8 ± 0.8	4.6 ± 0.8	10 ± 1	18 ± 1
k_{fwd}/K_d ($\varepsilon M^{-1} s^{-1}$)	9.6 ± 2.9	7.9 ± 1.4	4.8 ± 0.6	3.4 ± 0.1

Table 3-3. Kinetic constants[a] for phosphotransfer reactions in the absence and presence of glycerol. [a] The data used to calculate the values in this table were obtained in triplicate and the errors represent standard errors of the mean.

(k_{fwd}/K_d), the limit of eq 1 when [S] tends to zero and k_{rev} = 0, remained unchanged from 0 to 0.6 M NaCl. The highest concentration of NaCl (1 M) was not considered physiologically relevant (see discussion).

The phosphotransfer reactions between SLN1-RR~P and YPD1 in the presence of glycerol were done in a manner analogous to those in the presence of NaCl (Figure 3-2) with concentrations of glycerol as shown in Figure 3-3, Table 3-3. The concentrations of glycerol chosen reflect the range of intracellular levels observed during hyperosmotic stress (Hohmann 1997; Klipp, Nordlander *et al.,* 2005). The value of k_{fwd} increases from 27.0 ± 2.6 s^{-1} with no glycerol present to a value of 62.3 ± 1.0

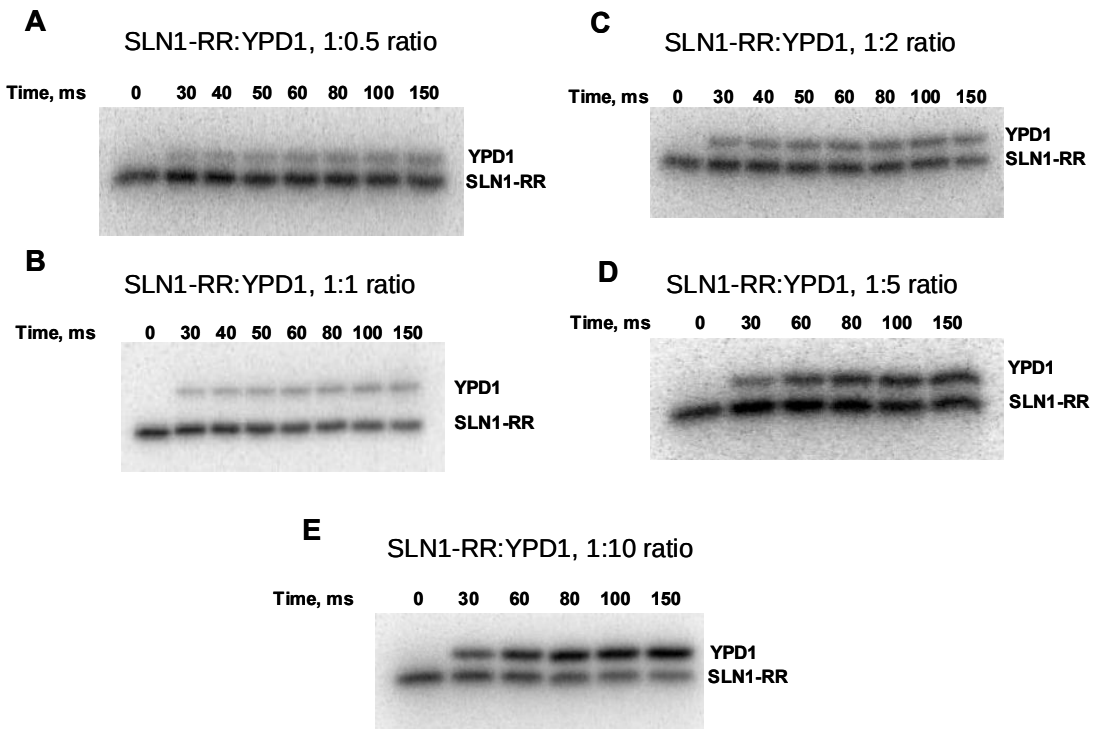

Figure 3-2. Phosphotransfer reaction from SLN1-RR to YPD1 in the presence of 0.75 M Glycerol. Rapid mixing of specific molar ratios of SLN1-RR~P and YPD1 in the presence of 0.75 M Glycerol followed by rapid quench with monitoring the disappearance of SLN1-RR~P and the appearance of YPD1~P . A) 1:0.5 ratio; B) 1:1 ratio; C) 1:2ratio; D) 1:5 ratio and E) 1:10 ratio.

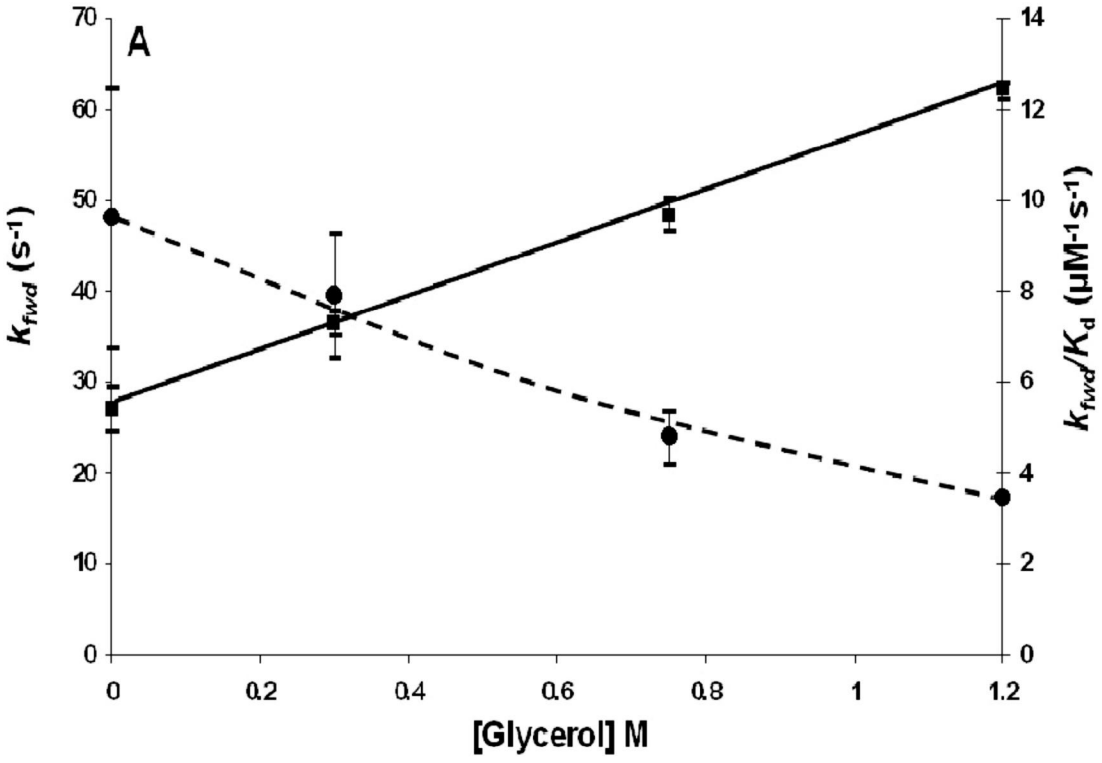

Figure 3-3. Phosphotransfer reactions SLN1-RR to YPD1. A) k_{fwd} and k_{fwd}/K_d for the SLN-RR~P·YPD1 phosphotransfer reaction at different concentrations of glycerol. Curves are drawn by hand for k_{fwd} (y) and k_{fwd}/K_d (•).

s^{-1} at 1.2 M glycerol and the value of k_{rev} increases from 9.2 ± 3.3 s^{-1} to 14.5 ± 0.1 s^{-1}, at 1.2 M glycerol. The dissociation constant increases approximately 6-fold (Figure 3-4) and the second order rate constant decreases approximately 3-fold in the presence of 1.2 M glycerol.

Rate constants were also measured in the presence of both NaCl and glycerol (Table 3-4). The maximum forward rate constant increased by about 2-fold at the

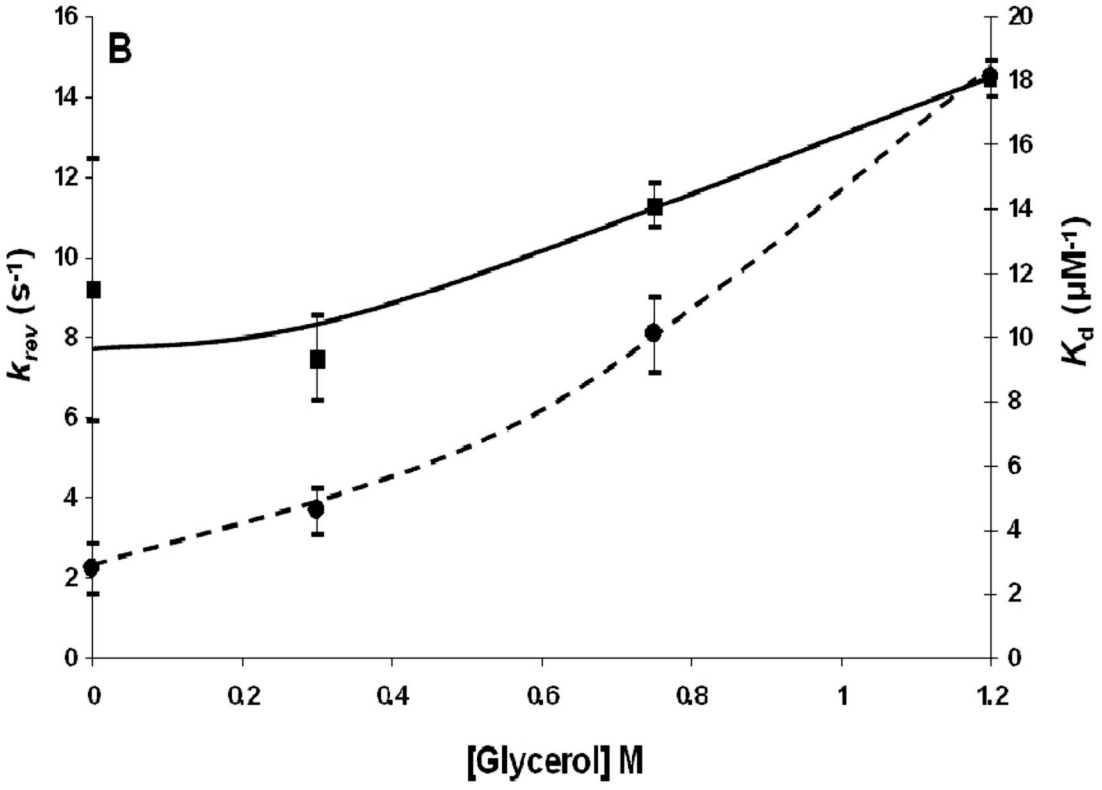

Figure 3-4. Phosphotransfer reactions SLN1-RR to YPD1.B) k_{rev} and K_d for the SLN1-RR~P·YPD1 phosphotransfer reaction at different concentrations of glycerol. Lines are drawn by hand for k_{rev} (y) and K_d (•).

highest concentration of both osmolytes (0.75 M glycerol, 0.6 M NaCl). The reverse rate constant and the K_d values remained unchanged. The combinatory effect of both osmolytes at the highest concentrations tested caused about a 3-fold increase in the second-order rate constant.

Reaction	SLN1-R1~P + YPD1			
[Glycerol]M/ [NaCl]M	**0/0**	**0.3/0.2**	**0.55/0.4**	**0.75/0.6**
k_{fwd} (s^{-1})	27.0 ± 2.6	53.8 ± 1.3	57.5 ± 0.4	66.0 ± 0.8
k_{rev} (s^{-1})	9.2 ± 3.3	5.4 ± 1.4	6.4 ± 0.5	7.2 ± 0.9
K_d (εM)	2.8 ± 0.8	3.2 ± 0.4	2.7 ± 0.1	2.3 ± 0.1
k_{fwd}/K_d ($\varepsilon M^{-1}s^{-1}$)	9.6 ± 2.9	16.8 ± 2.1	21.3 ± 0.8	28.7 ± 1.3

Table 3-4. Kinetic constants[a] for phosphotransfer reactions in the absence and presence of glycerol and NaCl. [a] The data used to calculate the values in this table were obtained in triplicate and the errors represent standard errors of the mean.

3.3.2 Effect of individual osmolytes on the phosphotransfer rates from YPD1 to SSK1-RR

To observe the effect of sodium chloride and glycerol on the phosphotransfer rates between YPD1~P and SSK1-RR, experiments similar to those described above were carried out. In this case, YPD1~P was mixed with SSK1-RR (Scheme 2):

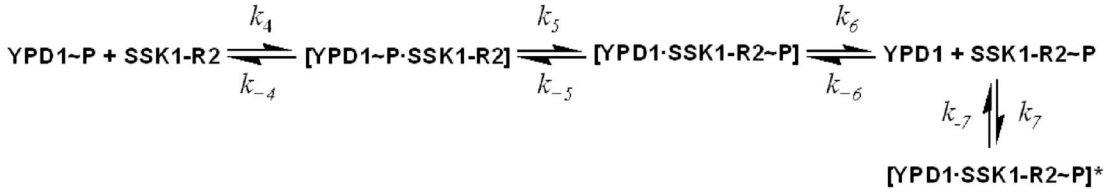

and the data were collected by following the appearance of SSK1-RR~P and disappearance of YPD1~P.

In the absence of osmolytes, the maximum forward rate constant, k_{fwd}, was 110 ± 8.0 s^{-1}. The reverse rate constant, k_{rev}, and K_d for the reaction were 4.1 ± 1.4 s^{-1} and 3.8 ± 1.5 μM, respectively, in good agreement with previously obtained data (Janiak-Spens, Cook *et al.,* 2005). The maximum forward (k_{fwd}) and reverse rate constants (k_{rev}) in the presence of NaCl are shown in Table 3-5, Figure 3-5. The value of k_{fwd} decreases from 110 ± 8.0 s^{-1} with no NaCl present to a value of 32.0 ± 3.2 s^{-1} at 1 M NaCl, while k_{rev} remained essentially the same. The dissociation constant in these experiments did not change significantly. However, there is a deviation on k_{rev} and K_d in going from 0 to 0.2 M, which might be due to systematic error or some unknown phenomenon. The second order rate constant remained unchanged from 0 to 0.6 M NaCl. The highest concentration of NaCl (1 M) was not considered physiologically relevant (see discussion).

In contrast to the effect of glycerol on the phosphotransfer reaction between SLN1-RR~P and YPD1, the effect of glycerol on the phosphotransfer reactions between YPD1~P and SSK1-RR was different. All experiments were conducted in a

Reaction	YPD1~P + SSK1-RR			
NaCl	**0 M**	**0.2 M**	**0.6 M**	**1 M[b]**
k_{fwd} ($s^{ï 1}$)	110 ± 8	77.0 ± 0.2	41.0 ± 0.5	32.0 ± 3.2
k_{rev} ($s^{ï 1}$)	4.1 ± 1.4	0.8 ± 0.3	2.2 ± 0.7	6.1 ± 2.9
K_d (ε M)	3.8 ± 1.5	2.2 ± 0.3	1.4 ± 0.1	3.0 ± 1.6
k_{fwd}/K_d ($\varepsilon M^{ï 1} s^{ï 1}$)	29 ± 4	35.0 ± 4.8	28.6 ± 2.0	10.6 ± 5.8

Table 3-5. Kinetic constants[a] for phosphotransfer reactions in the absence and presence of NaCl. [a] The data used to calculate the values in this table were obtained in triplicate and the errors represent standard errors of the mean. [b] 1 M NaCl is considered not physiologically relevant. [c] Undefined.

manner analogous to those obtained for SLN1-RR~P/YPD1 (Figure 3-6). The forward (k_{fwd}) and the reverse rate constants (k_{rev}) change in the same direction; that is, their values increase with increasing glycerol concentration. Specifically, the value of k_{fwd} increases from 110 ± 8.0 s^{-1} with no glycerol present to a value of 185.0 ± 4.0 s^{-1} at 1.2 M glycerol and the value of k_{rev} increases from 4.1 ± 1.4 s^{-1} to 9.5 ± 1.4 s^{-1}, at 1.2 M glycerol. The dissociation constant increases approximately 3-fold and the second order rate constant remains approximately the same in the presence of 1.2 M glycerol. The data are summarized in Table 3-6.

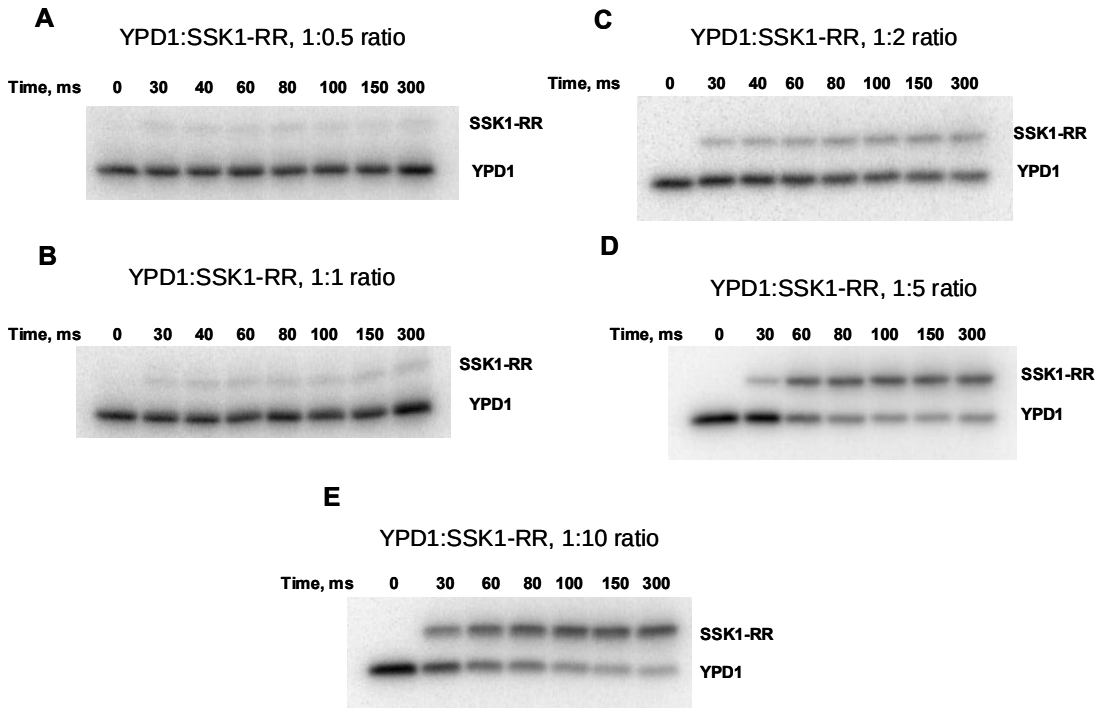

Figure 3-5. Phosphotransfer reaction from YPD1 to SSK1-RR in the presence of 0.6 M NaCl. Rapid mixing of specific molar ratios of YPD1~P and SSK1-RR in the presence of 0.6 M NaCl followed by rapid quench with monitoring the disappearance of YPD1~P and the appearance of SSK1-RR~P . A) 1:0.5 ratio; B) 1:1 ratio; C) 1:2ratio; D) 1:5 ratio and E) 1:10 ratio.

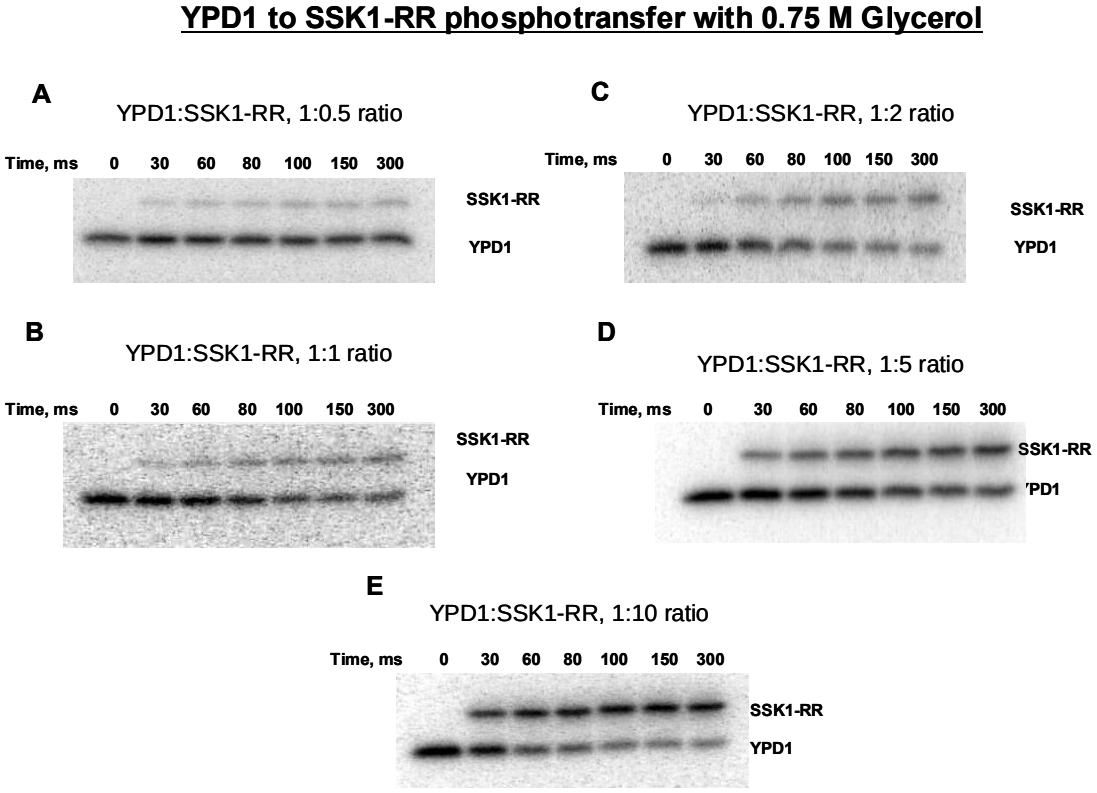

Figure 3-6. Phosphotransfer reaction from YPD1 to SSK1-RR in the presence of 0.75 M Glycerol. Rapid mixing of specific molar ratios of YPD1~P and SSK1-RR in the presence of 0.75 M Glycerol followed by rapid quench with monitoring the disappearance of YPD1~P and the appearance of SSK1-RR~P . A) 1:0.5 ratio; B) 1:1 ratio; C) 1:2ratio; D) 1:5 ratio and E) 1:10 ratio.

Reaction	YPD1~P + SSK1-RR			
Glycerol	**0 M**	**0.3 M**	**0.75 M**	**1.2 M**
k_{fwd} (s^{-1})	110 ± 8.0	107 ± 2	141 ± 1.0	185 ± 4.0
k_{rev} (s^{-1})	4.1 ± 1.4	3.8 ± 0.9	4.4 ± 0.6	9.5 ± 1.4
K_d (εM)	3.8 ± 1.5	2.1 ± 0.3	4.0 ± 0.1	11.5 ± 2.7
k_{fwd}/K_d ($\varepsilon M^{-1}s^{-1}$)	28.6 ± 4.3	28.2 ± 7.2	51.0 ± 9.2	35.2 ± 3.2

Table 3-6. Kinetic constants[a] for phosphotransfer reactions in the absence and presence of glycerol. [a] The data used to calculate the values in this table were obtained in triplicate and the errors represent standard errors of the mean.

Experiments carried out to determine the combined effect of NaCl and glycerol on the YPD1~P and SSK1-RR phosphotransfer reaction were conducted in the presence of varying concentrations of both NaCl and glycerol. As osmolyte concentrations increased, the maximum forward and reverse rate constants increased, while no change was observed in the second order rate constant or K_d (Table 3-7).

Reaction	YPD1~P + SSK1-R2			
[Glycerol]M/ [NaCl]M	**0/0**	**0.3/0.2**	**0.55/0.4**	**0.75/0.6**
k_{fwd} (s^{-1})	110 ± 8.0	136 ± 1.0	141 ± 2.1	160 ± 3.0
k_{rev} (s^{-1})	4.1 ± 1.4	3.6 ± 0.5	6.9 ± 0.9	10.2 ± 2.8
K_d (εM)	3.8 ± 1.5	4.4 ± 0.1	4.3 ± 0.2	4.3 ± 1.4
k_{fwd}/K_d ($\varepsilon M^{-1} s^{-1}$)	28.6 ± 4.3	30.9 ± 0.7	32.8 ± 1.6	37.2 ± 2.2

Table 3-7. Kinetic constants[a] for phosphotransfer reactions in the absence and presence of glycerol and NaCl. [a] The data used to calculate the values in this table were obtained in triplicate and the errors represent standard errors of the mean.

To differentiate between a true glycerol effect and an effect of viscosity on the phosphotransfer reactions, a control experiment was performed in the presence of Ficoll 400. Ficoll 400, as a high molecular weight polymer (macroviscosogen) is able to vary viscosity of the reaction mixture; however it has no effect on the rates of diffusion of the phosphotransfer reactions (Blacklow, Raines *et al.,* 1988). Glycerol (a microviscosogen), on the other hand, is capable of affecting both parameters. Kinetic data obtained in the presence of Ficoll 400 were similar to the data obtained in the

absence of osmolytes suggesting that the effects on the phosphotransfer reactions observed in the presence of glycerol are viscosity-independent.

3.3 Discussion

Osmotic shock can dramatically alter the intracellular concentrations of osmolytes. However, cells can adapt by modulating intracellular osmolyte concentrations in order to balance the external osmolarity of the cell. When homeostasis is restored, the osmotic pressure and the production of osmolytes are reduced and the activity of the osmoregulation pathway components returns to its default or prestimulus state.

In order to better understand the overall physiology of the cell response to hyperosmotic shock, detailed kinetic studies are important. Although many two-component systems have been identified in prokaryotes, only a small number of bacterial and eukaryotic phosphotransfer systems have been kinetically characterized (Fischer, Kim *et al.,* 1996; Stewart 1997; Grimshaw, Huang *et al.,* 1998; Mayover, Halkides *et al.,* 1999; Janiak-Spens, Cook *et al.,* 2005). As shown in Scheme 1, for phosphotransfer between SLN1-RR and YPD1, the ratio k_1/k_{-1} is defined as the K_d (the dissociation constant of the SLN1-RR~PÅYPD1 complex). The forward and reverse net rate constants for the phosphotransfer reaction are k_{fwd} and k_{rev}, respectively. Transfer of phosphoryl groups from YPD1~P to SSK1-RR, as depicted in Scheme 2, involves formation of the YPD1~P·SSK1-RR complex; the ratio k_4/k_{-4} is defined as the

K_d (the dissociation constant of the YPD1~PÅSSK1-RR complex). k_7 is the rate constant for the formation of the dead-end complex. In eq. 1 above, the observed rate constant is given in terms of a forward and reverse rate constant, k_{fwd} and k_{rev}. However, these rate constants are net rate constants, not microscopic rate constants. k_{fwd} is defined as in eq. 2.

$$k_{fwd} = \frac{k_2 k_3}{k_2 + k_{-2} + k_3} \tag{2}$$

and if k_{-1} is not greater than k_2, k_{rev} will be defined as in eq. 3

$$k_{rev} = \frac{k_{-1} k_{-2}}{k_2 + k_{-2} + k_{-1}} \tag{3}$$

This is likewise true for Scheme 2 where k_{fwd} and k_{rev} are given by eqs. 4 and 5

$$k_{fwd} = \frac{k_5 k_6}{k_{-5} + k_6 + k_5} \tag{4}$$

$$k_{rev} = \frac{k_{-4} k_{-5}}{k_{-4} + k_5 + k_{-5}} \tag{5}$$

The treatment of eq. 2-5 assumes a rapid pre-equilibrium (reflected in the Kd) of the initial encounter complex compared to the chemical steps and k_{-3} and k_{-6} are negligible under the conditions tested. If dissociation of the product complex, SLN1-RR·YPD1~P, is fast compared to the phosphotransfer step, $k_3 > k_2$, then $k_{fwd} = k_2$. This is the case for the kinetics of the reverse reaction, transfer of phosphate from YPD1 to SLN1-RR in the absence of osmolytes (Janiak-Spens, Cook *et al.,* 2005).

The kinetic data obtained in this study showed that in the presence of osmolytes, the rates of phosphoryl transfer were saturable at high YPD1 concentration suggesting the formation of a YPD1~P·SSK1-RR complex as observed previously (Janiak-Spens, Cook *et al.,* 2005). Phosphoryl transfer between SLN1-RR~P and YPD1 gives a significant k_{rev}, thus k_3 Ò k_2. This is also true for phosphoryl transfer between YPD1~P and SSK1-RR; k_{rev} is finite and k_6 Ò k_5. However, phosphoryl transfer from SSK-RR~P to YPD1 is not observed, and thus either the YPD1·SSK1-RR complex is not formed or is non-productive. However, attempts to demonstrate phosphoryl transfer from SSK1-RR~P to YPD1 were unsuccessful and thus a dead-end complex must form between SSK1-RR~P and YPD1. Scheme 2 shows the formation and dissociation of the dead-end complex with rate constant k_7 and k_{-7}. Thus, SSK1-RR~P and YPD1 can form either a [SSK1-RR~P·YPD1] or [SSK1-RR~P·YPD1]* complex, but the latter is more stable. The measurement of the observed rate constants (k_{fwd} and k_{rev}) and binding affinity (K_d) on the basis of eq 1 provides quantitative data for comparison of the phosphotransfer reactions between SLN1-RR and YPD1, and YPD1 and SSK1-RR in the absence and presence of osmolytes.

The maximum rate, k_{fwd}, will only be observed if the concentrations of the response regulator molecules (SLN1-RR or SSK1-RR) are significantly greater than the K_d for the YPD1·RR complex *in vivo*. However, the physiologic concentrations of these molecules are much lower than the K_d. As reported in the *Saccharomyces*

Genome Database (www.yeastgenome.org), the *in vivo* concentrations of SLN1-RR, YPD1, and SSK1-RR are estimated to be 0.03, 0.29, and 0.05 εM, respectively. Given a K_d of 2.8 εM for the SLN1-RR~P·YPD1 complex, the concentration of the complex formed is estimated to be 0.005 εM, 16 % of the limiting component, SLN1-RR. As a result, it is the second order rate constant, k_{fwd}/K_d that will be physiologically important. This is equally true of the YPD1~P·SSK1-RR complex. At limiting concentrations of the components in the reaction, the second order rate constant applies and includes all processes from the initial binding of the components to give a productive complex through the dissociation of the product complex. For Schemes 1 and 2, rate constants k_1 through k_3 and k_4 through k_6 will be included in k_{fwd}/K_d for the SLN1-RR~P to YPD1 and YPD1~P to SSK1-RR reactions, respectively. The rate constant for reformation of the SLN1-RR·YPD1~P complex from SLN1-RR and YPD1~P ($k_{i\,3}$) or the YPD1·SSK1-RR~P complex from YPD1~P and SSK1-RR ($k_{i\,6}$) are not included in the second order rate constant. Thus, any changes in the K_d values of the reactant complex, *i.e.*, the SLN1-RR~P·YPD1 and YPD1~P·SLN1-RR complexes, are accounted for in the second order rate constant. This would include a change in the half-life for the reactant complexes in the presence of viscosogen.

For both phosphotransfer reactions, SLN1-RR~P to YPD1 and YPD1~P to SSK1-RR in the presence of NaCl, no significant change in k_{fwd}/K_d or K_d is observed up to 0.6 M NaCl. Thus, NaCl exhibits no significant effect on the SLN1-RR~P and YPD1 or YPD1~P and SSK1-RR rates of phosphotransfer.

The concentration of NaCl at 1 M was not considered physiologically relevant for these experiments. Upon osmotic shock, the yeast cell volume can decrease by as much as 50-60%, which accordingly would increase the internal osmolyte concentration by only two- to three-fold (Morris, Winters *et al.,* 1983). Under normal conditions, a basal internal concentration of NaCl and KCl within *S. cerevisiae* is approximately 0.2 M (Ferrando, Kron *et al.,* 1995), consequently upon hyperosmotic shock this concentration will raise to approximately 0.6 M.

The effect of glycerol on phosphotransfer kinetics is in general different than the effect of NaCl. For the SLN-RR~P·YPD1 complex, the K_d increases by about 6-fold as the glycerol concentration increases to 1.2 M (Table 3-3), suggesting less initial complex is present at the same SLN1-RR~P and YPD1 concentrations, compared to the absence of glycerol. In addition, the second-order rate constant for the forward reaction (k_{fwd}/K_d), (Figure 3-3), decreases with an increase in glycerol concentration, and thus glycerol alone cannot contribute to an increase in phosphorylation of SSK1-RR in the osmoadaptation phase, once osmotic pressure has been re-established.

In the case of the YPD1~P·SSK1-RR complex, the K_d does not change as glycerol concentration increases to 1.2 M. Although, k_{fwd} and k_{rev} increase slightly, the second order rate constant (k_{fwd}/K_d) remains relatively constant. Therefore, the net effect of glycerol on the YPD1~P·SSK1-RR complex parallels the effect of glycerol

on SLN1-RR~P·YPD1 complex, and glycerol alone does not give a net increase in phospho-SSK1-RR.

The combinatory effects of NaCl and glycerol on the pathway, however, are more revealing. As shown in Table 3-4, in the case of SLN1-RR~P·YPD1 complex, the second order rate constant increases three-fold, as the concentration of glycerol and NaCl increase to 0.75 M and 0.6 M, respectively. A synergistic effect is observed that is different from the effect of glycerol or NaCl alone. For the YPD1~P to SSK1-RR phosphotransfer reaction (Table 3-7), k_{fwd}/K_d also increases, although by only 30%. The combined effect of NaCl and glycerol is thus to increase the level of phosphorylated SSK1-RR and return the pathway to its prestimulus state, *i.e.* the effect of osmotic stress has been attenuated.

The subtle effects of NaCl and glycerol on the SLN1-YPD1-SSK1 phosphorelay system reveal some important regulatory aspects of the cell response to osmotic shock. In the early stages of the cell's response to hyperosmotic stress, immediate water loss can lead to a modest increase in intracellular ion/solute concentrations. The half-life studies in the presence of osmolytes suggest a reduction in SSK1-RR~P·YPD1 complex stability; thereby leading to a higher rate of SSK1-RR dephosphorylation. This likely represents one contributing factor that leads to subsequent HOG1 pathway activation. However, in the osmoadaptation phase, after HOG1-dependent transcriptional targets such as *GPD1* have been upregulated and intracellular glycerol levels approach molar concentrations, our results indicate that

the combinatory effect of high levels of NaCl and glycerol on rates of phosphotransfer favors phosphorylation of SSK1 and signal attenuation. Thus, the studies on the phosphorelay kinetics in the presence of osmolytes provide insight into the post-hyperosmotic shock events, restoration of intracellular homeostasis and cessation of glycerol production. These studies explain for the first time the effects of osmolytes on the SLN1-YPD1-SSK1 phosphorelay and elucidate some basic aspects of the osmoregulation pathway including the presence of a feedback-like control mechanism and the combinatory effect of NaCl and glycerol.

References

Blacklow, S. C., Raines, R. T., Lim, W. A., Zamore, P. D. and Knowles, J. R. (1988). "Triosephosphate isomerase catalysis is diffusion controlled." Biochemistry **27**: 1158-1167.

Ferrando, A., Kron, S. J., Rios, G., Fink, G. R. and Serrano, R. (1995). "Regulation of cation transport in *Saccharomyces cerevisiae* by the salt tolerance gene HAL3." Mol Cell Biol **15**(10): 5470-5481.

Fischer, S. L., Kim, S. K., Wanner, B. L. and Walsh, C. T. (1996). "Kinetic comparisons of the specificity of the vancomycin resistance kinase VanS for two response regulators, VanR and PhoB." Biochemistry **35**: 4732-4740.

Grimshaw, C. E., Huang, S., Hanstein, C. G., Strauch, M. A., Burbulys, D., Wang, L., Hoch, J. A. and Whiteley, J. M. (1998). "Synergistic kinetic interactions between components of the phosphorelay controlling sporulation in *Bacillus subtilis*." Biochemistry **37**: 1365-1375.

Hohmann, S. (1997). Shaping up: The response of yeast to osmotic stress. Yeast Stress Responses. S. Hohmann and W. H. Mager. New York, Chapman & Hall**:** 101-145.

Janiak-Spens, F., Cook, P. F. and West, A. H. (2005). "Kinetic analysis of YPD1-dependent phosphotransfer reactions in the yeast osmoregulatory phosphorelay system." Biochemistry **44**(1): 377-386.

Janiak-Spens, F., Sparling, J. M., Gurfinkel, M. and West, A. H. (1999). "Differential stabilities of phosphorylated response regulator domains reflect functional roles of the yeast osmoregulatory SLN1 and SSK1 proteins." J. Bacteriol. **181**(2): 411-417.

Klipp, E., Nordlander, B., Krüger, R., Gennemark, P. and Hohmann, S. (2005). "Integrative model of the response of yeast to osmotic shock." Nature Biotech. **23**(8): 975-982.

Mayover, T. L., Halkides, C. J. and Stewart, R. C. (1999). "Kinetic characterization of CheY phosphorylation reactions: Comparison of P-CheA and small-molecule phosphodonors." Biochemistry **38**: 2259-2271.

Morris, G. J., Winters, L., Coulson, G. E. and Clarke, K. J. (1983). "Effect of osmotic stress on the ultrastructure and viability of the yeast *Saccharomyces cerevisiae*." J Gen Micro **129**: 2023-2034.

Stewart, R. C. (1997). "Kinetic characterization of phosphotransfer between CheA and CheY in the bacterial chemotaxis signal transduction pathway." Biochemistry **36**: 2030-2040.

Chapter 4

Biochemical characterization of the phosphorelay proteins CaYPD1 and CaSSK1 from *Candida albicans*

Candida albicans is pathogenic diploid yeast ï the cause of opportunistic oral and genital infections in humans (Calderone 2002). *C. albicans* is commensal and under normal environmental conditions can live in 80% of the human population with no harmful effects. However, in patient groups whose defense system is severely compromised (AIDS patients, prematurely born infants, leukemics and burn patients), *Candida albicans* turns into a deadly pathogen causing systemic infections with a mortality rate as high as 50% (Wenzel 1995). Although *C. albicans* is a threat as a human pathogen, mutational analysis revealed avirulent or attenuated species defective in host recognition, morphogenesis, enzymatic and oxidant adaptation functions.

The multi-step His-to-Asp signal transduction pathway is known as one of the major routes by which adaptation to general stress, morphogenesis, cell wall biosynthesis and virulence occurs in *C. albicans* (Calera, Zhao *et al.,* 2000; Chauhan, Inglis *et al.,* 2003; Chauhan, Latge *et al.,* 2008). In both *C. albicans* and *S. cerevisiae*, the SSK1 and CaSSK1-RR response regulator proteins are critical for downstream signaling via the HOG1 MAPK, except that the main function of this pathway is

osmoadaptation in *S. cerevisiae* and oxidant adaptation in *C. albicans*. In addition to oxidant adaptation, mutants deleted of CaSSK1 in *C. albicans* also are less able to adhere to human esophageal cells, survive in human PMNs and cause invasive disease (Calderone 2000; Calera, Zhao *et al.,* 2000; Bernhardt, Herman *et al.,* 2001). However, little is known about structure-function activities of the CaSSK1 in *C. albicans* and the role of specific amino acid residues in phosphotransfer and adaptation. In *S. cerevisiae*, several studies have focused upon the identification of domains that are essential for YPD1ï SSK1 interactions (Porter, Xu *et al.,* 2003; Porter, West 2005). *In vitro* phosphorylation assays have been established using expressed and purified domains of SLN1, YPD1 and SSK1 (Janiak-Spens, Sparling *et al.,* 1999; Janiak-Spens, West 2000).

We initiated studies that focus on *in vitro* reconstitution of the multi-step phosphorelay from *C. albicans* and biochemical characterization of the CaYPD1 (HPt protein) and CaSSK1 (response regulator protein). We examined heterologous phosphoryl transfer from SLN1-HK-RR Ÿ CaYPD1Ÿ CaSSK1 and measured the lifetime of the phosphorylated regulatory domain of CaSSK1. Mutational analysis of the CaSSK1 response regulator domain was also performed. Mutants were expressed, purified and their activities were analyzed using an *in vitro* phosphorylation assay.

4.2 Materials and methods

4.2.1 Materials

All chemicals and biochemicals used were of ultrapure grade. NdeI, XhoI and chitin beads were obtained from New England Biolabs. Gateway cloning kit, Pfu Turbo, Pfx DNA polymerase and T4 ligase were purchased from Stratagene. Low-melting agarose was purchased from Cambrex Bio Sciences. QIAquick® Plasmid DNA purification kit, QIAquick® Gel extraction kit and QIAprep® spin Miniprep kit were purchased from QIAGEN Inc. Sequencing was done by Microgen at the University of Oklahoma Health Sciences Center (OUHSC) to confirm designed mutations. [ɔ-^{32}P] ATP (30 Ci/mmol) was purchased from Amersham. Chromatography media were purchased from Pharmacia and Sigma. Plasmids pBR27 and pYPD1, containing the genes of CaSSK1-RR and CaYPD1, respectively, were a gift from Dr. Richard Calderone (Georgetown University). The expression vector pET16b was purchased from Novagen and expression vector pETCYB (IMPACT system) from New England Biolabs. Primers were purchased from Invitrogen. IPTG (Isopropyl-β-D-thiogalactoside) was from Gold Biotechnology.

4.2.2 Protein expression and purification

For protein expression in *E. coli* cells, gene fragments of the CaSSK1 response regulator domain (CaSSK1-RR, residues 499ï 674) and full length CaYPD1 (aa 1-184) were amplified by PCR using the pBR27 and pYPD1 plasmids with the sets of primers

listed in Table 4-1 (Szurmant, Muff *et al.,* 2004). The PCR reaction for CaYPD1 had the following parameters: denaturation temperature ï 94°C for 1.5 min, annealing temperature - 45°C for 30 s, extension temperature - 68°C for 1 min 45 s. Parameters for the CaSSK1-RR PCR reaction were identical to CaYPD1. The amplified products were digested with NdeI and XhoI restriction enzymes and introduced into the NdeI/XhoI cloning sites of pET16b (CaYPD1) and pETCYB (CaSSK1-RR) vectors. These plasmid derivatives were designated, pET-CaYPD1 and pETCYB-CaSSK1-RR, respectively.

Both plasmids were transformed first into DH5α cells. After transformation, selected colonies were grown overnight and plasmids were extracted using the QIAprep® spin Miniprep kit. Both plasmids were sent to Microgen (OUHSC) for DNA sequencing. Next, pET-CaYPD1 was introduced into the *E. coli* expression host strain BL21 (DE3) Star and the pETCYB-CaSSK1-RR plasmid was transformed into BL21 (DE3) RIL.

Protein constructs	Primer Pairs (Sequence 5` to 3`)
AW421 CaYPD1 FP	GGGAATTCCATATGTCAGAAGATAAATTAC
AW422 CaYPD1 RP	CCGCTCGAGCGGCTATTCGTAATATTCGTCC
AW425 CaSSK1-RR FP	GGGAATTCCATATGAATTTTCTCTATAACAATTCA
AW458 CaSSK1-RR RP	ATACTCGAGCGGAGCTTTGTTTAATCTTCG
AW524 CaSSK1-RR-D556N FP	CACTTGGTATTGATGAACATTCAATTGCCAGTG
AW525 CaSSK1-RR-D556N RP	CACTGGCAATTGAATGTTCATCAATACCAAGTG
AW522 CaSSK1-RR-D513K FP	CTGTATTGGTAGTTGAAAAAAATGCCATCAATCAAGC
AW523 CaSSK1-RR-D513K RP	GCTTGATTGATGGCATTTTTTTCAACTACCAATACAG

Table 4-1. Primer pairs used for gene cloning and site directed mutagenesis.

AW number was assigned in the lab for each individual primer. FP stands for a forward primer, while RP is a reverse primer.

CaYPD1 protein expression and purification

Escherichia coli BL21 (DE3) Star cells containing pET-CaYPD1 vector were grown in 1 L of LB medium in the presence of 100 ε g $mL^{ī 1}$ of ampicillin at 37°C. When the optical density (at 600 nm) of the culture reached 0.6, the cells were induced by the addition of IPTG to a final concentration of 0.4 mM. The culture was shaken for an additional 3 h at 37°C and then harvested, washed and suspended at 5 mL $g^{ī 1}$ (wet weight) of cells in lysis buffer (20 mM Tris-HCl, pH 7.6, 100 mM NaCl, 20 mM imidazole). Cells were lysed by sonication, and the lysate was clarified by centrifugation at 112, 000 *x g* for 1 h at 4°C. The supernatant was loaded onto a Ni^{2+}-NTA-affinity chromatography column pre-equilibrated in lysis buffer. CaYPD1 was

eluted using a step gradient of 200 mM imidazole and 300 mM imidazole. The protein was further purified by separation on a gel filtration column (Sephadex G50, 300 mL bed volume) equilibrated in 20 mM Tris-HCl, pH 7.6, 50 mM NaCl, 1 mM EDTA and 1.4 mM ß-mercaptoethanol. Fractions containing CaYPD1 were pooled and concentrated by using a Centricon 3 (Amicon) filter unit. The protein was judged to be 99% homogeneous based on analysis by SDS-PAGE. The protein concentration was determined by absorbance at 280 nm using a calculated extinction coefficient of 16 500 M^{-1} cm^{-1}. Typical yields were 4 mg L^{-1} of cells. Purified CaYPD1 protein was stored in gel filtration buffer in the presence of 10% glycerol at − 20°C.

CaSSK1-RR protein expression and purification

Escherichia coli BL21 (DE3) RIL cells containing the pETCYB-CaSSK1-RR vector were grown in 2 L of LB medium in the presence of 100 µg mL^{-1} of ampicillin and 25 µg mL^{-1} of chloramphenicol at 37°C. When the optical density (at 600 nm) of the culture reached 0.6, the cells were cooled to room temperature and expression of CaSSK1-RR was induced by the addition of IPTG to a final concentration of 1 mM. The cultures were shaken overnight at 16°C and then harvested, washed and resuspended at 5 mL g^{-1} (wet weight) of cells in lysis buffer (20 mM Tris-HCl, pH 8, 500 mM NaCl, 1 mM EDTA, 0.1% Triton X-100, 10% glycerol). Cells were lysed by French press, and the lysates were clarified by centrifugation at 27,200 *x g* for 1 h at 4°C. The supernatant was loaded onto a 3 mL chitin bead column equilibrated in lysis

buffer at 4°C. The column was washed sequentially with 100 mL of lysis buffer and 25 mL of cleavage buffer (20 mM Tris-HCl, pH 8, 50 mM NaCl, 1 mM EDTA, 5 mM ATP, 10 mM $MgCl_2$, 10% glycerol). Thereafter the column was washed immediately with 25 mL of cleavage buffer containing 30 mM ßME and incubated overnight at 4°C. The protein was eluted with cleavage buffer and further purified by separation on a gel filtration column (Sephadex G75, 300 ml bed volume) equilibrated in 20 mM Tris-HCl, pH 8, 50 mM NaCl, 1 mM EDTA, and 1.4 mM ßME. Fractions containing CaSSK1-RR were pooled and concentrated using a Centricon 10 (Amicon) filter unit. The protein was judged to be ~90% homogeneous based on analysis by SDS-PAGE. The protein concentration was determined by absorbance at 280 nm using a calculated extinction coefficient of 25, 440 $M^{-1}cm^{-1}$. Typical yields were 1 mg L^{-1} of cells. Purified CaSSK1-RR protein was stored in gel filtration buffer in the presence of 10% glycerol at − 20°C.

The *S. cerevisiae* YPD1 protein, SLN1-RR and GST-SLN1-HK were purified as described in Chapters 2 and 3 (Li, Ault *et al.,* 1998; Janiak-Spens, Sparling *et al.,* 1999; Xu, Nguyen *et al.,* 1999).

4.2.3 *In vitro* phosphorylation

Glutathione-Sepharose-bound GST-SLN1-HK (12.5 µM) was mixed with SLN1-RR (0.125 µM) and [ɔ-^{32}P]-ATP (4 µM) in 80 µL of reaction buffer (50 mM Tris pH 8.0, 100 mM KCl, 15 mM $MgCl_2$, 2 mM DTT, 20% glycerol) to generate

phosphorylated SLN1-RR via phosphoryl transfer from GST-SLN1-HK. The mixture was incubated at room temperature for 30 min. SLN1-RR was separated from GST-SLN1-HK by gentle centrifugation (1 min at 1000 *x g*). The SLN1-RR (8 εL) was added to reaction mixtures (total volume of 15 εL) containing designated phosphorelay components (0.67 εM YPD1; 0.67 εM CaYPD1; 0.67 εM YPD1 and 0.67 εM CaSSK1-RR; 0.67 εM CaYPD1 and 0.67 εM CaSSK1-RR). Phosphorelay reaction mixtures were incubated for 10 min at room temperature. Reactions were stopped by the addition of 5 εL of 4× stop buffer (0.25 M Tris, pH 6.8, 8% SDS, 40 mM EDTA, 40% glycerol, and 0.008 % bromophenol blue) and the reaction products were separated on a 15% SDS-PAGE gel. The wet gel was immediately wrapped in plastic film and subjected to phosphorimager analysis (Molecular Dynamics, Storm 840).

4.2.4 Measurement of CaSSK1-RR phosphorylated half-life

Phosphorylation of the response regulator domain CaSSK1-RR was achieved by incubation with GST-SLN1-HK and [γ-^{32}P] ATP. GST-tagged SLN1-HK (7 μM) bound to glutathione-Sepharose 4B resin was incubated with 7 μM [γ-^{32}P] ATP in 100 μL of 50 mM Tris-HCl (pH 8.0), 100 mM KCl, 10 mM $MgCl_2$, 2 mM DTT and 20% glycerol for 30 min at room temperature. The phosphorylated GST-SLN1-HK was recovered in the pellet after gentle centrifugation (1 min at 1000 *x g*). CaSSK1-RR (12 μM) in 50 mM Tris-HCl (pH 8.0), 100 mM KCl, 10 mM $MgCl_2$, 2 mM DTT was

added to the phosphorylated GST-SLN1-HK and incubated for 30 min at room temperature in a total reaction volume of 280 µL. The phosphorylated response regulator domain was recovered in the supernatant after gently pelleting the resin-bound GST-SLN1-HK. Aliquots (15 µL) were removed from the reaction mixture at indicated time points, mixed with 5 µL of 4X stop buffer (0.25 M Tris-HCl pH 8.0, 8% SDS, 60 mM EDTA, 40% glycerol, 0.008% bromophenol blue) to terminate the reaction, and kept at -20 ℃ until gel analysis. Reaction products were separated on 15% SDS-PAGE gel. The wet gel was immediately wrapped in plastic film and subjected to phosphorimager analysis to quantify the radioactivity of each band (Molecular Dynamics, Storm 840).

4.2.5 Construction, expression and purification of CaSSK1-D556N and CaSSK1-D513K mutants

Two aspartate residues (D513 and D556) within the CaSSK1-RR domain were mutated to lysine and asparagine, respectively, with the QuikChange method (Stratagene). Two oligonucleotide primers carrying the selected mutation were included with the pETCYB-CaSSK1-RR plasmid template in a PCR reaction (Table 4-1). PCR reaction conditions were: denaturation temperature ï 94°C for 1.5 min, annealing temperature - 50°C for 50 s, extension temperature - 68°C for 14 min. Pfu Turbo DNA Polymerase was used for PCR reaction. After 18 rounds of amplification, the reaction mixture was digested with Dpn I restriction enzyme to digest methylated

parental DNA while retaining newly synthesized one. The reaction mixture was subsequently transformed into *E. coli* DH5Ŭ competent cells. Plasmids were isolated from selected transformants and the mutations were confirmed via DNA sequencing analysis (Microgen, OUHSC). Confirmed plasmids were transformed into *E. coli* BL21 (DE3) RIL cells. Expression and purification of the mutant proteins were performed similar to that of CaSSK1-RR.

4.2.6 *In vitro* phosphorylation of CaSSK1-D556N and CaSSK1-D513K mutants

Phosphorylation of the CaSSK1-RR mutants (D513K and D556N) was performed similar to that of WT CaSSK1-RR with the following modifications. Reaction mixtures (total volume of 15 ε l) contained 2 ε M CaYPD1; 2 ε M CaYPD1 and 2 ε M CaSSK1-RR; 2 ε M CaYPD1 and 2 ε M CaSSK1-RR D556N; 2 ε M CaYPD1 and 2 ε M CaSSK1-RR D513K.

4.3 Results

4.3.1 Amino acid sequence analysis of the *C. albicans* CaSSK1-RR domain

The CaSSK1 response regulator domain sequence was aligned with sequences corresponding to *S. cerevisiae* SSK1 response regulator domain, *S. pombe* MCS4 response regulator domain and *E. coli* CheY protein using the Clustal W program (Figure 4-1)(Thompson, Higgins *et al.,* 1994).

The CheY RR from *Escherichia coli* served as a model for RR proteins. The CheY protein is required for cell motility of this microorganism by directing the clockwise-counterclockwise movement of flagella (Szurmant, Muff *et al.,* 2004). Of several conserved residues, D57 (site of phosphorylation) and D13 (metal binding site) have been shown to be the required for normal cell motility. One additional conserved residue Lys109 is required for phosphorylation of Asp57 residue (Bourret, Drake *et al.,* 1993). Compared to CheY, the response regulator domain of CaSSK1 contains Asp556 as the site of phosphorylation (Asp57 in CheY). Residue Asp513 is one of the pair of aspartates that are conserved among prokaryotic response regulators (Asp13 in CheY) and Lys638 corresponds to the conserved residue Lys109 in CheY protein (Parkinson 1993).

The secondary structure prediction of CaSSK1-RR using the web-based program APSSP (http://imtech.res.in/raghava/apssp/) revealed a typical RR protein core (CheY-like) consisting of doubly-wound $(\beta\alpha)_5$ fold. This fold contains a central five-stranded parallel ϐ sheet flanked on both faces by amphipathic helices. Highly conserved residues are located in the areas of an active-site groove formed by loops of ϐ1, ϐ3 and ϐ5 strands, and a pair of residues that form a diagonal path extending across the molecule from the active site (West, Stock 2001).

Next, protein sequences were introduced into the BLASTP program and it was shown, that the CaSSK1 response regulator domain shares homology with response

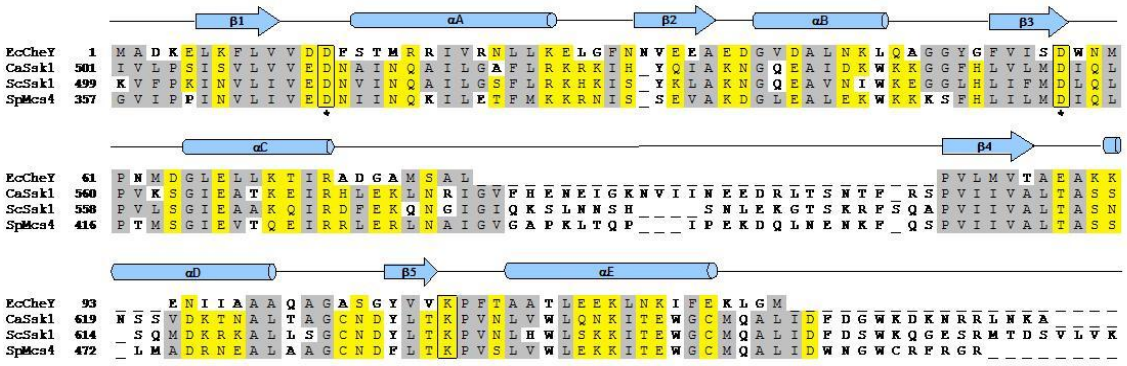

Figure 4-1. Alignment of the receiver domains of *C. albicans* CaSSK1, *S. cerevisiae* SSK1, *S. pombe* MCS4 with *E. coli* CheY (Menon, Li *et al.*, 2006). Above sequence alignment is the corresponding secondary structure for CheY. The numbers to the left of each line refer to the primary amino acid sequence. Conserved hydrophobic and hydrophilic residues are shaded grey and yellow respectively. The three amino acid residues that are invariant within the response regulator superfamily are boxed. The amino acid residues marked with an asterisk are the positions that were mutated in *C. albicans* SSK1-RR (D556 and D513).

regulator protein domains and the CheY RR protein. The highest similarity was shared with the SSK1-RR from *S. cerevisiae* (61.3% identity and 72.8% similarity) and MCS4-RR from *S. pombe* (59.5% identity and 71.6% similarity), respectively (Altschul, Gish *et al.,* 1990). The combined sequence analysis and structure prediction information allowed an accurate structure-based sequence alignment for mutational analysis. The assignment of functions to conserved amino acids of the *C. albicans* RR protein has not been reported, nor has the phosphoacceptor residue been established in this human pathogen. The BLASTP analysis also identified that the *C. albicans* D556

and D513 correspond to the D554 and D511 of the *S. cerevisiae* (SSK1) and D412 and D369 of the *S. pombe* (MCS4) RR proteins (Figure 4-1). The overall approach therefore was to mutate these residues in CaSSK1 to help understand the role of each in phosphotransfer and adaptation of *C. albicans*.

4.3.2 Phosphotransfer from SLN1-HK to CaYPD1 and CaSSK1-R2

The receiver domain of CaSSK1-RR (residues 499ï 674) was expressed, purified and phosphorylated *in vitro* using a heterologous phosphorelay assay (Janiak-Spens, Sparling *et al.,* 2000). The assay mixture consisted of GST-SLN1-HK, SLN1-RR and YPD1 proteins from *S. cerevisiae* and CaYPD1 and CaSSK1-RR proteins from *C. albicans* as indicated in Figure 4-2. GST-SLN1-HK was autophosphorylated in the presence of [ɔ-^{32}P]-ATP. Addition of purified SLN1-RR domain to GST-SLN1-HK allowed for the formation of phosphorylated SLN1-RR (Figure 4-2, lane 1). Phospho-SLN1-RR was then separated from GST-SLN1-HK and added to either YPD1 or CaYPD1. The radiolabel can be transferred from SLN1-RR to either HPt protein (Figure 4-2, lanes 2 and 3). If CaSSK1-RR is included (Figure 4-2, lanes 4 and 5), complete phosphorelay from SLN1-RR to YPD1 to CaSSK1 and SLN1-RR to

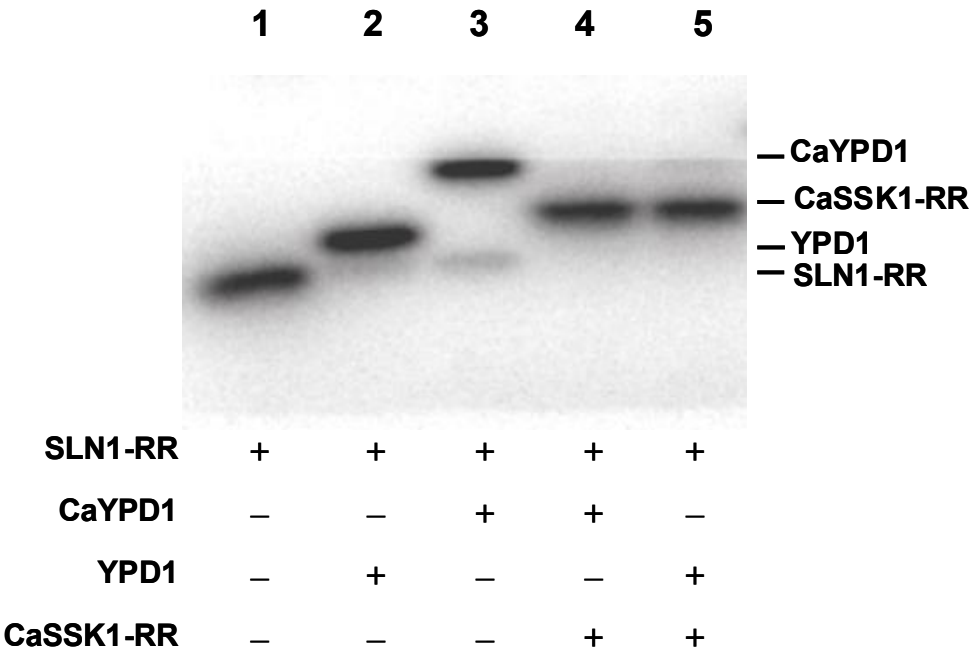

Figure 4-2. *In vitro* phosphorylation of CaSSK1-RR. The phosphorylation reaction mixtures contained SLN1-RR (lane 1); or equimolar amounts of SLN1-RR and YPD1 (lane 2); SLN1-RR and CaYPD1 (lane 3); SLN1-RR, CaYPD1 and CaSSK1-RR (lane 4); SLN1-RR, YPD1 and CaSSK1-RR (lane 5). After incubation for 10 min, reactions were quenched by addition of 5 εl of 4 × stop buffer. Reaction products were separated by 15% SDS-PAGE and the gel was then subjected to phosphorimager analysis.

CaYPD1 to CaSSK1 is observed. The steady-state level of phospho-CaSSK1-RR protein observed in this 10 min time frame suggests that both YPD1 and CaYPD1 can serve as equivalent phosphodonors for the CaSSK1-RR protein.

4.3.3 *In vitro* assay for testing phosphotransfer activities of CaSSK1-R2 mutants

Similar studies were performed to assess the ability of the D556N and D513K mutants of CaSSK1-RR to be phosphorylated compared with the wild-type CaSSK1-RR. Both mutants were expressed, purified and assayed as described above for the wild-type CaSSK1-RR protein. The CaSSK1-RR was phosphorylated as shown in Figure 4-3, lane 3. As expected for the D556N mutant, we observed little or no phosphorylation; the radiolabel primarily resides with the CaYPD1 protein and does not get transferred to the D556N mutant (Figure 4-3, lane 4). Likewise, the D513K mutant is also severely impaired in its ability to be phosphorylated by YPD1 (Figure 4-3, lane 5).

4.3.4 Stability of the phosphorylated CaSSK1-RR domain

The response regulators studied thus far differ in their phosphorylated half-lives, ranging from seconds for the bacterial chemotaxis protein CheY to about 10-12 h for the vancomycin resistance protein VanR (Hess, Oosawa *et al.,* 1988; Wright, Holman *et al.,* 1993). A half-life value of 13 ± 3 min, with a corresponding rate constant of 0.054 min^{-1} was previously reported for the half-life of phosphorylated SSK1-RR in *Saccharomyces cerevisiae* (Janiak-Spens, Sparling *et al.,* 1999). To address the stability of the phosphorylated form of CaSSK1-RR, and to compare it to SSK1-RR and other response regulator proteins, we measured rates of dephosphorylation of phospho-CaSSK1-RR.

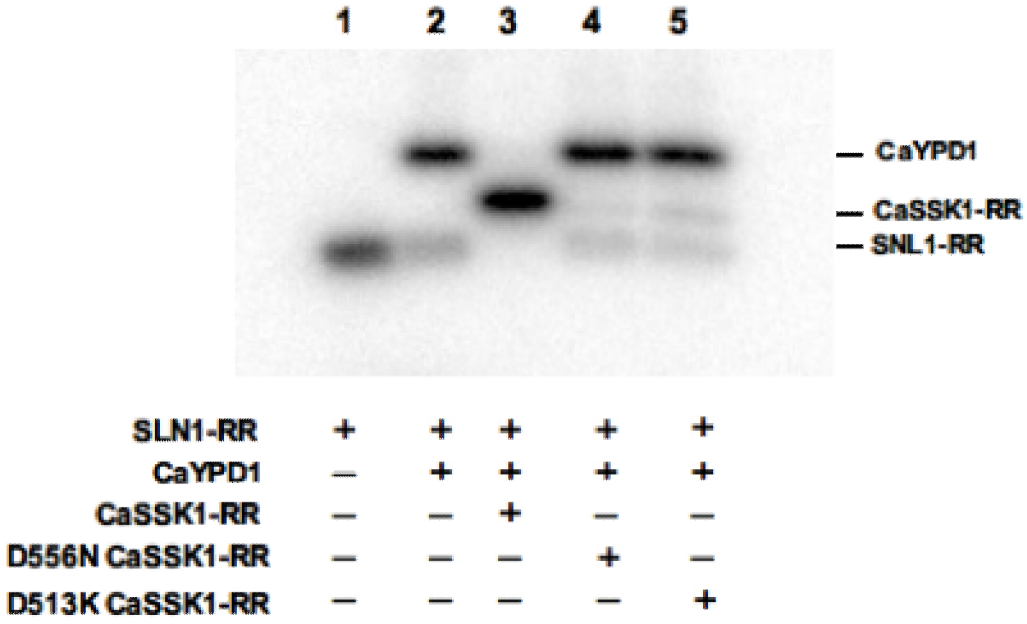

Figure 4-3. *In vitro* phosphorylation of the D556N-RR and D513K-RR domains. SLN1-RR (lane 1); SLN1-RR, CaYPD1 (lane 2); SLN1-RR, CaYPD1, CaSSK1-RR (lane 3); same as lane 3, but with D556N CaSSK1-RR (lane 4); and D513K CaSSK1-RR (lane 5).

Purified phospho-GST-HK (7 μM) was incubated with CaSSK1-RR (12 μM) in the presence of Mg^{2+} ions. Phosphoryl transfer from phospho-GST-HK to CaSSK1-RR was complete within 30 min. Aliquots were removed at designated time points thereafter, and stop buffer was added. The reaction products were separated on 15% SDS-PAGE gels and analyzed by phosphorimager analysis (Figure 4-4). Dephosphorylation of phospho-CaSSK1-RR followed first-order rate kinetics and the

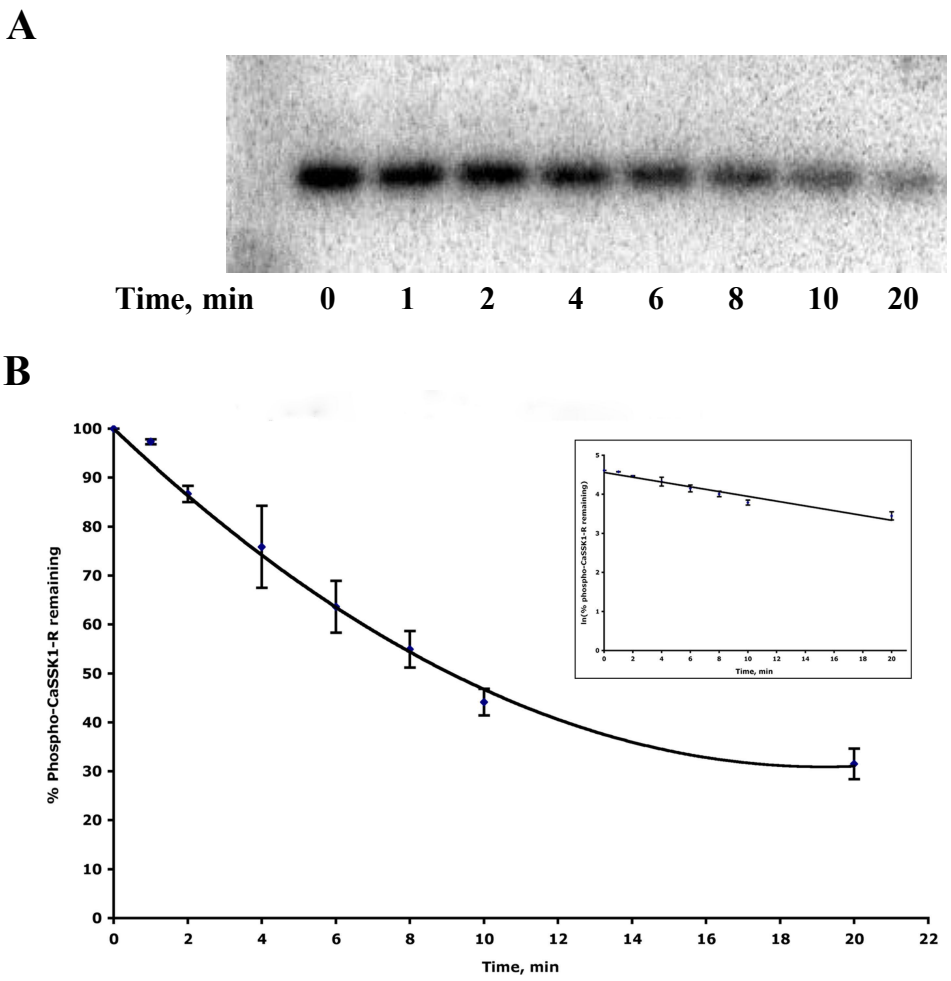

Figure 4-4. Dephosphorylation rate of CaSSK1-RR. (A) Dephosphorylation of CaSSK1-RR as a function of time. The reaction products were separated on SDS-PAGE gel and analyzed by phosphorimager analysis (Molecular Dynamics, Storm 840). (B) Image was further analyzed by ImageQuant™ TL Software (GE Heathcare) to determine the fraction of CaSSK1-RR remaining. The half-life of the CaSSK1 was determined by first-order rate kinetics accordingly.

half-life of phospho-CaSSK1-R2 was determined according to the formula $t_{1/2} = \ln 2/k$, where k is a rate constant for the dephosphorylation reaction. The results showed that

the phosphorylated response regulator domain of CaSSK1 has a half-life ($t_{1/2}$) of 8.9 ± 1.1 min (Figure 4-5) with a corresponding rate constant (k) of 0.078 min^{-1} (Figure 4-4).

4.4 Discussion

Response regulator proteins are critically placed in signaling pathways to regulate output responses of cells to a wide variety of environmental signals. All RR proteins contain a regulatory domain of approximately 125 amino acids, about 20ï 30% of which are identical (Stock, Ninfa *et al.,* 1989; Volz 1993). Probably the most studied of all RR proteins is CheY of *E. coli*. Its role in bacterial chemotaxis is to promote clockwise flagella rotation resulting in a 'smooth swimming' phenotype (Armitage 1999; Webre, Wolanin *et al.,* 2003; Szurmant, Muff *et al.,* 2004; Wadhams, Armitage 2004). Amino acid residues that compose the active site of CheY include three aspartates (D12, D13 and D57), which in turn position an essential Mg^{2+} ion, and a conserved lysine residue (K109) that interacts with the phosphate group when D57 is phosphorylated. The biological activities of RR proteins such as CheY include phosphotransfer, autodephosphorylation and regulation of the effector domain processes that are associated with enzymatic properties of the protein (Stock, West 2002).

Residues D556 and D513 of *C. albicans* CaSSK1 protein represent the invariant D57 and D13 of the CheY receiver domain and D554 and D511 of *S.*

cerevisiae SSK1. The reason for choosing these residues to construct point mutants was based upon studies in *E. coli* that demonstrated their importance to chemotaxis as stated above. While the function of RRs is diverse, invariant amino acid residues are critical for protein activity, so it is reasonable to compare the activities of disparate proteins.

D554 is the phosphoacceptor of the SSK1-RR, which as stated above works in cooperation with the upstream YPD1 phosphorelay protein to ensure phosphotransfer to SSK1 (Posas, Saito 1998). YPD1 becomes phosphorylated by the transmembrane histidine kinase, SLN1 (Posas, Wurgler-Murphy *et al.,* 1996). Thus, the flow of phosphate includes four phosphotransfer reactions involving four key amino acid residues of SLN1, YPD1 and SSK1 proteins (H576 and D695 of SLN1; H64 of YPD1; and D554 of SSK1). Previous studies have indicated that the *in vitro* half-lives of the phosphorylated SLN1-RR and SSK1-RR are approximately 13 min, while that of phosphorylated SSK1-RR in the presence of YPD1 is about 42 h such that the longer half-life of the SSK1 protein probably reflects the need to maintain the HOG1 pathway in an inactive state when cells are not osmotically or oxidatively stressed (Janiak-Spens, Sparling *et al.,* 1999).

In *sln1* deleted strains, HOG1 should be constitutively phosphorylated, but in the *S. cerevisiae* mutant, this causes lethality because cells overproduce glycerol (Hohmann 2002). In *C. albicans*, deletion of *sln1* is not lethal under any stress condition and HOG1 is phosphorylated (Nagahashi, Mio *et al.,* 1998; Yamada-Okabe,

Mio *et al.,* 1999). Our interpretation is that CaSSK1 is unphosphorylated in the *sln1* mutant and therefore CaSSK1 is capable of activating the HOG1 MAPK pathway via CaSSK2 but without a lethal event occurring.

In work described in this chapter, the D556 and D513 amino acids of SSK1 appear critical to oxidant adaptation and morphogenesis, respectively, of *C. albicans* ((Menon, Li *et al.,* 2006). However, the role of D513 in oxidant adaptation and morphogenesis is not as clear. The constitutive activation of HOG1 in the D513K mutant (as well as the D556R) supports the currently accepted dogma that RR proteins exist in a dynamic equilibrium between active and inactive conformational states (Menon, Li *et al.,* 2006). Phosphorylation likely stabilizes the active conformation and thus shifts the equilibrium in that direction as described for the *E. coli* CheY (Bourret, Hess *et al.,* 1990; Lukat, Lee *et al.,* 1991; Jiang, Bourret *et al.,* 1997). Thus, the D13K mutation (in CheY, and by analogy the D513K mutant in CaSSK1) is thought to mimic the active conformation in the absence of phosphorylation. In addition, D513K mutant is also unable to undergo the yeast-hyphal transition, suggesting that the inhibition of hyphal formation could be associated with the constitutive phosphorylation of HOG1 in the D513K mutant, which could change the activities of signal systems in cells. Perhaps a primary function of the HOG1 MAPK pathway is to prevent or attenuate cross-talking which may be abrogated in the D513K mutant.

The D556 residue of *C. albicans* CaSSK1 is required for peroxide adaptation, but the sensitivity of the D556N mutant to other oxidants such as menadione was

similar to WT cells, implying that other regulatory/signal processes may participate in adaptation to specific oxidants, such as described by (Enjalbert, Smith *et al.,* 2006; Menon, Li *et al.,* 2006). Perhaps the D556N mutant of CaSSK1 also interacts with other pathways that regulate oxidant adaptation, which obviously would not occur in the *ssk1* deletion mutant. Alternatively, the different sensitivities may indicate that nuclear translocation of HOG1 occurs at a low level.

4.5. Overall Summary

Phosphorylation and dephosphorylation of SSK1 RR functions as an on/off switch in controlling the activity of the downstream HOG1 mitogen-activated protein (MAP) kinase cascade, responsible for production of glycerol in response to hyperosmotic shock in *S. cerevisiae* (Posas, Saito 1998; Horie T., Tatebayashi K. *et al.,* 2008). The effect of osmolyte concentrations on the half-life of the phosphorylated SSK1-RR caused a reduction in the half-life of SSK1-RR~P in the presence of YPD1 by approximately 2-fold and had no effect on the intrinsic stability of SSK1-RR~P in the absence of YPD1. This showed that increasing osmolyte concentration has a negative effect on SSK1-RR~P·YPD1 and results in an increased rate of SSK1-RR~P phosphate hydrolysis.

Phosphotransfer rates within the SLN1-YPD1-SSK1 phosphorelay in the presence of NaCl or glycerol, individually, did not change significantly. However, the combined effect at low to moderate concentrations of both osmolytes negatively

affected the YPD1ÅSSK1~P interaction thereby facilitating dephosphorylation of SSK1 and activating the HOG1 MAP kinase cascade. At high combinatory osmolyte concentrations, the kinetics of the phosphorelay favored production of SSK1~P and inhibition of the HOG1 pathway.

The *Candida albicans* multi-step phosphorelay CaSLN1-CaYPD1-CaSSK1 is required for adaptation to oxidative stress. An established heterologous phosphotransfer system utilizing the SLN1 histidine kinase protein from *S. cerevisiae* enabled estimation of the phosphorylated CaSSK1-RR half-life (approximately 9 min). Two point mutants, D556N and D513K of the CaSSK1-RR protein were analyzed using an *in vitro* phosphotransfer assay, resulting in little or no phosphorylation of the CaSSK1-RR D556N mutant and a severely impaired D513K mutant. Both mutants were compromised in their ability to adapt cells to oxidants or to promote morphogenesis (Menon, Li *et al.,* 2006).

References

Altschul, S. F., Gish, W., Miller, W., Myers, E. W. and Lipman, D. J. (1990). "Basic local alignment search tool." J. Mol. Biol. **215**(3): 403-410.

Armitage, J. P. (1999). "Bacterial tactic responses." Adv Microb Physiol **41**: 229-289.

Bernhardt, J., Herman, D., Sheridan, M. and Calderone, R. (2001). "Adherence and invasion studies of *Candida albicans* strains, using in vitro models of esophageal candidiasis." J. Infect. Dis. **184**: 1170-1175.

Bourret, R. B., Drake, S. K., Chervitz, S. A., Simon, M. I. and Falke, J. J. (1993). "Activation of the phosphosignaling protein CheY II. Analysis of activated mutants by ^{19}F NMR and protein engineering." J. Biol. Chem. **268**(18): 13089-13096.

Bourret, R. B., Hess, J. F. and Simon, M. I. (1990). "Conserved aspartate residues and phosphorylation in signal transduction by the chemotaxis protein CheY." Proc. Natl. Acad. Sci. (USA) **87**(Jan.): 41-45.

Calderone, R. (2000). "*Candida albicans*: adherence, signaling and virulence." Med. Mycol. **38**(Suppl. 1): 125-137.

Calderone, R., Ed. (2002). *Candida* and Candidiasis. Washington, D.C., ASM Press.

Calera, J. A., Zhao, X.-J. and Calderone, R. (2000). "Defective hyphal development and avirulence caused by a deletion of the SSK1 response regulator gene in *Candida albicans*." Infect. Immun. **68**(2): 518-525.

Chauhan, N., Inglis, D., Roman, E., Pla, J., Li, D., Calera, J. A. and Calderone, R. (2003). "*Candida albicans* response regulator gene *SSK1* regulates a subset of genes whose functions are associated with cell wall biosynthesis and adaptation to oxidative stress." Euk. Cell **2**(5): 1018-1024.

Chauhan, N., Latge, J. P. and Calderone, R. (2008). "Two-component signal transduction proteins as potential drug targets in medically important fungi." Infect Immun **76**(11): 4795-4803.

Enjalbert, B., Smith, D., Alam, I., Nicholls, S., Brown, A. J. and Quinn, J. (2006). "Role of Hog1 stress-activated protein kinase in the global transcriptional response to stress in the fungal pathogen Candida albicans." Mol Biol Cell **17**: 1018-1032.

Hess, J. F., Oosawa, K., Kaplan, N. and Simon, M. I. (1988). "Phosphorylation of three proteins in the signaling pathway of bacterial chemotaxis." Cell **53**: 79-87.

Hohmann, S. (2002). "Osmotic stress signaling and osmoadaptation in yeasts." Microbiol. Mol. Biol. Rev. **66**(2): 300-372.

Horie T., Tatebayashi K., Yamada R. and H., S. (2008). "Phosphorylated Ssk1 prevents unphosphorylated Ssk1 from activating the Ssk2 mitogen-activated protein kinase kinase kinase in the yeast high-osmolarity glycerol osmoregulatory pathway." Mol Cell Biol **28**(17): 5172-5183.

Janiak-Spens, F., Sparling, D. P. and West, A. H. (2000). "Novel role for an HPt domain in stabilizing the phosphorylated state of a response regulator domain." J. Bacteriol. **182**(23): 6673-6678.

Janiak-Spens, F., Sparling, J. M., Gurfinkel, M. and West, A. H. (1999). "Differential stabilities of phosphorylated response regulator domains reflect functional roles of the yeast osmoregulatory SLN1 and SSK1 proteins." J. Bacteriol. **181**(2): 411-417.

Janiak-Spens, F. and West, A. H. (2000). "Functional roles of conserved amino acid residues surrounding the phosphorylatable histidine of the yeast phosphorelay protein YPD1." Mol. Microbiol. **37**(1): 136-144.

Jiang, M., Bourret, R. B., Simon, M. I. and Volz, K. (1997). "Uncoupled phosphorylation and activation in bacterial chemotaxis." J. Biol. Chem. **272**(18): 11850-11855.

Li, S., Ault, A., Malone, C. L., Raitt, D., Dean, S., Johnston, L. H., Deschenes, R. J. and Fassler, J. S. (1998). "The yeast histidine protein kinase, Sln1p, mediates phosphotransfer to two response regulators, Ssk1p and Skn7p." EMBO J. **17**(23): 6952-6962.

Lukat, G. S., Lee, B. H., Mottonen, J. M., Stock, A. M. and Stock, J. B. (1991). "Roles of the highly conserved aspartate and lysine residues in the response regulator of bacterial chemotaxis." J. Biol. Chem. **266**: 8348-8354.

Menon, V., Li, D., Chauhan, N., Rajnarayanan, R., Dubrovska, A., West, A. H. and Calderone, R. (2006). "Functional studies of the Ssk1p response regulator protein of *Candida albicans* as determined by phenotypic analysis of receiver domain point mutants." Mol. Micro. **62**: 997-1013.

Parkinson, J. S. (1993). "Signal transduction schemes of bacteria." Cell **73**: 857-871.

Porter, S. W. and West, A. H. (2005). "A common docking site for response regulators on the yeast phosphorelay protein YPD1." Biochim. Biophys. Acta **1748**: 138-145.

Porter, S. W., Xu, Q. and West, A. H. (2003). "Ssk1p response regulator binding surface on histidine-containing phosphotransfer protein Ypd1p." Euk. Cell **2**(1): 27-33.

Posas, F. and Saito, H. (1998). "Activation of the yeast SSK2 MAP kinase kinase kinase by the SSK1 two-component response regulator." EMBO J. **17**(5): 1385-1394.

Posas, F., Wurgler-Murphy, S. M., Maeda, T., Witten, E. A., Thai, T. C. and Saito, H. (1996). "Yeast HOG1 MAP kinase cascade is regulated by a multistep phosphorelay mechanism in the SLN1-YPD1-SSK1 "two-component" osmosensor." Cell **86**: 865-875.

Stock, A. M. and West, A. H. (2002). Response regulator proteins and their interactions with histidine protein kinases. Histidine kinases in signal transduction. M. Inouye and R. Dutta. New York, Academic Press**:** 237-271.

Stock, J. B., Ninfa, A. J. and Stock, A. M. (1989). "Protein phosphorylation and regulation of adaptive responses in bacteria." Microbiol. Rev. **53**: 450-490.

Szurmant, H., Muff, T. J. and Ordal, G. W. (2004). "*Bacillus subtilis* CheC and FliY are members of a novel class of CheY-P hydrolyzing proteins in the chemotactic signal transduction cascade." J. Biol. Chem. **279**(21): 21787-21792.

Thompson, J. D., Higgins, D. G. and Gibson, T. J. (1994). "CLUSTAL W: improving the sensitivity of progressive multiple sequence alignment through sequence weighting, position specific gap penalties and weight matrix choice." Nuc. Acids Res. **22**: 4673-4680.

Volz, K. (1993). "Structural conservation in the CheY superfamily." Biochemistry **32**(44): 11741-11753.

Wadhams, G. H. and Armitage, J. P. (2004). "Making sense of it all: bacterial chemotaxis." Nature Rev. Mol. Cell Biol. **5**(Dec.): 1024-1037.

Webre, D. J., Wolanin, P. M. and Stock, J. B. (2003). "Bacterial chemotaxis." Curr. Biol. **13**(2): R47-R49.

Wenzel, R. P. (1995). "Nosocomial candidemia: risk factors and attributable mortality." Clin. Infect. Dis. **20**: 1531-1534.

West, A. H. and Stock, A. M. (2001). "Histidine kinases and response regulator proteins in two-component signaling systems." Trends Biochem. Sci. **26**(6): 369-376.

Wright, G. D., Holman, T. R. and Walsh, C. T. (1993). "Purification and characterization of VanR and the cytosolic domain of VanS: A two-component regulatory system required for vancomycin resistance in *Enterococcus faecium* BM4147." Biochemistry **32**: 5057-5063.

Xu, Q., Nguyen, V. and West, A. H. (1999). "Purification, crystallization, and preliminary X-ray diffraction analysis of the yeast phosphorelay protein YPD1." Acta Cryst. **D55**: 291-293.

Appendix

Chapter 5

Measurements of YPD1/SSK1-R2 binding affinity

The branched multi-step phosphorelay signaling pathway from *Saccharomyces cerevisiae* is involved in adaptation to environmental stress-related responses such as hyperosmotic and oxidative stresses (Blomberg, Adler 1992; Maeda, Wurgler-Murphy *et al.,* 1994; Posas, Wurgler-Murphy *et al.,* 1996).

Under normal growth conditions, the SLN1-YPD1-SSK1 branch negatively regulates MAP (mitogen-activated protein) kinase cascade. Specifically, phosphoryl groups are being shuttled to SSK1 response regulator protein preventing its interaction with SSK2/SSK22 MAPKKK (Maeda, Wurgler-Murphy *et al.,* 1994; Posas, Wurgler-Murphy *et al.,* 1996). The actual dephosphorylation mechanism is not completely understood. Hyperosmotic stress leads to dephosphorylation of SSK1 and activation of the MAP kinase cascade resulting in HOG1 phosphorylation, followed by its translocation into the nucleus and activation of stress-related genes responsible for glycerol production (Albertyn, Hohmann *et al.,* 1994; Ferrigno, Posas *et al.,* 1998; Posas, Saito 1998; Rep, Krantz *et al.,* 2000). An increase in intracellular glycerol concentration plays a key role in the yeast cell survival upon hyperosmotic stress (Mager, Varela 1993). Furthermore, the cellular response to hyperosmotic stress involves rapid efflux of water and changes in intracellular ion and osmolyte concentration. It is our hypothesis that these changes may affect protein-protein

interactions involving YPD1 and SSK1-RR. Therefore, this chapter is focused on examining environmental conditions that affect YPD1·SSK1-RR complex formation and its stability via fluorescence spectroscopy. Specifically, experiments were conducted to examine the effect of ion or solute concentrations on YPD1·SSK1-RR interactions *in vitro* and to measure affinities between YPD1 and phosphorylated and unphosphorylated SSK1-RR.

5.2 Materials, methods

5.2.1 Materials

All chemicals and biochemicals were of ultrapure grade. Glutathione-Sepharose 4B resin was purchased from Amersham and Sephadex G25 from Sigma. HiTrapQ columns were purchased from GE Healthcare. [γ-^{32}P] ATP (3000 Ci/mmol) was purchased from Perkin-Elmer. Chymostatin, aprotinin, pepstain, phosphoramidon, E-64, leupeptin, antipain, sodium metabisulfite were purchased from Sigma and benzamidine was purchased from Fluka. D-(+)-trehalose, D-(+)-melezitose hydrate, betaine and stachyose tetrahydrate were purchased from Sigma-Alrdich. NaCl, KCl and glycerol were from Mallinckrodt Chemicals, EMD and Pharmco-Aaper, respectively. The fluorescence probe 5-iodoacetamidofluorescein (5-IAF) was purchased from Molecular Probes. Acetyl phosphate, carbamoyl phosphate, orthotungstate, orthovanadate, beryllium chloride and sodium fluoride were from Sigma.

5.2.2 Protein expression and purification

Bacterial strains used for protein purification are presented in the Table 5-1.

Protein expressed	Plasmid number	Plasmid name	Strain number	*E. coli* strain, antibiotic resistance
GST-SLN1-HK	OU70	pGEX-GST-HK	OU246	DH5α/Amp^R
YPD1	OU15	pUC12-YPD1	OU6	DH5α/Amp^R
SSK1-RR	OU26	pETCYB-SSK1-RR	OU357	BL21(DE3) Star/ Amp^R, Cm^R
YPD1-T12C	OU270	pET21a-YPD1T12C	OU340	BL21(DE3) Star/ Amp^R

Table 5-1. Plasmid constructs used for protein expression and purification. An OU number was assigned for each individual plasmid construct and transformed *E. coli* strain.

Purifications of GST-SLN1-HK, SLN1-RR, YPD1 and SSK1-RR were done following the same protocols presented in Chapters 2 and 3.

5.2.3 Construction, expression, purification of YPD1-T12C mutant (done by F. Janiak-Spens)

Both YPD1 and SSK1-RR proteins were examined first for internal tryptophan fluorescence. The SSK1-RR response regulator contained 4 tryptophans (W543, W638, W646 and W658) and the HPt protein YPD1 contained two (W11 and W80). However, W11 of YPD1 is buried and W80 is located on the surface outside of the hydrophobic patch, near the binding site for the SSK1-RR response regulator. No

change in intrinsic tryptophan fluorescence was observed when SSK1-RR was added to YPD1 protein (F. Janiak-Spens, unpublished data). Therefore an external probe was attached to the surface of YPD1 via an engineered cysteine residue.

The surface exposed residue Thr12 of YPD1 was mutated to cysteine via the QuikChange method (Stratagene). Two oligonucleotide primers (AW426 5`-GAAATCATCAATTGGTGTATCTTAAATGAAATT and AW137 3`-TTCTCGAGTTATAGGTTTGTGTTG) carrying the selected mutation were included with the pET21a-YPD1 plasmid template in a PCR reaction. PCR reaction conditions were: denaturation temperature ï 94°C for 2.5 min, annealing temperature - 50°C for 30 s, extension temperature - 68°C for 10 min. Pfu Turbo DNA Polymerase was used for PCR reaction. After 18 rounds of amplification, the reaction mixture was digested with DpnI restriction enzyme to digest methylated parental DNA while retaining newly synthesized one. The reaction mixture was subsequently transformed into *E. coli* DH5Ŭ competent cells (OU336). Plasmid DNA was isolated from selected transformants and the mutation was confirmed via DNA sequencing analysis (Microgen, OUHSC). The YPD1-T12C expressing plasmid was transformed into *E. coli* BL21 (DE3) Star cells (OU340, Table 5-1). For protein expression, cells were grown in 1 L of LB medium in the presence of 100 εg mL^{-1} of ampicillin at 37ºC. When the optical density (at 600 nm) of the culture reached 0.8, the cells were induced

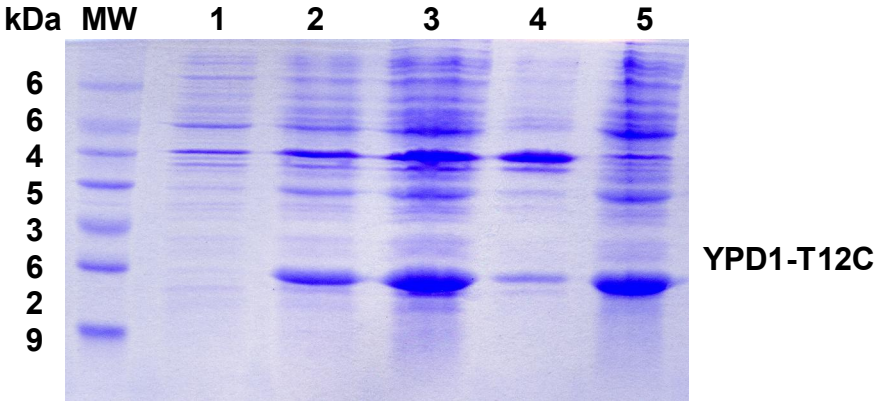

Figure 5-1. Expression profile of YPD1-T12C protein. Samples of *E. coli* BL21 (DE3) Star cells containing pET21a-YPD1T12C were removed from different stages of expression and analyzed on 15% SDS-PAGE. Lane 1, pre-induced sample of YPD1-T12C; lane 2, IPTG induced sample; lane 3, whole-cell lysate; lane 4, insoluble cell extract after sonication; lane 5, soluble cell extract after sonication.

by the addition of IPTG to a final concentration of 1 mM. The culture was cooled down and was shaken for an additional 22 hrs at 16ºC and then harvested. The expression profile is shown in Figure 5-1. Purification of the mutant protein was performed similar to that of the wild type YPD1 protein (Chapter 2) (Xu, Nguyen *et al.,* 1999).

5.2.4 *In vitro* phosphorylation of the YPD1-T12C mutant

Phosphorylation of the YPD1-T12C was achieved by incubation with GST-SLN1-HK, SLN1-RR and [γ-^{32}P] ATP. GST-tagged SLN1-HK (7 µM) bound to glutathione-Sepharose 4B resin was incubated with 7 µM [γ-^{32}P] ATP in 65 µL of 50

mM Tris-HCl (pH 8.0), 100 mM KCl, 10 mM $MgCl_2$, 2 mM DTT and 20% glycerol for 30 min at room temperature. Phosphorylated GST-SLN1-HK was recovered in the pellet after three consecutive centrifugation steps (1 min at 100 × *g*). Purified SLN1-RR (6 µM) in 50 mM Tris-HCl (pH 8.0), 100 mM KCl, 10 mM $MgCl_2$, 2 mM DTT was added and the mixture was incubated for 30 min at room temperature in a total reaction volume of 65 µL. Phospho-SLN1-RR was recovered in the supernatant after gently pelleting the resin-bound GST-SLN1-HK. The isolated phosphorylated SLN1-RR (5 εL) was added to different reaction mixtures containing either: 6 µM YPD1; 6 µM YPD1 and 6 µM SSK1-RR; 6 µM YPD1-T12C; 6 µM YPD1-T12C and 6 µM SSK1-RR in a total reaction volume of 15 µL. The reaction mixtures were incubated for 5 min at room temperature and then mixed with 5 µL of 4X stop buffer (0.25 M Tris-HCl pH 8.0, 8% SDS, 60 mM EDTA, 40% glycerol, 0.008% bromophenol blue) to terminate the reaction, and kept at - 20 ^{0}C until gel analysis. Samples were analyzed by SDS-PAGE followed by phosphorimager analysis (STORM 860, Molecular Dynamics) (Figure 5-2).

5.2.5 Fluorescence labeling of YPD1-T12C mutant

The YPD1-T12C protein 500 εL (75 εM) was loaded on the Sephadex G-25 column (1.5 cm x 18 cm) pre-equilibrated with 50 mM sodium phosphate, pH 7, 1 mM EDTA to remove DTT and collect 1 mL samples. Fractions were pulled and concentrated via centricon (YM-10, Millipore) for further labeling. The stock of 5-IAF

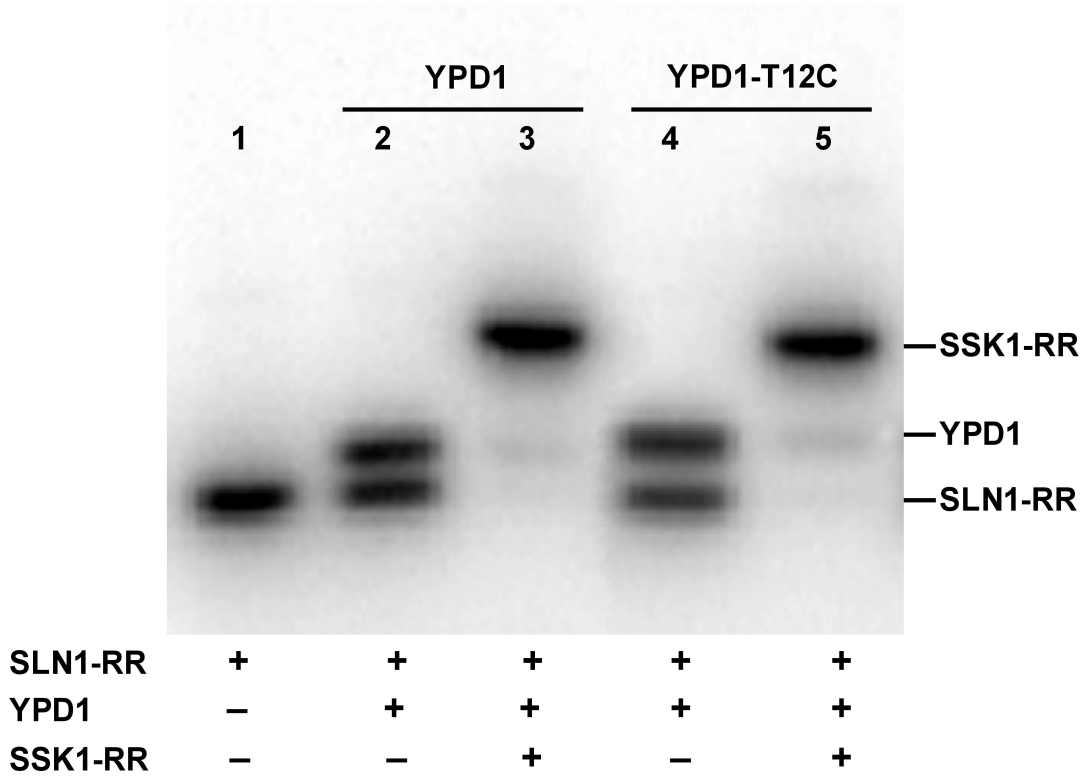

Figure 5-2. YPD1 and YPD1-T12C-dependent phosphoryl transfers. Samples were phosphorylated *in vitro* in total volume of 15 εL. Lane 1, phosphorylated SLN1-RR; lane 2, phosphoryl transfer from SLN1-RR to YPD1; lane 3, phosphoryl transfer from SLN1-RR to YPD1 to SSK1-RR; lane 4, phosphoryl transfer from SLN1-RR to YPD1-T12C; lane 5, phosphoryl transfer from SLN1-RR to YPD1-T12C to SSK1-RR.

was made by dissolving 1 mg of 5-IAF in 200 εL of DMSO. The stock solution (5 εL) was dissolved in 1 mL of 50 mM K_3PO_4, pH 9.0. The 5-IAF concentration was

determined (extinction coefficient, Ů =75 900 M^{-1} cm^{-1}) via spectrophotometer measuring absorbance at ∂ = 492 nm.

The 10x molar excess of 5-IAF stock was added to YPD1-T12C protein in the glass tube, mixed gently and incubated for 1-2 hrs at room temperature in the dark. The reaction was quenched by 5 mM DTT and incubated for 5 min at room temperature.

The YPD1-T12C-F (labeled by 5-IAF YPD1-T12C) protein was loaded onto Sephadex G-25 column to remove unreacted 5-IAF from the mixture, 1 mL fractions were collected. The concentration was determined via spectrophotometer measuring absorbance at ∂ = 280 and 492 nm. Binding efficiency was estimated according to the formula: [A_{492}/ 75900] / [A_{280}/ 15280], where 75900 ï extinction coefficient of 5-IAF and 15280 ï extinction coefficient of YPD1-T12C. All fractions were pooled and glycerol was added to the final concentration of 15%, aliquoted (100 µL) and frozen.

5.2.6 Fluorescence-based protein binding assay

Fluorescence-based YPD1-T12C-F assay was performed as follows: 12.5 µL of YPD1-T12C-F (10 µM) was mixed with 50 mM Tris-HCl, pH 8.0, 10 mM $MgCl_2$ and 1 mM DTT in total volume of 300 µL and placed in the quartz cuvette (QS 10.00, HELMA). The cuvette was placed in the fluorospectrophotometer ( ) and the fixed excitation wave length was set to ∂ = 495 nm, while the emission wave length was set to the range of ∂ = 500 - 550 nm. Subsequently YPD1-T12C-F was titrated with

SSK1-RR by adding it to the reaction mixture in the final concentrations from 0 to 4 µM.

The experiments with osmolytes were performed in similar manner; however YPD1-T12C-F was mixed with 200 mM trehalose or 200 mM glycerol or 200 mM KCl or 20 mM melezitose or 500 mM betaine or 50 mM stachyose or 500 mM NaCl and titrated with SSK1-RR by adding it to the reaction mixture in the final concentrations from 0 to 3 µM.

Similar experiments were performed with 5 mM, 20 mM and 50 mM acetyl phosphate; 0.5 mM, 5 mM and 20 mM carbamyl phosphate; 0.5 mM, 5 mM and 10 mM orthotungstate; 0.5 mM, 2 mM and 5 mM orthovanadate; and 7 mM beryllium fluoride (1 mM $BeCl_2$ and 7 mM NaF mix). All substances were incubated for 5 min with SSK1-RR and added to the reaction mixture with YPD1-T12C-F. The reaction mixture was titrated with SSK1-RR in the final concentrations from 0 to 2 µM.

All the obtained data was corrected for the volume, F/F_0. The data were analyzed using the least squares fitting of Excel (Microsoft Office v. 10.1.12) and Enzfitter (version 2.04, Biosoft, Cambridge, U.K.). Individual datasets were analyzed using equation:

$$\Delta F = \Delta F_{max} \cdot [L]/(K_d + [L]),$$

to calculate dissociation constant, K_d, values.

5.2.7 YPD1-T12C•SSK1-RR complex stability in the presence of osmolytes

Twelve osmolytes were found to be present in yeast such as: glycerol, trehalose, glycine betaine, glycerophosphocholine, proline, betaine, stachyose, melezitose, sucrose, glucose, NaCl and KCl (Blomberg, Adler 1992; Aiba, Yamada *et al.,* 1995; Hohmann 2002; Burg, Ferraris 2008).

Osmolyte	K_d, μM
NaCl (500 mM)	**0.48 ± 0.08**
KCl (200 mM)	**0.44 ± 0.11**
Glycerol (200 mM)	**0.90 ± 0.02**
Trehalose (200 mM)	**0.67 ± 0.03**
Melezitose (20 mM)	**0.58 ± 0.06**
Stachyose (50 mM)	**0.68 ± 0.05**
Betaine (500 mM)	**0.65 ± 0.04**

Table 5-2. Effect of osmolytes on the complex stability of YPD1-T12C-F and unphosphorylated SSK1-RR Dissociation constants were calculated on the bases of data collected from fluorescence-based binding assay. The data used to calculate the values in this table were obtained in triplicate and the errors represent standard errors of the mean.

The binding affinity was first measured for the YPD1-T12C·SSK1-RR complex. Analysis of the data indicated that the dissociation constant for the unphosphorylated

YPD1-T12C-F·SSK1-RR complex is 0.40 ± 0.08 εM. The effect of osmolytes on the complex stability of YPD1-T12C-F ·SSK1-RR was estimated. The K_d values obtained are presented in Table 5-2.

5.2.8 YPD1-T12C•SSK1-RR complex stability in the presence of small molecules phosphodonors.

In attempt to mimic the phosphorylation state of SSK1-RR and determine its binding affinity towards YPD1-T12C-F protein, small molecules phosphodonors and transition state analogs were incubated with SSK1-RR and then added to the reaction mixture for the fluorescence assay. The following small molecules phosphodonors were examined: acetyl phosphate, carbamoyl phosphate and beryllium fluoride. The following transition state analogs were examined: orthovanadate and orthotungstate. The effect of small molecules phosphodonors and transition state analogs on the complex stability of YPD1-T12C-F and SSK1-RR was estimated. The K_d values obtained are presented in Table 5-3.

Phosphate mimic	Concentration, mM	K_d, μM
Acetyl Phosphate	5	0.24 ± 0.05
	20	0.28 ± 0.05
	50	0.57 ± 0.04
Carbamoyl Phosphate	0.5	0.33 ± 0.01
	5	0.39 ± 0.01
	20	0.50 ± 0.12
Orthotungstate	0.5	0.30 ± 0.02
	5	0.45 ± 0.07
	10	0.50 ± 0.13
Orthovanadate	0.5	0.24 ± 0.12
	2	0.38 ± 0.06
	10	0.73 ± 0.01
Beryllium fluoride	7	0.52 ± 0.09

Table 5-3. Effect of phosphate mimics on the complex stability of YPD1-T12C-F and SSK1-RR Dissociation constants were calculated on the bases of data collected from fluorescence-based binding assay. The data used to calculate the values in this table were obtained in triplicate and the errors represent standard errors of the mean.

5.4. Discussion

The histidine phosphotransfer protein YPD1 is able to form a complex with the phosphorylated response regulator SSK1-RR (Janiak-Spens, Sparling *et al.,* 2000), however, it is still remains unclear what conditions/interactions trigger complex dissociation, phosphoryl group hydrolysis from SSK1-RR, and subsequent MAP kinase cascade activation.

We have hypothesized that changes in intracellular ion and osmolyte concentrations may affect protein-protein interactions involving YPD1 and SSK1-RR. In the current study we have examined environmental conditions that affect YPD1·SSK1-RR complex formation and its stability via fluorescence spectroscopy. Specifically, experiments were conducted to examine the effect of ino or solute concentrations on YPD1-SSK1-RR interactions *in vitro* and measure affinities between YPD1 and potentially phosphorylated SSK1-RR.

I have corroborated Fabiola Janiak-Spens initial results that YPD1-T12C-F can form a complex with SSK1-RR with a measured dissociation constant of the unphosphorylated SSK1-RR·YPD1-T12C-F of 0.40 ± 0.08 εM using the fluorescence assay described herein. However, there did not appear to be a significant effect of osmolytes on complex stability of the YPD1-T12C-F·SSK1-RR. There was a small 2-fold increase in the K_d observed for glycerol (200 mM) (Table 5-2), however it is impossible to draw conclusions if this change has significant effect on complex stability.

Small molecules phosphodonors were chosen for this study to functionally activate SSK1-RR domain, as it has been shown for other response regulators such as CheY and NtrC (Yan, Cho *et al.,* 1999; Lee, Cho *et al.,* 2001). These structural analogs are capable of binding to aspartyl side chain in the tetrahedral geometry, mimicking phosphoryl group conformation within the target molecule. My experimental data, however, showed no significant change in the dissociation constant values (Table 5-3). However, I have been unable to confirm the extent of phosphorylation of SSK-RR using small molecule phosphodonors.

Alternatively, transition state analogs, such as orthovanadate and orthotungstate were used to activate the SSK1-RR. In contrast to tetrahedral conformation of small molecules phosphodonors, these compounds mimic the transition state for a phosphoryl transfer reaction and are assumed to have a penta-coordinated geometry (Barford, Flint *et al.,* 1994; Holtz, Stec *et al.,* 1999). Both analogs had no significant effect on the dissociation constant of YPD1-T12C-F·SSK1-RR complex. Again, I have no data to confirm whether these transition state analogs actually bind to SSK1-RR. There are several questions that remain unclear:

a) Does the small molecules change in dissociation constant between YPD1-T12C-F and SSK1-RR represent a true osmolyte effect?
b) Is the SSK1-RR domain activated when incubated with small molecules phosphodonors and transition state analogs?

c) If the SSK1-RR is activated, what is the effect of osmolytes on YPD1-T12C-F·SSK1-RR complex stability?

All these questions need to be addressed in future studies to assess whether ion or solute concentration affects YPD1-SSK1-RR interactions.

List of Abbreviations

General Abbreviations

ATP	Adenosine-5′-triphosphate
DTT	Dithiothreitol
EDTA	Ethylenediaminetetraacetic acid
GST	Glutathione-S-transferase
HK	Histidine kinase
RR	Response regulator
HPt	Histidine-containing phosphotransfer
IPTG	Isopropyl-β-D-thiogalactopyranoside
PAGE	Polyacrylamide gel electrophoresis
PCR	Polymerase chain reaction
MAP	Mitogen-activated protein
MAPK	MAP kinase;
MAPKK	MAP kinase kinase
MAPKKK	MAP kinase kinase kinase
SDS	Sodium dodecyl sulfate

Gene designations

GPD1	Glycerol-3-phosphate dehydrogenase 1

Protein designation

CheY	Chemotaxis protein Y; *E. coli*
ArcB	Anoxic redox control B; *E. coli*
HOG1	High osmolarity glycerol response; *S. cerevisiae*
SKN7/CaSKN7	
SLN1/CaSLN1	Synthetic lethal of the N-end rule 1; *S. cerevisiae/C. albicans*
SSK1/CaSSK1	Suppressor of the sensor kinase 1; *S. cerevisiae/C. albicans*
YPD1/CaYPD1	Tyrosine (Y) phosphatase dependent 1;*S. cerevisiae/C. albicans*
CaNIK1	
CaHK1	Histidine kinase 1; *C. albicans*

References

Aiba, H., Yamada, H., Ohmiya, R. and Mizuno, T. (1995). "The osmo-inducible *gpd1*$^{+}$ gene is a target of the signaling pathway involving Wis1 MAP-kinase kinase in fission yeast." FEBS Lett. **376**: 199-201.

Albertyn, J., Hohmann, S. and Prior, B. A. (1994). "Characterization of the osmotic-stress response in *Saccharomyces cerevisiae*: osmotic stress and glucose repression regulate glycerol-3-phosphate dehydrogenase independently." Curr. Genet. **25**: 12-18.

Barford, D., Flint, A. J. and Tonks, N. K. (1994). "Crystal structure of human protein tyrosine phosphatase 1B." Science **263**(Mar. 11): 1397-1404.

Blomberg, A. and Adler, L. (1992). "Physiology of osmotolerance in fungi." Adv. Micro. Physiol. **33**: 145-212.

Burg, M. B. and Ferraris, J. D. (2008). "Intracellular organic osmolytes: function and regulation." *J. Biol. Chem.* **283**: 7309-7313.

Ferrigno, P., Posas, F., Koepp, D., Saito, H. and Silver, P. A. (1998). "Regulated nucleo/cytoplasmic exchange of HOG1 MAPK requires the importin β homologs NMD5 and XPO1." EMBO J. **17**(19): 5606-5614.

Hohmann, S. (2002). "Osmotic stress signaling and osmoadaptation in yeasts." Microbiol. Mol. Biol. Rev. **66**(2): 300-372.

Holtz, K. M., Stec, B. and Kantrowitz, E. R. (1999). "A model of the transition state in the alkaline phosphatase reaction." J. Biol. Chem. **274**(13): 8351-8354.

Janiak-Spens, F., Sparling, D. P. and West, A. H. (2000). "Novel role for an HPt domain in stabilizing the phosphorylated state of a response regulator domain." J. Bacteriol. **182**(23): 6673-6678.

Lee, S.-Y., Cho, H. S., Pelton, J. G., Yan, D., Berry, E. A. and Wemmer, D. E. (2001). "Crystal structure of activated CheY." J. Biol. Chem. **276**(19): 16425-16431.

Maeda, T., Wurgler-Murphy, S. M. and Saito, H. (1994). "A two-component system that regulates an osmosensing MAP kinase cascade in yeast." Nature **369**: 242-245.

Mager, W. H. and Varela, J. C. S. (1993). "Osmostress response of the yeast *Saccharomyces*." Mol. Microbiol. **10**(2): 253-258.

Posas, F. and Saito, H. (1998). "Activation of the yeast SSK2 MAP kinase kinase kinase by the SSK1 two-component response regulator." EMBO J. **17**(5): 1385-1394.

Posas, F., Wurgler-Murphy, S. M., Maeda, T., Witten, E. A., Thai, T. C. and Saito, H. (1996). "Yeast HOG1 MAP kinase cascade is regulated by a multistep phosphorelay mechanism in the SLN1-YPD1-SSK1 "two-component" osmosensor." Cell **86**: 865-875.

Rep, M., Krantz, M., Thevelein, J. M. and Hohmann, S. (2000). "The transcriptional response of *Saccharomyces cerevisiae* to osmotic shock." J. Biol. Chem. **275**(12): 8290-8300.

Xu, Q., Nguyen, V. and West, A. H. (1999). "Purification, crystallization, and preliminary X-ray diffraction analysis of the yeast phosphorelay protein YPD1." Acta Cryst. **D55**: 291-293.

Yan, D., Cho, H. S., Hastings, C. A., Igo, M. M., Lee, S.-Y., Pelton, J. G., Stewart, V., Wemmer, D. E. and Kustu, S. (1999). "Beryllofluoride mimics phosphorylation of NtrC and other bacterial response regulators." Proc. Natl. Acad. Sci. (USA) **96**(26): 14789-14794.